



**CALIFORNIA
ENERGY COMMISSION**



ENERGY RESEARCH AND DEVELOPMENT DIVISION

FINAL PROJECT REPORT

Maximizing Water and Energy From New Anaerobic Wastewater Treatment Technology

May 2024 | CEC-500-2024-044



PREPARED BY:

Chungheon Shin Aleksandra Szczuka Juliana P. Berglund-Brown
Hannah K. Chen Amanda N. Quay Jessica A. MacDonald
Felipe Chen
Silicon Valley Clean Water

Sebastien Tilmans Alexandre Miot Arvind Akela
Eric Hansen William A. Mitch Craig Criddle
Codiga Resource Recovery Center at Stanford

Primary Authors

Christian Fredericks
Project Manager
California Energy Commission

Agreement Number: EPC-16-017

Cody Taylor
Branch Manager
INDUSTRY & CARBON MANAGEMENT BRANCH

Jonah Steinbuck, Ph.D.
Director
ENERGY RESEARCH AND DEVELOPMENT DIVISION

Drew Bohan
Executive Director

DISCLAIMER

This report was prepared as the result of work sponsored by the California Energy Commission (CEC). It does not necessarily represent the views of the CEC, its employees, or the State of California. The CEC, the State of California, its employees, contractors, and subcontractors make no warranty, express or implied, and assume no legal liability for the information in this report; nor does any party represent that the uses of this information will not infringe upon privately owned rights. This report has not been approved or disapproved by the CEC, nor has the California Energy Commission passed upon the accuracy or adequacy of the information in this report.

ACKNOWLEDGEMENTS

The authors of this report are deeply grateful to the leadership of Silicon Valley Clean Water, who had the vision to pursue this bold project, and the many Silicon Valley Clean Water staff who have graciously supported the project with their time and effort. It is exceptionally difficult to sustain the effort required to develop new technologies while fulfilling a public utility's core mission of producing clean water 24 hours per day, 365 days per year. The entire team at Silicon Valley Clean Water deserves great credit for the contribution they are making to improving the sustainability of the clean water industry.

The project team also expresses heartfelt thanks to numerous project partners who provided in-kind match contributions, including equipment, labor, technical support, and in-kind services. These partners include SUEZ, Stanford University, Valley Water, Trojan Technologies, Tanner Pacific International, Flo-line Technology, Sulzer, Endress Hauser, Ovivo, LG NanoH₂O, Kennedy/Jenks Consultants, and JF Shea/Parsons Joint Venture. This project would not have been a success without them.

Finally, the Codiga family and Olivia Chen have been instrumental in supporting the salaries of numerous project staff. The team is deeply grateful for their support.

PREFACE

The California Energy Commission's (CEC) Energy Research and Development Division supports energy research and development programs to spur innovation in energy efficiency, renewable energy and advanced clean generation, energy-related environmental protection, energy transmission, and distribution and transportation.

In 2012, the Electric Program Investment Charge (EPIC) was established by the California Public Utilities Commission to fund public investments in research to create and advance new energy solutions, foster regional innovation, and bring ideas from the lab to the marketplace. The EPIC Program is funded by California utility customers under the auspices of the California Public Utilities Commission. The CEC and the state's three largest investor-owned utilities—Pacific Gas and Electric Company, San Diego Gas and Electric Company, and Southern California Edison Company—were selected to administer the EPIC funds and advance novel technologies, tools, and strategies that provide benefits to their electric ratepayers.

The CEC is committed to ensuring public participation in its research and development programs that promote greater reliability, lower costs, and increase safety for the California electric ratepayer and include:

- Providing societal benefits.
- Reducing greenhouse gas emission in the electricity sector at the lowest possible cost.
- Supporting California's loading order to meet energy needs first with energy efficiency and demand response, next with renewable energy (distributed generation and utility scale), and finally with clean, conventional electricity supply.
- Supporting low-emission vehicles and transportation.
- Providing economic development.
- Using ratepayer funds efficiently.

For more information about the Energy Research and Development Division, please visit the [CEC's research website \(www.energy.ca.gov/research/\)](http://www.energy.ca.gov/research/) or contact the Energy Research and Development Division at ERDD@energy.ca.gov.

ABSTRACT

Municipal wastewater treatment processes in the United States typically rely on aerobic secondary treatment, an energy-intensive process, for removal of dissolved organic contaminants. Aerobic treatment consumes 0.4-0.65 kilowatt-hours per cubic meter (kWh/m³) or 1,500-2,500 kilowatt-hours per million gallons (kWh/MG) and produces large quantities of surplus biosolids that must be hauled away and disposed.

A new, anaerobic secondary wastewater treatment process, the staged anaerobic fluidized bed membrane bioreactor (SAF-MBR), was installed at Silicon Valley Clean Water, a full-scale wastewater treatment facility in Redwood City, California, that serves about 220,000 people and businesses in several cities. The SAF-MBR was tested at its design flow of about 90.2 cubic meters per day (24,000 gallons/day) and is achieving US secondary effluent standards in a treatment volume and footprint that are more compact than typical aerobic systems. Because of energy efficiency and increased energy production, the SAF-MBR can be net-energy positive. A full-scale wastewater treatment plant employing an SAF-MBR for secondary treatment could produce a renewable energy surplus of 0.35 kilowatt-hours per meters cubed (1,320 kWh/MG) while cutting secondary biosolids production by about 90 percent. This anaerobic system thus would enable wastewater treatment plants to transform from large power consumers into renewable energy power plants.

SAF-MBR effluent contains sulfides and ammonia, which will interfere with disinfection using chlorine or ultraviolet light. To overcome these challenges, a treatment process consisting of sulfide oxidation by hydrogen peroxide, pathogen inactivation by UV irradiation, and chloramination was investigated. This process is capable of meeting disinfection and chlorine residual requirements established by California water reuse regulations.

Potable water reuse treatment processes were tested on SAF-MBR effluent. These processes achieved potable reuse requirements, while reducing fouling of reverse osmosis membranes and reducing the toxicity of disinfection byproducts in the final water compared to conventional aerobic systems. Further scale-up could unlock large energy and water quality benefits.

Keywords: Anaerobic secondary treatment, staged anaerobic fluidized bed membrane bioreactor, Silicon Valley Clean Water, non-potable water reuse, potable water reuse, wastewater treatment, energy efficiency

Please use the following citation for this report:

Shin, Chungheon; Aleksandra Szczuka, Juliana P. Berglund-Brown, Hannah K. Chen, Amanda N. Quay, Jessica A. MacDonald, Felipe Chen, Sebastien Tilmans, Alexandre Miot, Arvind Akela, Eric Hansen, William A. Mitch, and Craig Criddle. 2023. *Maximizing Water and Energy From New Anaerobic Wastewater Treatment Technology: Final Report*. California Energy Commission. Publication number: CEC-500-2024-044.

TABLE OF CONTENTS

Acknowledgements	i
Preface.....	ii
Abstract	iii
Executive Summary.....	1
Demonstration Results	1
Benefits to California	2
CHAPTER 1: Introduction	3
1.1 Project Objective.....	3
1.2 Technology Description	3
1.3 System Layout, Process Flow Diagram, Dimensions.....	4
CHAPTER 2: Process Performance for Secondary Treatment.....	8
2.1 System Sampling and Analysis Schedule.....	8
2.2 Analysis Methods	9
2.3 Secondary Treatment Performance	9
2.3.1 Treatment Process Results	9
2.3.2 Energy Performance	21
2.3.3 Costs	27
2.4 Secondary Treatment Discussion.....	30
2.4.1 SAF-MBR Compared to Other AnMBR Configurations.....	30
2.4.2 Carbon Footprint Comparison: Conventional Aerobic WWTP Versus AnMBR.....	33
CHAPTER 3: Non-potable Reuse Process Performance.....	36
3.1 Non-potable Water Reuse Criteria and Challenges for Anaerobic Effluent.....	36
3.2 Methods	37
3.2.1 Materials	37
3.2.2 Water Sample and Buffer Preparation	38
3.2.3 Kinetics Experiments.....	38
3.2.4 UV Experiments.....	39
3.2.5 Analyses	39
3.3 Non-potable Reuse Results and Discussion	40
3.3.1 General Water Quality.....	40
3.3.2 Timescale and Products of Sulfide Oxidation by H ₂ O ₂	41
3.3.3 Effect of H ₂ O ₂ Dose.....	44
3.3.4 Effect of Sulfides on Log Inactivation of MS ₂	45
3.3.5 Effect of H ₂ O ₂ Pre-treatment on MS ₂ Inactivation.....	48
3.3.6 Free Chlorine Doses to Achieve Total Chlorine Residuals for Distribution	49
3.3.7 Comparison of Treatment Costs.....	50

3.3.8	Implications of Results for SVCW	51
CHAPTER 4:	Potable Reuse Process Performance	53
4.1	Motivation for Potable Reuse of Anaerobic Effluent	53
4.2	Materials and Methods	54
4.2.1	Pilot- and Lab-Scale SAF-MBR Reactors	54
4.2.2	Sample Pretreatment	55
4.2.3	RO Flux Decline Measurements.....	56
4.2.4	Polarity Rapid Assessment Method (PRAM).....	57
4.2.5	Post-Treatment of RO and O ₃ /BAC Effluents.....	58
4.2.6	Analyses and Toxicity Calculation.....	58
4.3	Results and Discussion	59
4.3.1	Water Quality	59
4.3.2	RO Membrane Fouling.....	59
4.3.3	Correlation of Flux Decline with DOC Hydrophobicity	61
4.3.4	DBP Formation Along Potable Reuse Trains	62
4.3.5	Environmental Implications	65
CHAPTER 5:	Technology Transfer	67
5.1	Technology/Knowledge Dissemination Target Audience.....	67
5.2	Technology/Knowledge Dissemination Activities.....	67
5.2.1	Activities to Date:	68
5.3	Policy Development Activities.....	70
CHAPTER 6:	Future Work to Commercialize Technology	71
6.1	Demonstration of Water Reuse Trains at Pilot Scale	71
6.2	Modeling Platform to Predict SAF-MBR Performance in Different Contexts	71
6.3	Pathway for System Scale-up and Adoption	72
CHAPTER 7:	Conclusion.....	73
	Glossary and List of Acronyms	76
	References	80

LIST OF FIGURES

Figure 1:	Benefits of Replacing Aerobic Secondary Treatment With SAF-MBR.....	3
Figure 2:	Process Flow Diagram for SAF-MBR at SVCW.....	4
Figure 3:	Photograph of SAF-MBR Installed at SVCW.....	5
Figure 4:	Salsnes Filter During Installation.....	6
Figure 5:	Influent and Permeate COD Concentrations and HRT.....	10

Figure 6: COD Mass Balance During Startup Periods (Based on Estimated CH ₄)	17
Figure 7: COD Mass Balance During Steady State Operations in Periods I, II, and III (Based on Estimated CH ₄)	17
Figure 8: COD Mass Balance in Period III, Including Measured CH ₄	18
Figure 9: Net Flux and TMP	20
Figure 10: Energy Requirement for SAF-MBR Operation by Operational Period, Including Energy Requirement for Dissolved CH ₄ Recovery	22
Figure 11: Breakdown of Head Loss in the FBR for GAC Fluidization	23
Figure 12: Electricity (Blue) and Heat (Red) Energy Production Potential With Unrecovered Energy (Gray) From CHP Based on Estimated CH ₄ Production by Operational Period	24
Figure 13: Electricity (Blue) and Heat (Red) Energy Production Potential with Unrecovered Energy (Gray) from CHP Based on Measured CH ₄ Production in Period III	25
Figure 14: Energy Balance of the SAF-MBR by Operational Period	25
Figure 15: A Flow Diagram for Solids Waste Management and Calculation of Heat Energy Requirement (kWh/m ³)	27
Figure 16: Influent and Permeate COD Concentrations From CSTR-AnMBR and SAF-MBR.....	31
Figure 17: Color Map of MLSS Concentration Depending on HRT and SRT	33
Figure 18: Re Carbon Footprint (kgCO ₂ eq/m ³) of an SAF-MBR-based WWTP and a Conventional WWTP.....	34
Figure 19: Concentration of (A) Total Sulfide, (B) Hydrogen Peroxide, (C) Sulfate, and (D) UV ₂₅₄ When 500 μM Sulfide and 2000 μM Hydrogen Peroxide Were Spiked Into SAF- MBR Effluent Over a One-Hour Reaction Time. Error Bars Represent the Range of Experimental Duplicates.	41
Figure 20: Concentrations of (A) Total Sulfide, (B) H ₂ O ₂ , (C) Sulfate, and (D) UV ₂₅₄ Measured 30 Minutes After Addition of H ₂ O ₂ at Various Molar Ratios Relative to 500 μM Sulfides Spiked Into SAF-MBR Effluent. Error Bars Represent the Range of Experimental Duplicates.	44
Figure 21: Inactivation of Coliphage MS ₂ in Phosphate Buffer by UV Light (A) in the Presence of 0.5 mM Sulfides at pH 5.6, 7.2, and 9.2 and (B) in the Presence of 0.5 mM Sulfides (ST), 1 mM Thiosulfate (S ₂ O ₃ ²⁻), 1 mM Sulfite (SO ₃ ²⁻), or 1 mM Sulfate (SO ₄ ²⁻) Buffered at pH 9.2.	46
Figure 22: Inactivation of Coliphage MS ₂ in Phosphate Buffer (pH 9.2) by UV Light in the Presence of 0.5 mM Sulfides (ST), 2.9 mM N-acetyl-tyrosine, and 1 mM Thiosulfate with 2.0 mM N-acetyl-tyrosine.....	47
Figure 23: Inactivation of Bacteriophage MS ₂ in SAF-MBR Effluent by UV Light.....	48

Figure 24: Laboratory-scale Advanced Treatment Train Options for Treating Pilot-scale SAF-MBR or Laboratory-scale FBR Effluents	55
Figure 25: (A) Normalized RO Flux (J/J0) Over Time for Representative Untreated Controls of Pilot-scale SAF-MBR and Lab-scale FBR (Groups I and II) Effluents. (B) Normalized RO Flux (J/J0) After 25 h for Pilot-scale SAF-MBR Effluent Treated With Different Doses of Chloramines and Different Combinations of Chloramines (3.5 mg/L as Cl ₂), Ozone (0.8 mg O ₃ /mg DOC) and BAC (30 min EBCT). (C) Relationship Between the Fraction of DOC Retained on C18 or Diol SPE Cartridges and the Normalized RO Flux Measured After 25 h for Samples of RO Influent From the Pretreated and Control SAF-MBR Effluent Samples From Panel B. Error Bars Represent the Standard Deviations of Triplicate (A, B) or Duplicate (C) Measurements.....	57
Figure 26: DBPs Measured in the Pilot-scale SAF-MBR Influent and Effluent After Chloramine UFC Treatment on a Mass and Toxicity-weighted Basis.	63
Figure 27: DBPs Measured After Various Pretreatments on a Mass and Toxicity-weighted Basis Directly in the RO Influent Without Post-chloramination (A, C) and in the Final Effluent After Treatment by RO, the UV/H ₂ O ₂ AOP and Post-chloramination Using the Chloramine UFC Protocol (B, D)	64
Figure 28: DBPs Measured on a Mass and Toxicity-weighted Basis After Treatment of the Pilot-scale SAF-MBR Effluent by O ₃ /BAC, the UV/H ₂ O ₂ AOP and Post-chloramination Using the Chloramine UFC Protocol Without and With RO Treatment Between the BAC and the UV/H ₂ O ₂ AOP.....	65

LIST OF TABLES

Table 1: Sampling Schedules, Methods, and Analysis Contents	8
Table 2: Operational Periods and Mean Operating Conditions	9
Table 3: COD and VFA Concentrations and COD Removal Efficiency by Operational Period	11
Table 4: BOD ₅ Concentrations and Removal Efficiency	12
Table 5: Suspended Solids Concentration and Removal Efficiency by Operational Period	13
Table 6: Influent and Effluent Sulfate Concentration and Its Reduction	14
Table 7: Gas Composition in Period III (Days 153-243)	16
Table 8: SAF-MBR VSS Loading and Destruction Efficiency, Hydrolysis Rate Constant, and Biosolids Production Rate by Operational Period.....	19
Table 9: Energy Balance of Potential Future Wastewater Treatment Plant	26
Table 10: Operating Costs of Wastewater Treatment Plant, Depending Upon Conventional Aerobic Process and SAF-MBR	28

Table 11: Capital Costs and Assumptions for a SAF-MBR Processing 12 MGD (45,360 m ³)	29
Table 12: Unit Process Capital Costs for a Conventional Aerobic WWTP Processing 12 MGD (45,360 m ³), Assuming a Total Plant Cost of \$90M.....	30
Table 13: Required SRT to Retain <i>Methanothrix</i> at Various Temperatures.....	32
Table 14: Conversion Factor to Carbon Footprint (kgCO ₂ eq).....	34
Table 15: Treatment Costs for Reuse of an Aerobically Treated Effluent or Anaerobically Treated Effluent Spiked with 500 µm Sulfide and Treated with H ₂ O ₂ Dosed at Either a 6:1 or 4:1 H ₂ O ₂ :sulfide Ratio	51
Table 16: Users and Uses of Project Results	67
Table 17: Activities and Target Audience for Technology/Knowledge Dissemination	67
Table 18: Partial List of Stakeholders Engaged in Technology/Knowledge Dissemination Activities.....	69

Executive Summary

Current wastewater treatment is an energy-intensive process. Most treatment plants in the U.S. and California rely on aerobic secondary treatment, a process in which oxygen is injected into the wastewater to sustain bacteria and allow them to decompose the organic matter in the water. Aeration accounts for approximately 50 percent of the energy costs, and it results in the generation of large quantities of biosolids for disposal. Management of these biosolids is costly, and their transport is energy intensive.

An alternative to conventional aerobic secondary treatment is to eliminate the aeration and instead rely on anaerobic treatment to decompose the organic material. In contrast to the aerobic microbes at the core of conventional treatment, anaerobic microbes do not require oxygen to function. Instead of “burning” organic material into carbon dioxide like aerobic microbes, anaerobic microbes mostly transform that material into methane, the principal component of natural gas. The resulting biogas, a mixture of methane, carbon dioxide, and small amounts of other components, can be used beneficially for many applications, including electricity generation or heat, but also emerging applications like food production or production of advanced biodegradable polymers. It can also be upgraded and injected into existing pipelines as renewable natural gas.

Although anaerobic digestion of solid wastes is widely commercialized, including at wastewater treatment plants, conventional wisdom has always held that anaerobic treatment of the *liquid* wastewater stream could not achieve US effluent standards for discharge or for water reuse. This widely held but incorrect perception has confined most wastewater energy efficiency efforts to achieving marginal improvements to the aerobic paradigm, which consumes vast energy while also wasting up to 50 percent of the embodied energy of the wastewater. A shift from an aerobic to an anaerobic paradigm, however, has the potential to flip the energy balance of wastewater treatment from energy negative to renewable energy positive.

The goal of this project was to dispel antiquated perceptions of anaerobic technology and demonstrate anaerobic secondary treatment of wastewater at Silicon Valley Clean Water, a full-scale wastewater treatment facility in Redwood City, California, that serves about 220,000 people and businesses.

Demonstration Results

The staged anaerobic fluidized-bed membrane bioreactor (SAF-MBR) reliably achieved typical US secondary effluent standards for environmental discharge. The energy required to operate the system at its current flux is approximately 0.25 kWh/m³ (kilowatt-hours per cubic meter) or 950 kWh/MG (kilowatt-hours per million gallons). This performance represents a 17 percent improvement over typical aerobic systems, which consume about 0.3 kWh/m³ (1,140 kWh/MG), but the energy efficiency advantage of anaerobic treatment is compounded with large increases in renewable energy production. When capturing biogas and the dissolved methane from the effluent, and assuming typical energy conversion efficiencies from a combined heat and power plant, the total energy production potential of the SAF-MBR is about 0.60 kWh/m³

(2,270 kWh/MG) of electricity and 0.67 kWh/m³ (2,530 btu/MG) of heat. This energy generation potential would enable energy-positive secondary treatment, with a power surplus of about 0.35 kWh/m³ (1,320 kWh/MG) for export to the grid. When adding in the energy potential of primary solids, a full-scale wastewater treatment process employing a SAF-MBR for secondary treatment could produce a renewable energy surplus of 0.4 kWh/m³ (1,560 kWh/MG) for export to the grid. At SVCW, this would be equivalent to a whole-plant renewable power surplus of about 760 kW (kilowatts). By contrast, a typical conventional aerobic wastewater treatment plant consumes 0.4–0.65 kWh/m³ (1,500–2,500 kWh/MG). The SAF-MBR could transform wastewater treatment plants from large energy consumers into renewable power plants. The project team is unaware of any other secondary treatment process that can allow plants to export renewable energy without importing high-strength organic material.

In addition to energy benefits, the SAF-MBR reduced production of wastewater biosolids, which are costly to manage and dispose of. The biosolids production rate of the SAF-MBR is approximately 0.02 gVSS/gCOD_{removed}, about a 92 percent reduction in secondary solids production compared to the 0.218 gVSS/gCOD_{removed} of conventional aerobic secondary treatment processes. Eliminating energy use and reducing disposal of biosolids production at a full-scale treatment plant would eliminate approximately 35 percent of operating expenses at typical wastewater treatment plants, or about \$130/MG. Rough estimates indicate a potential capital cost savings of about \$14 million compared to an aerobic plant for a 12 MGD (million gallons per day) system. Finally, the SAF-MBR could enable reduction in greenhouse gas emissions. Assuming the existing California grid carbon intensity, the SAF-MBR could reduce the impact of wastewater treatment and the electric grid by about 620 kgCO₂e/MG (kilograms of carbon dioxide equivalent per million gallons).

Tests of strategies to further purify SAF-MBR effluent to standards suitable for non-potable or potable reuse were promising. A treatment process consisting of sulfide oxidation by hydrogen peroxide, pathogen inactivation by ultraviolet irradiation, and residual formation by chlorine addition was shown to achieve the water quality objectives needed for compliance with California's Title 22 regulations for non-potable water reuse. For potable reuse, purification of anaerobic secondary effluent using conventional full advanced treatment approaches appears viable, with potential advantages of reduced flux decline and reduced formation of disinfection byproducts. These advantages are compounded with the previously observed superior removal of pharmaceutical compounds in SAF-MBR systems. However, further testing is necessary to ensure proper management of sulfides and to evaluate the impact of seasonal sulfide variations.

Benefits to California

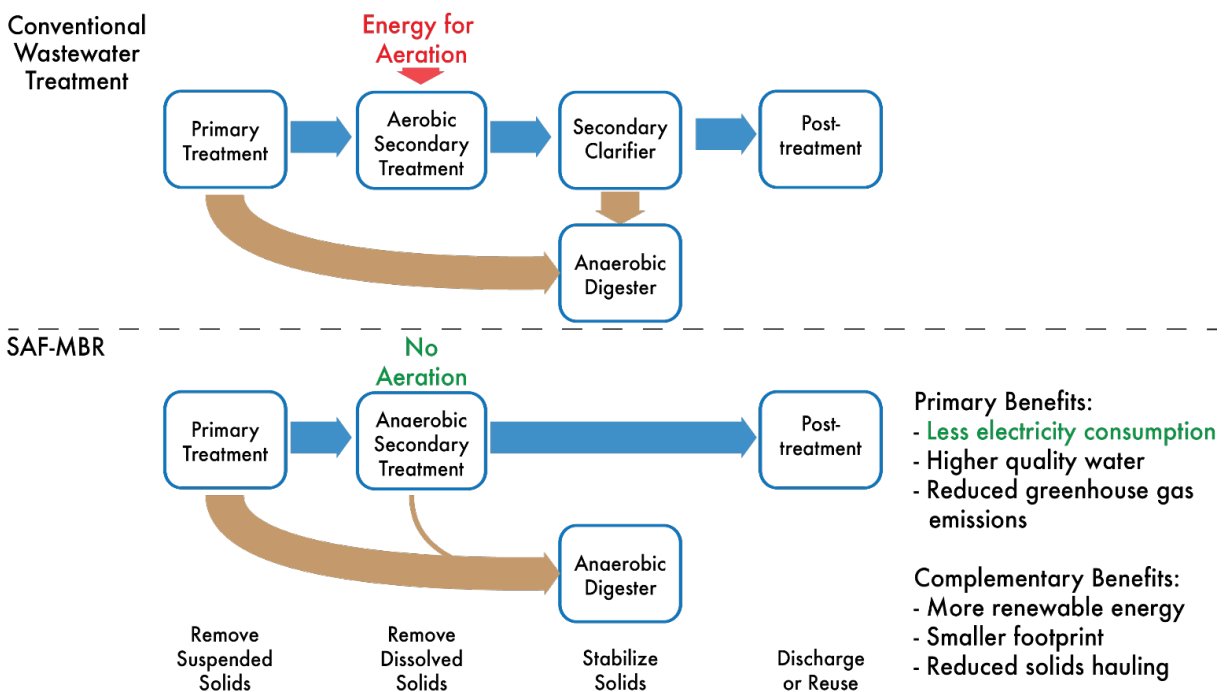
Adoption of the SAF-MBR at wastewater treatment systems would advance the state's statutory goals, as expressed in Senate Bill 350 (De León, Chapter 547, Statutes of 2015), to increase electricity and natural gas efficiency (the SAF-MBR reduces the use of electricity and could offset the use of fossil gas). By reducing nitrogen oxide (NO_x) emissions from secondary treatment and energy needs for electricity and biosolids transport, such systems also directly address Assembly Bill 32. Ratepayers would potentially benefit from reduced wastewater utility fees, reduced electric utility fees, and reduced greenhouse gases.

CHAPTER 1: Introduction

1.1 Project Objective

The overall goal of this project was to demonstrate optimized treatment trains featuring anaerobic secondary treatment at Silicon Valley Clean Water (SVCW), a full-scale wastewater treatment facility serving about 220,000 people and businesses in a service area including Redwood City, West Bay Sanitary District, the City of San Carlos, and the City of Belmont. Average summer flows at SVCW are about 45,000 cubic meters per day (m³/d) or 12 million gallons per day (MGD), and peak winter flows can reach up to 300,000 m³/d or 80 MGD. This project documented energy and cost benefits achieved by replacing conventional aerobic secondary treatment with a staged anaerobic fluidized-bed membrane bioreactor (SAF-MBR) system, as shown in Figure 1. It is important to note that the SAF-MBR is conceived as a replacement for aerobic secondary treatment, not conventional anaerobic digestion (AD). This project also evaluated the potential of the SAF-MBR to function as the centerpiece of novel treatment trains that generate non-potable and potable water for reuse applications.

Figure 1: Benefits of Replacing Aerobic Secondary Treatment With SAF-MBR



Source: Codiga Resource Recovery Center at Stanford

1.2 Technology Description

The SAF-MBR consists of two major components. The first is a fluidized-bed reactor (FBR), which is the reactor in which organic material and wastewater solids are decomposed and

converted into biogas. The FBR contains a bed of granular activated carbon, a material commonly used in water filtration. In an FBR, water is circulated vertically up through the bed of carbon to “fluidize” it, such that the grains of carbon are suspended in the turbulence of the water without flowing out of the reactor top. Anaerobic microorganisms accumulate on the surface and inside the pores of the carbon, forming layers of biofilm that intercept and degrade the organic material in the wastewater flowing by.

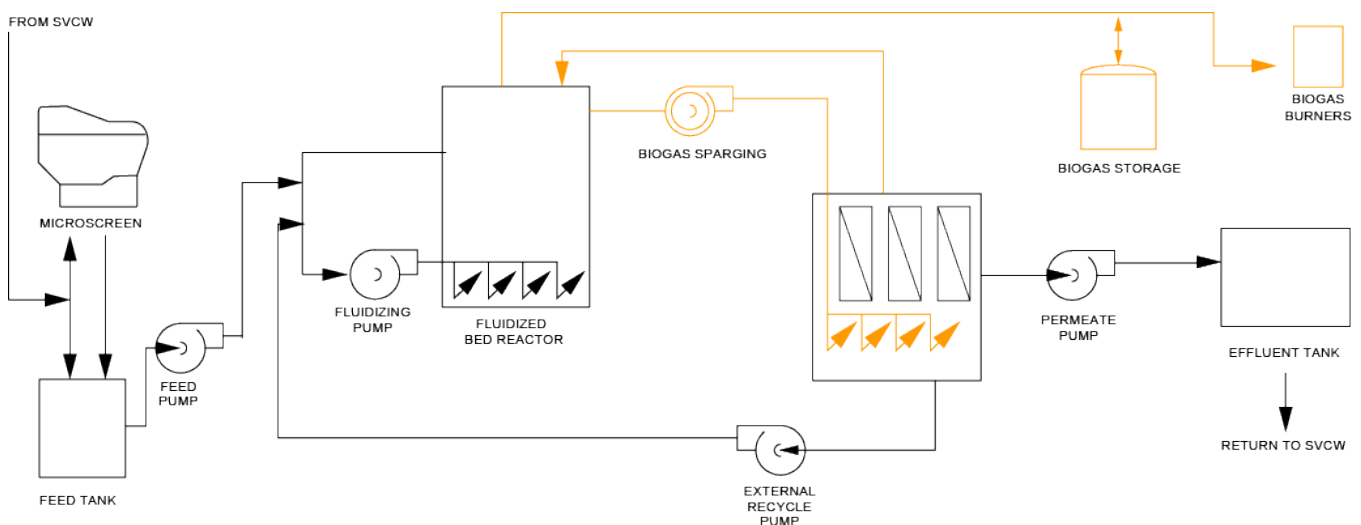
The second component of the SAF-MBR is a membrane tank, in which membranes filter the water to retain solids within the system. Those solids are recycled back to the FBR to allow them more contact with the microorganisms and more time to decompose. The membranes have a porosity of 0.04 μm (micrometers), which is about 10 percent of the size of typical bacteria. This small pore size enables very high solids removal in the system but causes solids to accumulate on the surface of the membranes and clog them. Biogas is recirculated into the bottom of the membrane tank to bubble past the membranes, agitating them to knock solids off the membrane surface and keep the membranes clean. The membranes can also be cleaned using sodium hypochlorite (bleach) and citric acid.

The two major consumers of energy in the SAF-MBR are: 1) the pumps required to continuously circulate water through the carbon bed to fluidize it, and 2) the blowers needed to circulate biogas into the base of the membranes for membrane cleaning. The SAF-MBR can nevertheless produce an energy surplus because excess biogas can be used for energy generation.

1.3 System Layout, Process Flow Diagram, Dimensions

A demonstration SAF-MBR system was installed at SVCW and started operating in 2021. A process flow diagram for the complete system is shown in Figure 2. A photograph of the SAF-MBR system is shown in Figure 3.

Figure 2: Process Flow Diagram for SAF-MBR at SVCW



Source: Codiga Resource Recovery Center at Stanford

Figure 3: Photograph of SAF-MBR Installed at SVCW



Source: Codiga Resource Recovery Center at Stanford

The demonstration system was constructed to be able to receive two distinct water streams from the main SVCW plant. First, the system can continuously receive SVCW primary effluent, which is pumped to the demonstration system from a sample tap downstream of SVCW's conventional primary clarifiers. As an alternative, the system can also continuously receive SVCW primary influent, which is pumped from a sample tap downstream of SVCW's influent bar screens. Both streams can be fed directly to the SAF-MBR feed tank or passed through a Salsnes SF1000 microscreen filter. The Salsnes filter is equipped with a filter belt with a 350 μ m porosity. A photo of the Salsnes filter and associated equipment is shown in Figure 4.

Figure 4: Salsnes Filter During Installation



Source: Codiga Resource Recovery Center at Stanford

From the feed tank, water is pumped into the first tank of the SAF-MBR, the fluidized bed reactor (FBR). This reactor is a concrete tank with a square cross-section with interior dimensions of 1.8m x 1.8m x 6m (6'x6'x20'). The FBR contains a bed of granular activated carbon (GAC) occupying about 3m (10 feet) of depth when static. A recirculation loop recirculates water from the top of the reactor into the bottom via a set of 36 nozzles designed to distribute flow evenly across the cross section of the reactor. This recirculation creates a continuous upward flow of water in the reactor that keeps the GAC bed fluidized.

Feed to the SAF-MBR is pumped into the recirculation loop of the reactor and pumped up through the GAC bed. Effluent from the SAF-MBR overflows by gravity to the membrane tank (MT). The membrane tank has dimensions of 0.84m x 0.67m x 3m (2.75' x 2.2' x 10') and contains nine Zeeweed 500D ultrafiltration membrane modules (Suez) with nominal porosity of 0.04 μ m. SAF-MBR effluent, also referred to as membrane permeate, is sucked through the membranes by a pump and sent to an effluent tank for use in potential downstream pilot treatment units.

The membranes filter out solids, which would accumulate in the MT if not processed. The solids and water in the MT are continuously pumped back to the recirculation loop of the FBR to ensure that the solids get adequate contact with the anaerobic microbes for treatment. A portion of the recycle flow is periodically wasted to control the accumulation of solids inside the SAF-MBR.

As the membranes filter water, solids intercepted on the membranes can clog the membranes, a process referred to as fouling, which decreases membrane performance. To control membrane fouling, a blower recirculates biogas from the headspace of the FBR into the base of the MT, a process known as gas sparging, wherein the bubbles of gas agitate the membranes to remove particulates and fouling. Gas in the headspace of the MT returns passively by pipe to the headspace of the FBR.

Excess biogas from the SAF-MBR is stored in a quasi-spherical Ovivo Ultrastore™ gas storage system, which has a storage capacity of approximately 2.8 Nm³ (normal cubic meters), or 100 ft³, and an external diameter of approximately 1.8m (6'). Biogas is periodically treated to remove hydrogen sulfide and burned to maintain adequate storage capacity.

CHAPTER 2:

Process Performance for Secondary Treatment

Although conventional aerobic treatment reliably achieves US secondary effluent standards for environmental discharge, it is a costly, energy-intensive process. Aerobic wastewater treatment plants consume 0.4-0.65 kWh/m³ (1,500-2,500 kWh/MG) of wastewater treated (Scherson and Criddle, 2014), and provoke operating costs of about \$0.11/m³ (\$416/MG) (costwater.com).

2.1 System Sampling and Analysis Schedule

SAF-MBR influent and permeate were collected using composite samplers (5800 Refrigerated Sampler, Teledyne Iso). At each process stage, 500 mL (milliliter) samples were collected every 30 minutes and mixed in a container prior to analysis. Grab samples were collected for mixed liquor suspended solids (MLSS) from the FBR and the membrane tank, as these concentrations were less susceptible to diurnal fluctuations than constituent concentrations in raw wastewater. Grab samples were also collected for biogas, including from the off-gas line and dissolved methane in the permeate. Samples of produced biogas were collected in a Tedlar gas bag for gas composition analysis. Samples of SAF-MBR permeate were collected in 530-mL gas-tight serum bottles without air contact, to analyze dissolved methane content. The collected samples were transported from SVCW to a laboratory on the Stanford Campus (approximately 30 minutes travel time) and immediately analyzed (chemical oxygen demand/suspended solids/5-day biochemical oxygen demand/gas chromatography equipped with a thermal conductivity detector [COD/SS/BOD₅/GC-TCD]) or pretreated for later analysis. Samples for ion chromatography (IC) analysis were filtered with a 0.1 μm membrane filter and stored at 39°F (4°C) until analysis. Samples for dissolved methane were alkalinized in the serum bottles by adding 2 mL of 3N NaOH (sodium hydroxide) solution to prevent any potential biological methane consumption. The sampling schedule and analyses are summarized in Table 1.

Table 1: Sampling Schedules, Methods, and Analysis Contents

Sample	Sampling day	Sampling method	Analyses
Influent	Tues/Thur	Composite	COD/ IC/ SS(Tues)/ BOD ₅ (Thur)
Permeate	Tues/Thur	Composite	COD/ IC/ SS(Tues)/ BOD ₅ (Thur)/ Turbidity
FBR MLSS	Tues/Thur	Grab	COD/ SS(Tues)
Membrane tank MLSS	Tues/Thur	Grab	COD/ SS(Tues)/ BOD ₅ (Thur)
Gas sample	Tues	Grab	GC-TCD
Permeate	Tues	Grab	Dissolved CH ₄ (GC-TCD)

IC: ion-chromatography for acetate, propionate and sulfate measurements

GC-TCD: for CH₄, CO₂ and N₂ composition analysis in a biogas sample

Source: Codiga Resource Recovery Center at Stanford

2.2 Analysis Methods

COD was analyzed using a spectrophotometric method (EPA 410.4) using COD test kits (Method 8000, Hach). Total and volatile suspended solids (TSS and VSS) and 5-day BOD₅ were analyzed according to standard methods (APHA, 1998). Acetate, propionate and sulfate concentrations in influent and permeate samples were analyzed by ion chromatography (IC, Dionex™, Integrion™, HPIC™ System, Thermo Scientific; Column: Dionex IonPac AS11, Thermo Scientific). Turbidity was monitored with a turbidity meter (HI 98713, Hanna Instruments). Gas composition was analyzed using a GC-TCD (Series 580, GOW-MAC, Bethlehem, PA). Dissolved methane concentration was measured using the serum bottle technique, as described in Shin et al., 2011.

2.3 Secondary Treatment Performance

2.3.1 Treatment Process Results

2.3.1.1 Operating Conditions

The SAF-MBR system proceeded through five operational periods corresponding to different net flux conditions, including two startup periods and three steady state periods, as summarized in Table 2.

Table 2: Operational Periods and Mean Operating Conditions

Operational period	Operational day	Influent flow rate (m ³ /d)	Permeate flow rate (m ³ /d)	MBR bulk wasted (m ³ /d)	HRT (h)	SRT (d)	Net flux (L/m ² /h)	Temp (°C)	OLR** (kgCOD/m ³ /d)
Startup (a)	1 ~ 40*	22.0	21.8	0.218	21.1	88.9	2.9	19.8	0.5
Startup (b)	41 ~ 54	26.4	26.1	0.261	17.6	74.1	3.5	19.6	0.7
I	55 ~ 110	44.9	44.4	0.444	10.4	43.6	6.0	24.1	1.1
II	111 ~ 152	74.8	74.0	0.740	6.2	26.1	10.0	25.0	2.0
III	153 ~ 243	90.2	89.3	0.893	5.2	21.7	12.0	22.8	2.6

* ~: approximately

** OLR: organic loading rate

Source: Codiga Resource Recovery Center at Stanford

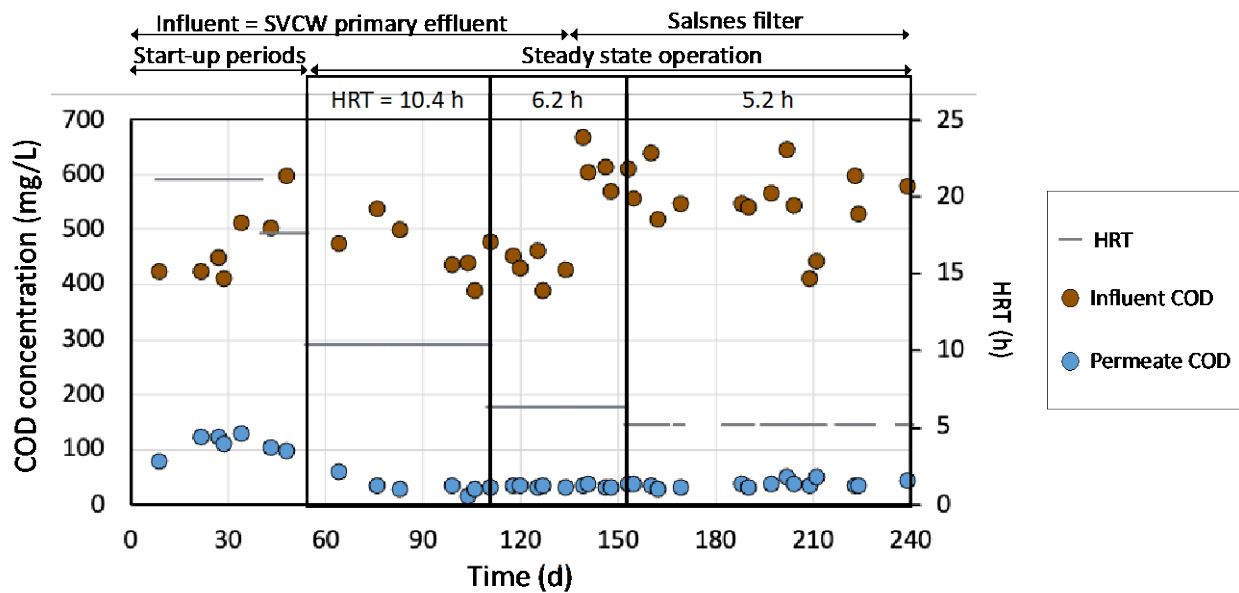
The SAF-MBR system was operated for more than 240 days without any temperature control. The system startup lasted 54 days, split into two periods. First, the system was operated at a hydraulic retention time (HRT) of 21.1 hours (h) and, second, the system was operated at an HRT of 17.6 h. System startup was deemed complete when the net flux was increased to 6 L/m²/h (liters per square meter hour), but flow was further increased over three steady state periods to achieve target flow objectives: Period I with an HRT of 10.4 h at 6 L/m²/h net flux, Period II with an HRT of 6.2 h at 10 L/m²/h net flux, and Period III with a HRT of 5.2 h at 12 L/m²/h net flux.

For the first 139 days of operation, encompassing the startup and steady state periods I and II, the system was fed primary effluent from the primary clarifiers of SVCW's main plant. In the middle of steady state Period III (day 140), the system feed was switched to SVCW primary influent downstream of SVCW's fine screens when the primary effluent supply was removed from service to accommodate necessary maintenance to the SVCW main plant. Prior to introduction into the SAF-MBR system, the SVCW primary influent was treated using the Salsnes filter to remove bulky materials and approximate typical primary effluent.

2.3.1.2 COD and BOD₅ Removal

Influent and permeate COD concentrations during the startup and steady state operation periods are shown in Figure 5.

Figure 5: Influent and Permeate COD Concentrations and HRT



Source: Codiga Resource Recovery Center at Stanford

During the startup periods, permeate COD concentration was ~ 100 mg/L (milligrams per liter), indicating that the microbial community had not fully colonized the system. Permeate COD concentration gradually decreased and stabilized at ~30 mg/L by the 76th day of operation in Period I (10.4 h). Thereafter, the SAF-MBR maintained robust performance, producing high quality permeate even under more demanding operating conditions of shorter HRT and higher influent COD concentrations. Permeate COD concentration was steady as HRT was reduced during Period II (6.2 h) and Period III (5.2 h). There was no change in permeate COD concentration when the SAF-MBR influent concentration increased from about 460 mg/L (SVCW primary effluent) to about 560 mg/L (SVCW primary influent with Salsnes filter treatment).

COD concentrations throughout the treatment process are summarized in Table 3. Residual acetate and propionate concentrations in permeate (mg/L as COD), and COD removal efficiency are also summarized for the operational period previously listed in Table 2.

Table 3: COD and VFA Concentrations and COD Removal Efficiency by Operational Period

Operational period		COD concentration (mg/L)				VFA concentration (mg/L as COD)		COD removal (%)
		Influent	Permeate	FBR MLSS	MT MLSS	Acetate	Propionate	
Startup (a) Days 1–40	mean	442	111	1733	2034	91	0.5 >	75
	±	41	20	693	836	79	0	4
	n	5	5	5	5	3	3	5
Startup (b) Days 41–54	mean	549	99	2480	2835	94	0.5 >	82
	±	68	4	0	233	4	0	3
	n	2	2	2	2	2	2	2
I Days 55–110	mean	461	32	2825	3308	5	0.5 >	93
	±	53	15	741	703	5	0	3
	n	6	6	6	6	3	3	6
II Days 111–152	mean	508	31	2248	3137	6	0.5 >	94
	±	96	2	341	468	2	0	1
	n	10	10	10	10	4	4	10
III Days 153–243	mean	550	36	3325	4513	9	0.5 >	94
	±	64	6	1237	1540	4	0	1
	n	15	15	15	15	9	9	4

VFA: volatile fatty acid

Source: Codiga Resource Recovery Center at Stanford

The high permeate COD concentration during the startup periods was mostly acetate, constituting ~ 90 percent of permeate COD. This high permeate acetate concentration indicated insufficient acetate consumption by acetoclastic methanogens, specifically *Methanothrix*, which is responsible for achieving low acetate concentrations in anaerobic membrane bioreactor (AnMBR) effluents (Shin et al., 2012; Shin et al., 2021a). During the startup period, propionate was not detected, indicating that degradation of propionate and other metabolic intermediates produced before propionate are not a limiting step in the SAF-MBR, even during startup. Instead, acetate utilization by *Methanothrix* is rate limiting. This implies that permeate acetate concentration is the key parameter that represents the degree of maturity of the system and therefore needs to be monitored during startup.

During steady state operations, permeate COD concentration was as low as ~ 33 mg/L with low acetate concentration (5 to [~] 9 mgCOD/L). These effluent concentrations can satisfy US secondary treatment standards for COD (60 mg/L; Lim et al., 2019). The low acetate concentration in the permeate indicates that the SAF-MBR is capable of accumulating and culturing *Methanothrix*, the organism that is indispensable for achieving low permeate COD concentrations anaerobically. The critical distinction in the SAF-MBR compared to other AnMBRs is the

use of GAC as a biocarrier. The GAC enables *Methanothrix* and other anaerobic organisms to form a biofilm and reach very long retention times (i.e., > 600 days, Shin et al., 2021b) even when there is a short solids retention time (SRT) for solids dispersed in the bulk fluid (43.6 days [d]) in Period I, 26.1 d in Period II, and 21.7 d in Period III). These high microbial retention times are critical, as *Methanothrix* requires approximately 70 days of retention time at local ambient temperatures to avoid being washed out of a reactor.

We expect that SAF-MBR permeate quality will further improve with longer operation to allow full system acclimation. In previous systems, peak process performance was achieved after ~ 400 days of operation (Shin et al., 2014), after which acetate concentration in the permeate could be lower than the detection limit (less than [$<$] 0.5 mgCOD/L, Shin et al., 2014; Evans et al., 2018; Shin et al., 2021a). Such a reduction in permeate acetate in the present system would yield permeate COD concentrations of approximately ~ 25 mg/L at SVCW.

COD removal efficiency was stable during steady state operations, with removal efficiencies > 93 percent, even at an HRT of 5.2 h during Period III. This high organic removal rate is confirmed by BOD₅ measurements from Period II, as shown in Table 4.

Table 4: BOD₅ Concentrations and Removal Efficiency

Operational period		BOD ₅ concentration (mg/L)			BOD ₅ removal efficiency (%)
		Influent	Permeate	MT MLSS	
II (Days 111–152)	mean	243	14	1110	94
	±	56	2	565	1
	n	5	5	5	5
III (Days 153–243)	mean	257	16	2395	94
	±	38	4	911	1
	n	9	9	9	9

MT: membrane tank

Source: Codiga Resource Recovery Center at Stanford

BOD₅ removal efficiency was as high as ~ 94 percent, enabling low permeate BOD₅ concentration of approximately 15 mg/L, which can satisfy US secondary treatment standards (BOD₅ = 30 mg/L, 40 Code of Federal Regulations 133.102, EPA). This performance indicates that the SAF-MBR reliably removes biodegradable organic contaminants from wastewater influent. The SAF-MBR permeate BOD₅ concentration may improve further, to as low as ~ 10 mg/L after colonization and acclimation by *Methanothrix*, as addressed above.

The high organic removals achieved at 5.2 h HRT are exceptional for a secondary treatment process. Conventional aerobic secondary treatment aeration basins require an HRT of ~ 6 h (Metcalf and Eddy, 1991), which then needs to be followed by a secondary clarifier for an additional ~ 2 HRT (Metcalf and Eddy, 1991). The overall HRT for conventional aerobic secondary system is thus about ~ 8 h. The short HRT capability of the SAF-MBR can therefore enable an approximately 35 percent smaller reactor volume than conventional aerobic systems, yielding reductions in plant footprint. At this low HRT, the OLR was 2.6 kgCOD/m³/d or

1.2 kgBOD₅/m³/d. Conventional aerobic secondary treatment systems can manage an OLR of about 0.5 kgBOD₅/m³/d (Metcalf and Eddy, 1991). Previous research has shown that FBRs, the main biological process in the SAF-MBR system, are capable of managing > 10 kgCOD/m³/d OLR (Shin et al., 2012), approximately 20 times more than the OLR that can be applied in conventional aerobic secondary treatment. Thus, the SAF-MBR system should be more robust to increases in influent COD concentration that are currently resulting from increased water conservation. Furthermore, the SAF-MBR system can operate at a shorter HRT because of its capability of managing high OLR. Future tests can further optimize the SAF-MBR, based on ambient temperatures, HRT, water quality, and membrane fouling.

2.3.1.3 Suspended Solids (SS) Removal

Suspended solids concentrations and removal efficiency during each operational period are summarized in Table 5.

Table 5: Suspended Solids Concentration and Removal Efficiency by Operational Period

Operational period		SS concentration (mg/L)								SS removal (%)
		Influent		Permeate		FBR MLSS		MT MLSS		
		TSS	VSS	TSS	VSS	TSS	VSS	TSS	VSS	
Startup (a) Days 1–40	mean	91	74	2	1	1128	893	1224	970	98
	±	8	5	1	1	246	191	250	176	2
	n	4	4	4	4	4	4	4	4	4
Startup (b) Days 41–54	mean	101	81	2	2	1325	1075	1208	971	98
	±	11	11	0	1	N.A.	N.A.	342	289	0
	n	2	2	2	2	1	1	2	2	2
I Days 55–110	mean	84	74	1	1	1507	1210	1643	1303	98
	±	20	18	0	0	503	360	383	281	0
	n	5	5	5	5	5	5	5	5	5
II Days 111–152	mean	108	92	1	1	1130	951	1695	1417	99
	±	38	31	1	1	231	176	263	209	1
	n	6	6	6	6	6	6	6	6	6
III Days 153–243	mean	136	116	1	1	1484	1233	2775	2255	99
	±	24	24	1	1	362	294	1724	1349	0
	n	10	10	10	10	10	10	10	10	10

MT: membrane tank; N.A.: not available

Source: Codiga Resource Recovery Center at Stanford

The SAF-MBR maintained > 98 percent suspended solids removal efficiency from the beginning of operations, yielding permeate concentration of approximately 1 mg/L, which

readily satisfy US secondary treatment standards (30 mg/L, 40 CFR 133.102, EPA). Effluent turbidity also remained low, at < 1.5 FNU (Formazin Nephelometric Units).

Typical suspended solids concentrations in the bulk fluid (the MLSS) of FBR and MT, approximately 2,800 mg/L, are much lower than reported MLSS concentrations in other MBRs (~10,000 mg/L), including both aerobic MBRs and AnMBRs. The low MLSS concentration is possible because the GAC biocarrier ensures long retention of microbial biomass, and therefore the reactor does not need to be operated at a high SRT to avoid microbial washout. A low SRT yields a low MLSS concentration, which in turn favors reduced membrane fouling rates. The low MLSS concentration in the SAF-MBR did not cause the significant membrane fouling that is commonly observed in MBRs operating at high MLSS concentrations (> 10,000 mg/L, Robles et al., 2013). Low membrane fouling rates, in turn, facilitate cost- and energy-efficient membrane operation.

In this study, the SAF-MBR demonstrated the capability of achieving US secondary effluent standards for organics (COD and BOD) and suspended solids (TSS) while operating at an HRT that is competitive with typical aerobic wastewater treatment systems (5.2 h). Critically, such performance has not been observed in other AnMBRs in temperate climates to date. There is the potential that the HRT could be further reduced. This performance positions the SAF-MBR as a unique alternative to the conventional energy-intensive aerobic wastewater treatment paradigm.

2.3.1.4 Sulfate and Sulfides

Under anaerobic conditions, sulfate present in the influent is a strong electron acceptor, used by sulfate-reducing bacteria (SRB). SRB compete with methanogens (methane-producing bacteria) for electron donor (BOD) and produce sulfide. Sulfide is a toxic constituent that causes issues for downstream processes, as discussed in Chapters 3 and 4. Influent and effluent sulfate concentrations and the removal rate of sulfate during each operational period are shown in Table 6.

Table 6: Influent and Effluent Sulfate Concentration and Its Reduction

		Sulfate concentration (mgSO ₄ ²⁻ /L)		Sulfate reduction (%)
		Influent	Effluent	
Startup (a) Days 1--40	mean	42	7	82
	±	4	3	8
	n	3	3	3
Startup (b) Days 41--54	mean	41	8	79
	±	3	2	6
	n	2	2	2
I Days 55--110	mean	32	12	65
	±	2	10	33
	n	3	3	3

		Sulfate concentration (mgSO ₄ ²⁻ /L)		Sulfate reduction (%)
		Influent	Effluent	
II Days 111– 152	mean	34	7	79
	±	4	1	4
	n	5	5	5
III Days 153– 243	mean	50	17	71
	±	24	23	20
	n	10	10	10

Source: Codiga Resource Recovery Center at Stanford

The sulfate removal rate was relatively higher during startup periods (79% ~ 82%) than during steady state periods (65% ~ 79% in periods I to III). This result implies that SRB required less acclimation time than methanogens in the beginning of operation but that, once established, methanogens may be able to partially outcompete SRB by lowering ambient acetate concentrations below optimal levels for SRB.

During Period III, the mean influent sulfate concentration was higher than in previous periods. Beginning on day 200, mean influent sulfate concentrations were ~ 76 mgSO₄²⁻/L because influent sulfate concentrations at SVCW increase during the wet season. The sulfate removal rate remained consistent during this period, yielding higher effluent sulfate concentrations than in other operational periods. These results also imply higher permeate sulfide concentrations in the colder months.

In general, about 30 mgSO₄²⁻/L of sulfate is reduced in the SAF-MBR system, corresponding to a sulfide production of about 10 mgS₂⁻/L. The pH within the SAF-MBR system was about 7.0, close to the pK_a (acidity) of H₂S (hydrogen sulfide), where about 50 percent of sulfide exists as HS⁻ (hydrogen sulfide ion) and the other 50 percent exists as H₂S. Because H₂S is very soluble (Henry's constants of 0.113 M/atm [molarity per atmospheric pressure at sea level] for 20°C and 0.1000 M/atm for 25°C), calculations based on Henry's law indicate that more than 90 percent of the produced H₂S was dissolved in the liquid phase. Based on Henry's law and sulfide speciation, more than 95 percent (= 50% from HS⁻ + 50%×90% from H₂S) of the produced sulfide remains in the SAF-MBR effluent.

The sulfide in the effluent can cause several downstream issues, including scale deposits on the effluent line, quenching of oxidant for disinfection or inhibition of ultraviolet (UV) disinfection, or clogging reverse osmosis (RO) membranes. An approach to managing sulfide for disinfection and reuse applications is discussed in Chapter 3.

2.3.1.5 Gas Production and Composition

Gaseous biogas production and dissolved methane concentration were monitored in tandem beginning on the 190th day of operation, in Period III. The biogas produced by the SAF-MBR consists primarily of CH₄ (methane), CO₂ (carbon dioxide), and N₂ (nitrogen), with trace amounts of H₂S (hydrogen sulfide). Measured biogas concentrations of CH₄, CO₂, and N₂ and estimates of H₂S in Period III are summarized in Table 7. H₂S composition was estimated

using Henry’s law. The composition of the biogas produced by the SAF-MBR will appear quite unusual to experts accustomed to biogas from conventional anaerobic digestion, dairies, or other high-strength anaerobic bioreactors. Biogas from these applications has a typical composition of 65 percent CH₄ and 35 percent CO₂, with negligible N₂. The biogas from the SAF-MBR is different because the SAF-MBR is processing wastewater with a much lower influent organic strength (about 500-1,000 mg/L COD as opposed to 10,000+ mg/L COD). CO₂ is more soluble in water than CH₄. At low influent COD concentrations, CO₂ production is not high enough to reach saturation levels in water. As a result, a larger fraction of produced CO₂ remains dissolved in the liquid phase. The lower water temperatures also contribute to increased solubility of CO₂, but the main driver of low CO₂ content in the biogas is the low strength of the wastewater. The nitrogen in the biogas is from the nitrogen dissolved in the effluent due to equilibrium with the atmosphere. This dissolved nitrogen achieves equilibrium with the reactor headspace (the biogas). Whereas in conventional AD the methane and CO₂ production is so large as to “dilute” the concentration of nitrogen to less than 1 percent of the gas, the lower productions in low strength wastewater do not dilute out the nitrogen. The concentrations of different gases observed in the present study are consistent with previous studies and with values predicted from Henry’s law on the solubility of gases (McCarty et al., 2015; Shin et al., 2021b).

Table 7: Gas Composition in Period III (Days 153-243)

	Gas composition (%)			
	CH ₄	CO ₂	N ₂	H ₂ S*
mean	85.5	4.7	9.8	2.8 × 10 ⁻³
±	3.1	0.6	3.5	N.A.
n	9	9	9	N.A.

* Estimated H₂S composition

N.A.: not available

Source: Codiga Resource Recovery Center at Stanford

Gas production was monitored with a mass flow meter (Alicat Scientific, MW-10SLPM-D-X, Tucson, Arizona). The monitored mean gas production was 5.2 slpm (standard liter per minute) or 0.182 scfm (standard cubic foot per minute), corresponding to 83 (±14) L biogas/m³ (liters per cubic meter) wastewater treated (11,000 ft³/MG or cubic feet per million gallons). It should be noted, however, that the monitored biogas production rate is an underestimate due to biogas losses in the demonstration system. At the time of report writing, several biogas leaks were identified and remedied, but the data at present do not yet capture the resulting improvements in measurements. The underestimates of gas production are addressed using a COD mass balance in Section 2.3.1.6.

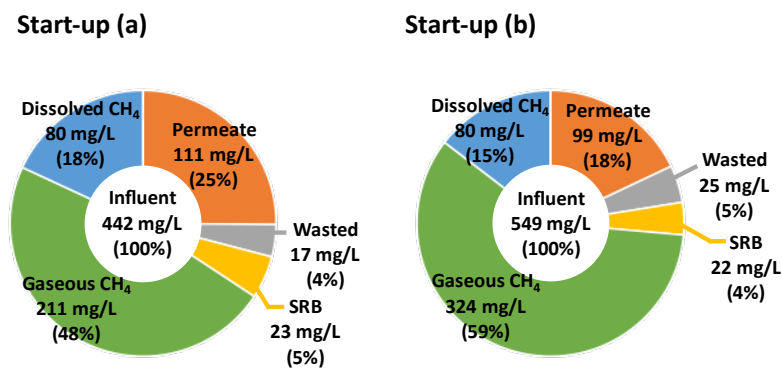
A portion of the biogas remains dissolved in the liquid phase and exits the reactor through the permeate. The concentration of dissolved methane in the SAF-MBR effluent was measured with the serum bottle technique established in Shin et al. (2011). The mean measured dissolved methane concentration was 20.2 (±1.4) mgCH₄/L. Measured concentrations of dissolved methane were consistent with theoretical predictions based on Henry’s law, assu-

ming saturation of methane. Therefore, the SAF-MBR effluent is not supersaturated with dissolved methane.

2.3.1.6 COD Mass Balance

A COD mass balance was developed for the startup periods (Figure 6) and steady state operation (Figures 7 and 8). The gaseous CH₄ production and dissolved CH₄ concentrations shown in Figures 6 and 7 were derived from the measured COD concentrations and the AnMBR gas simulation model introduced in Shin et al., 2021b. Methane values in Figure 8 rely on measured dissolved and gaseous CH₄ data in Period III.

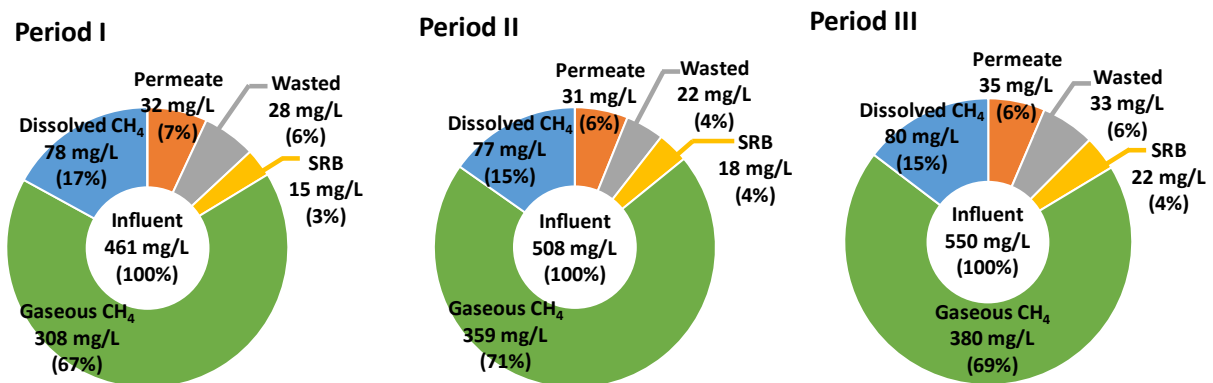
Figure 6: COD Mass Balance During Startup Periods (Based on Estimated CH₄)



Source: Codiga Resource Recovery Center at Stanford

During the startup periods (Figure 6), permeate COD constituted 25 percent and 18 percent of influent COD, largely due to acetate concentration in the permeate (Table 7). Beginning in steady state Period I (Figure 7, left), permeate COD declined to 7 percent of influent COD due to maturing biological activity, especially from *Methanothrix*. The increased biological activity produced more methane. During steady state operation (Periods I to III, Figures 7), ~85 percent of influent COD was converted to methane, including dissolved methane, and only ~10 percent of influent COD was discharged through permeate and wasted MLSS.

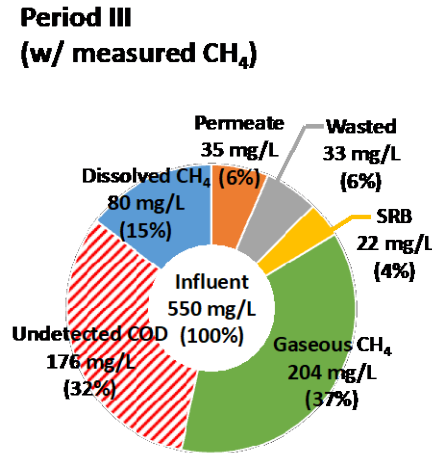
Figure 7: COD Mass Balance During Steady State Operations in Periods I, II, and III (Based on Estimated CH₄)



Source: Codiga Resource Recovery Center at Stanford

The estimated CH₄ data in Period III (Figure 7, right) has a large discrepancy with the measured CH₄ data in Figure 8. Simulations estimate that 69 percent of influent COD is converted to CH₄ (Figure 7, right), but measured gaseous CH₄ constitutes only 37 percent of influent COD in Figure 8. We expect that the missing 32 percent of influent COD is largely due to gas losses from the demonstration system (Section 2.3.1.5).

Figure 8: COD Mass Balance in Period III, Including Measured CH₄



Source: Codiga Resource Recovery Center at Stanford

2.3.1.7 VSS Destruction and Biosolids Production Rate

VSS destruction efficiency was calculated with Equation 2.1.

$$VSS \text{ destruction efficiency } (\%) = \frac{VSS_{in} - VSS_{wasted}}{VSS_{in}} \quad (2.1)$$

where VSS_{in} is the mass of VSS entering the system through the influent (grams/day[g/d]) and VSS_{wasted} is the VSS mass removed through MLSS wasting (g/d).

The VSS hydrolysis rate constant (k_{hyd} , 1/d) was estimated with Equation 2.2, based upon VSS destruction efficiency.

$$k_{hyd} = \frac{VSS \text{ destruction efficiency } (\%)}{1 - VSS \text{ destruction efficiency } (\%)} \times \frac{1}{SRT} \quad (2.2)$$

The biosolids production rate was calculated using Equation 2.3, where $COD_{removed}$ is the mass of COD removed each day (g/d).

$$Biosolids \text{ production rate } \left(\frac{gVSS}{gCOD_{removed}} \right) = \frac{VSS_{wasted}}{COD_{removed}} \quad (2.3)$$

Calculated VSS destruction efficiency, hydrolysis rate constant, and biosolids production rate are summarized in Table 8.

Table 8: SAF-MBR VSS Loading and Destruction Efficiency, Hydrolysis Rate Constant, and Biosolids Production Rate by Operational Period

Operational Period		VSS				Biosolids Production Rate (gVSS/gCOD _{removed})
		VSS _{in} (g/d)	VSS _{wasted} (g/d)	Destruction (%)	k _{hyd} (1/d)	
Startup (a) Days 1–40	mean	1619	194	88	0.086	0.027
	±	119	42	3	0.024	0.006
	n	4	4	4	4	4
Startup (b) Days 41–54	mean	2127	281	N.A.	N.A.	0.027
	±	289	N.A.	N.A.	N.A.	N.A.
	n	2	1	N.A.	N.A.	1
I Days 55–110	mean	3323	537	84	0.124	0.027
	±	808	160	4	0.039	0.005
	n	5	5	5	5	5
II Days 111–152	mean	6095	704	89	0.362	0.019
	±	2284	130	4	0.201	0.007
	n	6	6	6	6	5
III Days 153–243	mean	10426	1100	89	0.404	0.023
	±	2168	262	2	0.104	0.005
	n	10	10	10	10	10

Source: Codiga Resource Recovery Center at Stanford

The system achieved high VSS destruction efficiencies, 84 percent ~ 89 percent. In particular, the superior VSS destruction efficiency of 89 percent in Periods II and III indicates that the SAF-MBR enabled ~ 90 percent degradation of introduced VSS into the system. Hydrolysis rate constants (k_{hyd}) were relatively low during the startup periods, 0.086 d⁻¹, likely due to insufficient biological activity. During steady state operation (Periods I to III), hydrolysis rate constants (k_{hyd}) gradually increased from 0.124 to 0.404 d⁻¹, enabling rapid VSS destruction, even at short SRT (21.7 d) in Period III.

Biosolids production rates decreased from 0.027 to 0.023 gVSS/gCOD_{removed} as hydrolysis improved. The specific biosolids production in Period III, 0.023 gVSS/gCOD_{removed}, is much lower than the specific secondary sludge production from a conventional aerobic wastewater treatment process, typically about 0.218 gVSS/gCOD_{removed} (under 3-days SRT, Rittmann and McCarty, 2020). Thus, the SAF-MBR enables an 89 percent reduction in secondary sludge production compared to conventional aerobic systems.

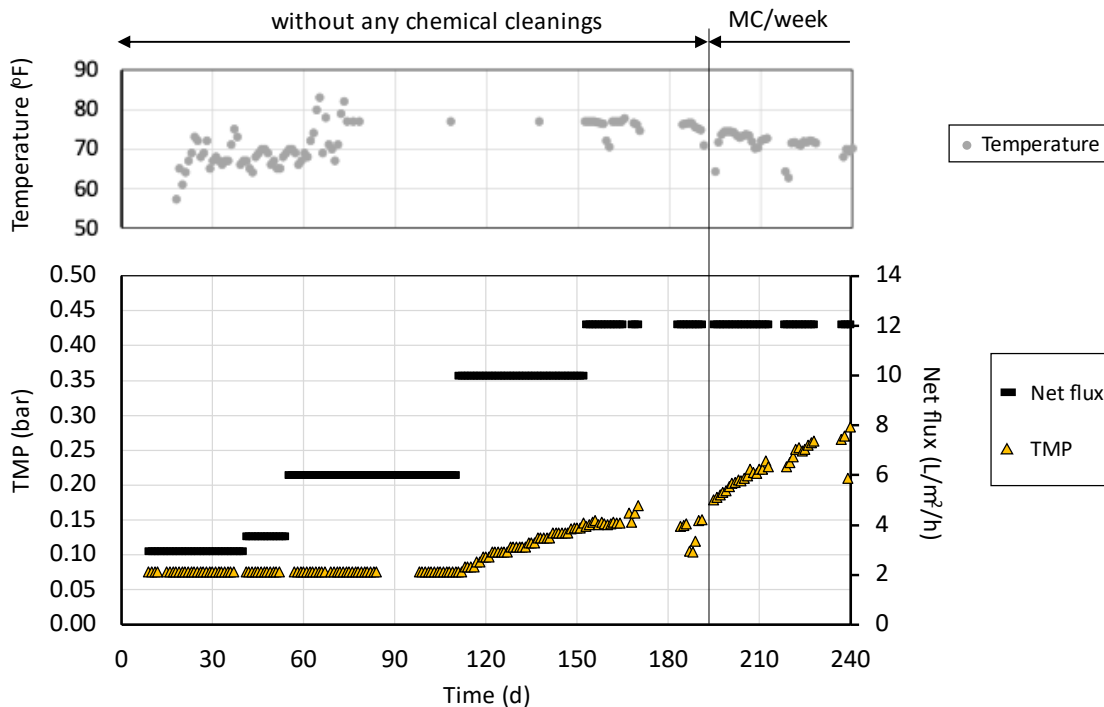
2.3.1.8 Membrane Fouling Control

The SAF-MBR system was operated for ~ 190 days without any chemical membrane cleaning or backwashing. A periodic membrane operation cycle (8 minutes of production followed by 2 minutes of membrane relaxation) and continuous gas sparging of 0.09 Nm³/m²/h (normal

meter cubed per hour), the recommended minimum gas sparing intensity from Suez, were sufficient strategies to control membrane fouling.

Trans-membrane pressure (TMP), the vacuum required to suck water through the membranes, was monitored as an indicator of membrane fouling. The evolution of TMP with operating conditions and time is shown in Figure 9. At a net flux of 6 L/m²/h, TMP remained steady, indicating no membrane fouling. At a net flux of 10 L/m²/h, TMP gradually increased from 0.08 to 0.15 bar without any spike or TMP jump, indicating there was no meaningful membrane fouling. When flux was further increased to 12 L/m²/h, there was no substantial change in TMP. TMP remained close to ~ 0.15 bar until day ~ 190.

Figure 9: Net Flux and TMP



Source: Codiga Resource Recovery Center at Stanford

When the water temperature decreased, beginning around day 190, weekly chemical maintenance cleanings (MC) were initiated to mitigate increased fouling. MC consisted of two sequences of chemically enhanced backwashing (CEB). The first sequence used a 500 mg/L sodium hypochlorite solution; the second sequence used a 2,000 mg/L citric acid solution. Each MC sequence began with a 2-minute initial CEB pulse followed by four 30-second CEB pulses at a flux of 20 L/m²/h, each separated by a membrane relaxation period of 4.5 minutes. It should be noted that the 4 CEB pulses each lasting 30 seconds were only half of the number of 30-second CEB pulses recommended by Suez (8 pulses), but this regime was adequate to control membrane fouling for the SAF-MBR while reducing chemical use by 33 percent compared to typical manufacturer recommendations (Shin et al., 2021a).

Even with the weekly practiced MC, the TMP value continued to increase due to further decrease in water temperature and accumulation of foulants from the long-term operation

(~ 240 days). Under these conditions, a recovery cleaning (RC) is warranted. A RC is conducted when the TMP reaches an upper limit set point (0.3 bar). During RC, the membrane tank is filled with a 1,100 mg/L sodium hypochlorite solution, and the membranes are soaked in this solution for 24 hours to eliminate organic foulant deposits. The tank is then flushed and filled with a citric acid solution of 2,200 mg/L, and the membranes are soaked for another 24 hours to remove inorganic foulants.

It should be noted here that the stable membrane operation of the SAF-MBR at high flux (10 and 12 L/m²/h) is exceptional compared to previous AnMBR studies. Conventional AnMBR tests have relied on a continuously stirred tank reactor (CSTR-AnMBR), a configuration in which anaerobic microbes are dispersed and mixed within the bulk fluid (MLSS) of the reactor. CSTR-AnMBRs rely on the membranes to retain the microbes within the system, in contrast to the SAF-MBR, which uses a GAC biocarrier to retain the microbes.

The SAF-MBR can achieve high relative performance because it retains biomass on the GAC biocarrier, enabling a low MLSS concentration (< 3,000 mg/L) that minimizes membrane fouling. By contrast, the CSTR-AnMBR in the recent study had to operate at much greater MLSS concentrations (~10,000 mg/L) to provide a sufficiently long SRT for retention of anaerobic microorganisms.

A recent study of a CSTR-AnMBR (Evans et al., 2018) that incorporated membranes identical to those in the SAF-MBR suffered major membrane fouling issues that constrained operations to < 10 L/m²/h net flux, even when applying much greater gas sparging intensity (0.3 ~ 0.5 Nm³/m²/h versus 0.09 Nm³/m²/h) and more intensive chemical cleanings (two maintenance cleanings per week, with twice the CEB pulses, and quarterly recovery cleaning). These more intensive chemical cleanings require a higher chemical cost of \$9.6×10⁻³/m³, which is three times greater than what the SAF-MBR achieved in this project.

2.3.2 Energy Performance

2.3.2.1 Energy Requirements

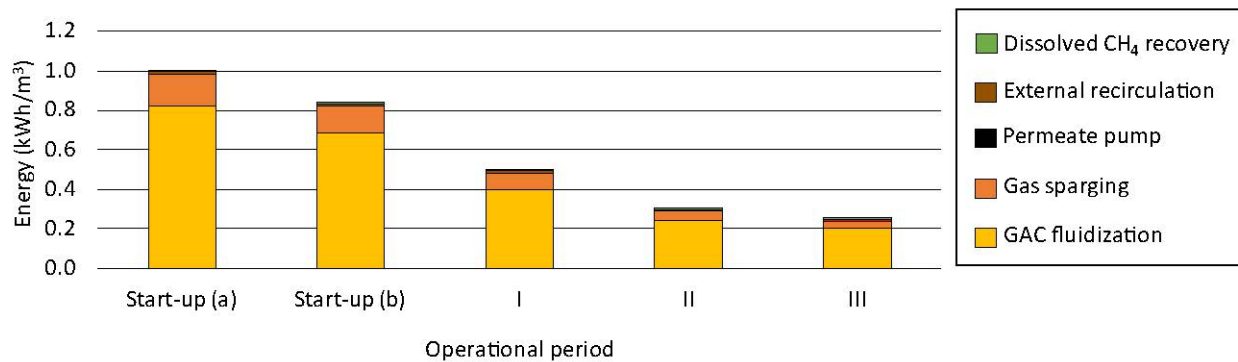
In conventional aerobic systems, 0.4-0.65 kWh of electricity is consumed for every cubic meter of wastewater treated (1,500-2,500 kWh/MG) (Scherson and Criddle, 2014). Aeration accounts for approximately 50 percent of the energy costs, and it results in the generation of large quantities of biosolids for disposal (Scherson and Criddle, 2014). Management of these biosolids is costly, and their transport is energy intensive. The SAF-MBR eliminates aeration, offering substantial energy savings potential, but the system does have energy-consuming equipment.

The key power-consuming processes of the SAF-MBR include: (1) pumping water to fluidize the GAC, (2) recirculating biogas to sparge membranes and control fouling, (3) pumping permeate through the membranes, and (4) pumping water to recycle water between the biological reactor and the membrane tank. Of these, pumping water for GAC fluidization and recirculating biogas for membrane sparging are the major energy-consuming components (Shin et al., 2021a). Both processes are continuous, requiring a constant power input. The system energy requirement is calculated as the power required divided by the wastewater flow rate and thus varies with HRT. Power required for pumping and gas blowing were calculated

using measured flow rates and pressure loss and assuming a pump and blower efficiency of 65 percent (Lim et al., 2019), as illustrated in Shin et al., 2021a. Because SAF-MBR effluent includes dissolved CH₄ that should be recovered before discharge to a water body or a post-treatment process, energy required for the dissolved CH₄ recovery process needs to be considered. As a generic assumption, we considered a conventional air stripping tower used to recover dissolved CH₄ in SAF-MBR effluent, enabling high dissolved CH₄ recovery of 98 percent and a low energy requirement of < 0.002 kWh/m³ (Galdi and Luthy, 2021).

Energy requirements for the SAF-MBR are summarized by operational period in Figure 10.

Figure 10: Energy Requirement for SAF-MBR Operation by Operational Period, Including Energy Requirement for Dissolved CH₄ Recovery



Source: Codiga Resource Recovery Center at Stanford

GAC fluidization and gas sparging were the major energy-consuming components, while the energy required for permeate pump, external recirculation, and dissolved CH₄ recovery was relatively small. The energy required was high during the startup periods when the system was operated at long HRT. The energy requirement decreased from Period I to Period III because energy consumption remained essentially constant while flow rate increased. The best energy requirement performance to date, 0.25 kWh/m³ (950 kWh/MG) was achieved at the shortest HRT (5.2 h in Period III).

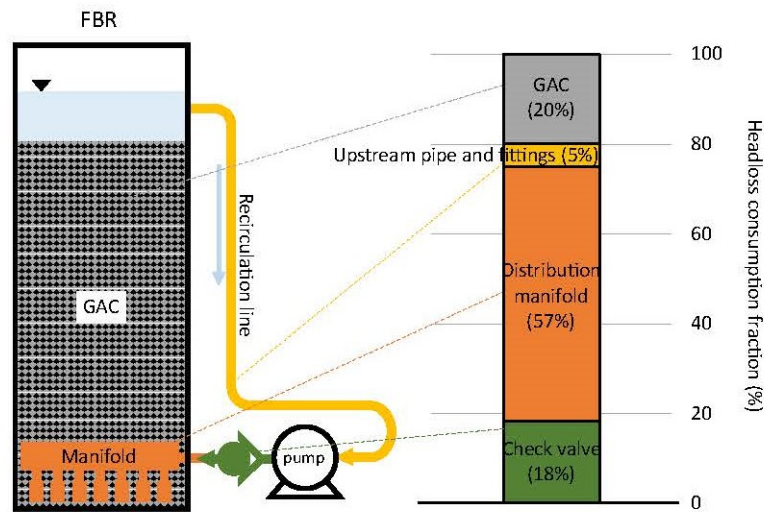
The single largest driver of system energy consumption is GAC fluidization, consuming about 0.20 kWh/m³ (760 kWh/MG) or 80 percent of the total system energy requirement. This high energy consumption contrasts with previous pilot-scale SAF-MBR studies that reported ~ 0.02 kWh/m³ (76 kWh/MG) (Shin et al., 2014; Evans et al., 2018) or ~ 0.08 kWh/m³ (300 kWh/MG) (Shin et al., 2021a) to fluidize GAC in anaerobic fluidized bed reactors (FBRs).

One reason for the higher energy demand for GAC fluidization is the higher GAC packing ratio in this study (65 percent) compared to previous studies that had a lower GAC packing ratio (25 percent in the FBR, Shin et al., 2014; Evans et al., 2018). The greater depth of GAC provokes a larger hydraulic head loss (ΔH) during fluidization. Another explanation is scale of the FBR. Previous tests (Shin et al., 2014, Shin et al., 2021a) used pilot-scale FBRs with a volume of about 1 m³ (264 gallons), while this study used a full-scale FBR with a volume of 17.6 m³ (4,640 gallons). The pilot-scale systems employed water diffusers that were custom-designed, using computational fluid dynamics to minimize head losses while maintaining a uniform distribution of flow throughout the reactor cross section. For the demonstration scale,

we adopted a conventional, proven design for the recirculation system that deliberately induces head loss in the distribution nozzles to ensure uniform flow distribution. There is a potential that the distribution system could be further optimized to reduce energy requirements while maintaining a uniform distribution of flow.

In FBRs, a pump recirculates water through an external pipe to provide a consistent upflow velocity of about 0.5 m/min (meters per minute) or 12.3 gpm/sf (gallons per minute per square foot) inside the reactor and fluidizes the GAC, as illustrated in Figure 11. Because the water elevation head at the suction and the discharge of the pump are essentially identical, the major driver of pump head is friction losses through the recirculation piping and the GAC. The head loss provoked by different elements along the flow path, including upstream pipe and fittings, a check valve, the distribution manifold, and the GAC, was measured using pressure measurements along the line. A head loss analysis within the FBR is shown in Figure 11.

Figure 11: Breakdown of Head Loss in the FBR for GAC Fluidization



Source: Codiga Resource Recovery Center at Stanford

In the current FBR, the distribution manifold is the major component, inducing 57 percent of the total head loss. In pilot-scale FBRs, however, the distribution manifold induced only about 14 percent of the total head loss. Conventional FBR design norms stipulate that the head loss in the diffuser nozzles must be a minimum of 30 percent of the head loss in the GAC bed. The manifold used in the current design far exceeds this requirement, indicating that optimization of the header design is possible while remaining within established FBR design norms. Such an optimization could reduce energy consumption of the FBR by up to 50 percent, or about 0.1 kWh/m³ (380 kWh/MG).

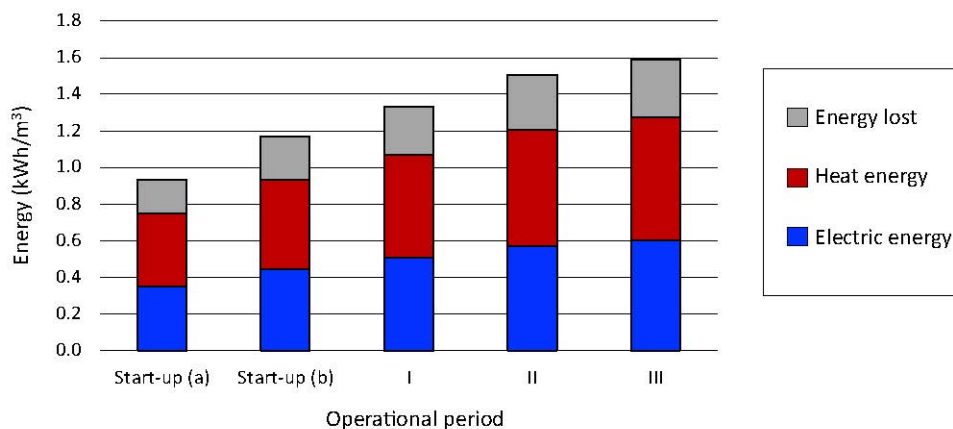
2.3.2.2 Energy Production

As an anaerobic system, the SAF-MBR converts biodegradable organic matter into methane that can be used to generate energy. We assume energy recovery from methane (0.222 kWh/mole CH₄) via combined heat and power (CHP) with a combined energy recovery efficiency of 80 percent (EPA), consisting of recovery of 38 percent as electric energy (Lang et al., 2017)

and 42 percent as heat energy. Energy production potentials were calculated with estimated CH₄ production (based on Figures 6 and 7) for all operational periods and with measured CH₄ data (based on Figure 8). For energy production potential from dissolved CH₄, the mean dissolved CH₄ recovery efficiency of 98 percent (Galdi and Luthy, 2021) was considered.

Figure 12 summarizes calculated energy production potentials based on estimated CH₄ production in all operational periods.

Figure 12: Electricity (Blue) and Heat (Red) Energy Production Potential With Unrecovered Energy (Gray) From CHP Based on Estimated CH₄ Production by Operational Period



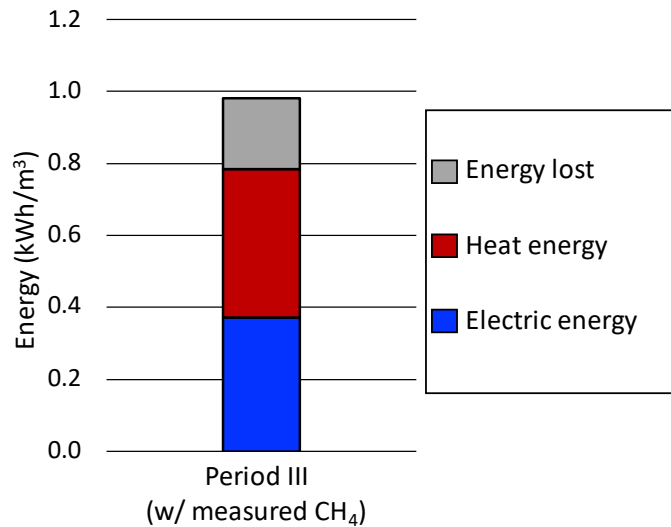
Source: Codiga Resource Recovery Center at Stanford

In all periods, including startup, electric energy production potential was greater than 0.35 kWh/m³ (1,320 kWh/MG), and the heat energy production potential was greater than 0.39 kWh/m³ (1,470 kWh/MG). Energy production potentials gradually increased from startup through Period II, as the microbial community activity matured. The energy production potential further increased in Period III because of the higher influent COD of the filtered primary influent. The energy production potential in Period III was 0.60 kWh/m³ (2,270 kWh/MG) of electrical energy and 0.67 kWh/m³ (2,530 kWh/MG) of heat. It is important to note that the calculated values for electricity potential represent a relatively conservative estimate.

Alternative technologies, such as fuel cells, have higher electrical conversion efficiencies than CHP and could further improve the electrical energy production of a typical wastewater treatment plant. Depending on several factors, including cost, local demand for heat, and air emissions standards, different alternatives for energy recovery may be preferable.

Figure 13 summarizes calculated energy production potentials based on measured CH₄ data in Period III.

Figure 13: Electricity (Blue) and Heat (Red) Energy Production Potential with Unrecovered Energy (Gray) from CHP Based on Measured CH₄ Production in Period III



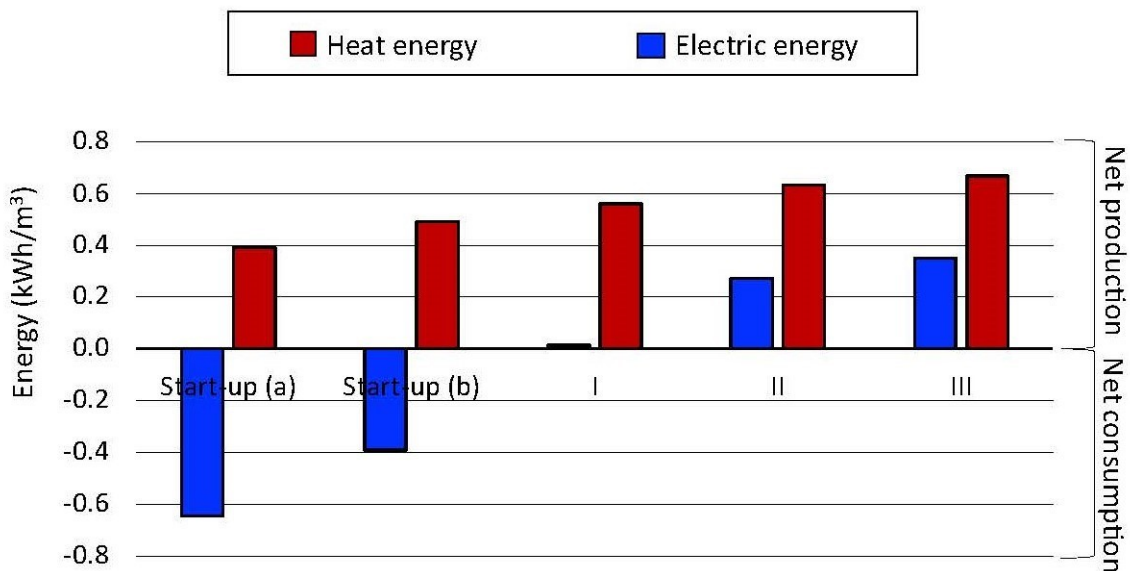
Source: Codiga Resource Recovery Center at Stanford

The energy production potential based on measured CH₄ data in Period III was 0.37 kWh/m³ (1,400 kWh/MG) of electrical energy and 0.41 kWh/m³ (1,550 kWh/MG) of heat, which is only 62 percent of the energy production potential, assuming estimated CH₄ production. Measured CH₄ is an underestimate, as discussed in previous sections.

2.3.2.3 Energy Balance

An energy balance of the SAF-MBR, consolidating both power consumption and energy production (relying on simulated CH₄ production), is shown in Figure 14.

Figure 14: Energy Balance of the SAF-MBR by Operational Period



Source: Codiga Resource Recovery Center at Stanford

During the startup periods, the system had a high volumetric energy requirement due to the low flow rates, and low energy production potential due to immature biological activity. As reactor flow rate and biological activity increased, system volumetric energy consumption declined while energy production potential increased. In Periods II and III, the SAF-MBR system enabled net energy positive operations. In Period III, the system had a net power production potential of 0.35 kWh/m³ (1,320 kWh/MG). Although the electrical generation potential based on measured gaseous CH₄ production was lower at 0.37 kWh/m³ (1,400 kWh/MG), this lower electricity generation potential still enabled an energy surplus of 0.12 kWh/m³ (455 kWh/MG). We know of no other secondary wastewater treatment process that is capable of such a performance.

The net power production potential of the SAF-MBR, summarized in Figure 14, can enable the entire wastewater treatment plant to be a net energy exporter. An energy balance of a potential future wastewater treatment plant, including typical energy consumption values for additional treatment processes and energy production from digestion of primary solids, is shown in Table 9. Using a SAF-MBR for secondary treatment, a wastewater treatment plant could shift from being a substantial energy consumer to producing a net surplus of about 0.39 kWh/m³ (1,470 kWh/MG).

Table 9: Energy Balance of Potential Future Wastewater Treatment Plant

Energy Consumption	kWh/m³	kWh/MG
Influent Pumps ^a	-0.04	-150
Preliminary Treatment ^a	-0.07	-270
Grit Removal ^a	-0.007	-30
Microscreen ^a	-0.02	-80
SAF-MBR	-0.25	-950
Total Consumption	-0.387	-1480

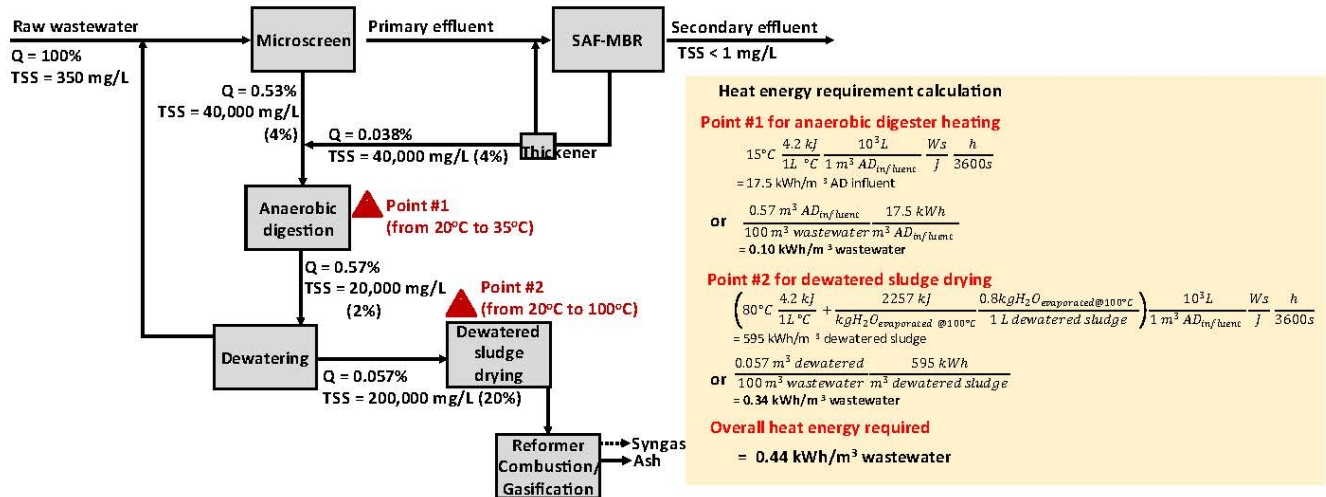
Energy Production	kWh/m³	kWh/MG
Digestion of Primary Solids ^b	0.18	680
SAF-MBR	0.60	2,270
Total Production	0.78	2,950
Net Energy Production	0.393	1,470

^a Longo et al., 2017; ^b McCarty et al., 2011
Source: Codigra Resource Recovery Center at Stanford

In addition to power, the heat production potential from the SAF-MBR could enable improved biosolids management. The waste heat from CHP can be used to treat primary sludge and the solids from the SAF-MBR, minimizing solids waste disposal and enabling further energy recovery. Primary and SAF-MBR solids can first be digested anaerobically. Dewatered digested sludge can be dried and further treated in a reformer consisting of solids combustion and gasification to produce ash and syngas (Scherson and Criddle, 2014). Heat energy is required

for anaerobic digester heating, specifically to heat solids from 20°C to 35°C (68°F to 95°F) and to dry the dewatered sludge, as illustrated in Figure 15.

Figure 15: A Flow Diagram for Solids Waste Management and Calculation of Heat Energy Requirement (kWh/m³)



Source: Codiga Resource Recovery Center at Stanford

The estimated overall heat energy demand for the solids management process is 0.44 kWh/m³ (5,675,000 btu/MG). The heat energy recoverable from the SAF-MBR in Period III is 0.67 kWh/m³ (8,642,000 btu/MG). With consideration of a heat exchanger efficiency of 72 percent (Errico et al., 2018), the available heat is 0.48 kWh/m³ (6,191,000 btu/MG), which is sufficient to supply the overall heat energy required for solids waste management.

2.3.3 Costs

2.3.3.1 Operating Costs

Compared to conventional aerobic-based systems, the SAF-MBR would reduce operating expenses by eliminating electrical energy costs and by reducing production of biosolids that need to be managed and disposed. A comparison of operating costs between a conventional aerobic secondary treatment process and the SAF-MBR is shown in Table 10.

Electricity is a major operating expense for wastewater treatment plants. A typical net energy consumption (= production – consumption) in a conventional domestic wastewater is 0.3 kWh/m³ (1,140 kWh/MG, costwater.com), comprising a 27 percent fraction of overall operating costs. In the case of SAF-MBR, however, the plant would not require any imported energy, implying that the plant can save at least a 27 percent fraction of operating expenses.

The solids produced from secondary treatment are a major constituent of wastewater biosolids, constituting about two-thirds of total sludge production (McCarty et al., 2011). Transport and disposal of biosolids typically constitute 13 McCarty of plant operating expenses (costwater.com). The SAF-MBR would reduce production of secondary solids by almost 90 percent, thereby reducing typical plant operating expenses by about 10 percent.

The chemical membrane cleanings represent a new cost. Based on the practiced weekly MC from the 190th operational day and the predicted RC requirements, the operational expenses for chemical cleanings can be calculated. We assume operation of the SAF-MBR at a net flux of 12 L/m²/h with weekly MC frequency (MC/week) and annual RC. As-purchased unit prices for chemicals in this project are \$279/m³ of 14-percent sodium hypochlorite solution and \$835/m³ of a 50-percent citric acid solution. Corresponding operational expenses are $2.8 \times 10^{-3}/\text{m}^3$ (\$10/MG) of treated wastewater for MC and $2.7 \times 10^{-4}/\text{m}^3$ (\$1/MG) of treated wastewater for RC. It should be noted that RC costs in this test are lower than reported in previous SAF-MBR studies ($1.5 \times 10^{-3}/\text{m}^3$, Shin et al., 2021a). This project employed a more efficient membrane packing ratio, fitting more membranes in a tighter tank volume. Because RC requires a specific chemical concentration in the membrane tank, independent of the number of membrane modules, a membrane tank with a greater membrane packing density would require less chemicals and a lower cost per unit of treated wastewater. The membrane tank in this project had a liquid volume of 1.5 m³ for 9 membrane modules (308.7 m² of membrane surface area), yielding a membrane packing density of 205.8 m² (membrane surface area)/m³ (reactor volume).

Table 10: Operating Costs of Wastewater Treatment Plant, Depending Upon Conventional Aerobic Process and SAF-MBR

Operating cost	Conventional aerobic secondary treatment ^a	SAF-MBR (this study at SVCW)	SAF-MBR at colder regions
Energy usage	$3.0 \times 10^{-2}/\text{m}^3$ (\$113/MG)	$0.0/\text{m}^3$ (\$0/MG)	$0.0/\text{m}^3$ (\$0/MG)
Secondary biosolids transport and disposal	$9.5 \times 10^{-3}/\text{m}^3$ (\$35/MG)	$9.5 \times 10^{-4}/\text{m}^3$ (\$4/MG)	$9.5 \times 10^{-4}/\text{m}^3$ (\$4/MG)
Chemical membrane cleaning	$0.0/\text{m}^3$ (\$0/MG)	$3.1 \times 10^{-3}/\text{m}^3$ (\$11/MG)	$6.7 \times 10^{-3}/\text{m}^3$ ^c (\$26/MG)
Other ^b (such as water discharge fee and staff cost)	$7.1 \times 10^{-2}/\text{m}^3$ (\$268/MG)	$7.1 \times 10^{-2}/\text{m}^3$ (\$268/MG)	$7.1 \times 10^{-2}/\text{m}^3$ (\$268/MG)
Total	$1.1 \times 10^{-1}/\text{m}^3$ (\$416/MG)	$7.5 \times 10^{-2}/\text{m}^3$ (\$283/MG)	$7.9 \times 10^{-2}/\text{m}^3$ (\$298/MG)

^a costwater.com; ^b assumed to be the same for all cases; ^c with the maximum chemical cleaning frequencies recommended by Suez (2MC/week and 4 RC/year)

Source: Codiga Resource Recovery Center at Stanford

The operating costs due to chemical membrane cleaning, $3.1 \times 10^{-3}/\text{m}^3$ (\$11/MG) are much smaller than cost savings achievable using the SAF-MBR, relative to conventional aerobic treatment, specifically $3.0 \times 10^{-2}/\text{m}^3$ (\$113/MG) for the use of electricity and $8.6 \times 10^{-3}/\text{m}^3$ (\$31/MG) for 90-percent reduced secondary biosolids transport and disposal (costwater.com). The net operating cost reduction would be about $0.035/\text{m}^3$ (\$133/MG). Assuming a typical unit cost for conventional aerobic wastewater treatment of $0.11/\text{m}^3$ (costwater.com), the resulting operating cost of a SAF-MBR-based treatment plant would be $0.075/\text{m}^3$, for overall cost savings of about 32 percent in a climate like Redwood City.

The fouling rate of the SAF-MBR membranes can vary considerably, depending on water temperature, with lower rates in warmer regions such as Southern California and higher rates in winter in locations such as New York or Michigan. Further tests in these geographies would be necessary to verify that chemical cleaning would be able to mitigate any additional fouling in cold climates without increasing the gas sparging rate. Assuming the maximum chemical cleaning frequencies recommended by Suez, 2 MC/week and 4 RC/year, the cost of chemical cleanings would reach $\$6.7 \times 10^{-3}/\text{m}^3$ ($\$26/\text{MG}$). The cost savings associated with energy savings and reduced biosolids hauling would still far offset the increased chemical costs.

2.3.3.2 Capital Costs

The SAF-MBR can achieve capital cost savings relative to conventional aerobic systems for several reasons. First, the SAF-MBR is capable of managing a higher organic loading rate, OLR, of up to $2.6 \text{ kgCOD}/\text{m}^3/\text{d}$ (21,800 lbs/MG/day) compared to less than $1.5 \text{ kgCOD}/\text{m}^3/\text{d}$ (12,500 lbs/MG/day) for aerobic processes. A higher OLR capability means that a SAF-MBR can process more wastewater in a smaller reactor volume, yielding savings in reactor construction costs. Second, because the SAF-MBR produces 90 percent less secondary biosolids waste than conventional aerobic systems, resulting in a two-thirds overall reduction in biosolids production, the size of solids dewatering and disposal facilities can be correspondingly reduced. Third, the SAF-MBR relies on membranes to separate solids from the wastewater, enabling much smaller reactor footprints compared to the secondary clarifiers and dual media filtration systems of conventional aerobic systems.

The SAF-MBR does, however, incur new capital costs in the form of membranes and associated equipment, GAC, and additional biogas management infrastructure.

A set of cost assumptions, quantities, and general capital cost estimates for a full-scale SAF-MBR treating 12 MGD ($45,360 \text{ m}^3/\text{d}$) is shown in Table 11. Cost estimates exclude land costs.

Table 11: Capital Costs and Assumptions for a SAF-MBR Processing 12 MGD ($45,360 \text{ m}^3$)

Component	Life (years)	Unit cost	Quantity	Cost	Reference for unit costs
Reactor tanks	30	$\$280/\text{m}^3$	8,400	$\$2,350,000$	Lin et al., 2011
Membranes	10	$\$25/\text{m}^2$	157,500	$\$11,810,000$	Suez ZeeWeed 500 (2022 ver)
Water pumps	15	$\$60/(\text{m}^3/\text{h})$	48,900	$\$5,860,000$	Lin et al., 2011
Gas sparging diffuser	10	$\$2.3/(\text{L}/\text{min})$	229,800	$\$1,610,000$	Lin et al., 2011
GAC	30	$\$2/\text{kg}$	1,726,800	$\$3,450,000$	USEPA, 2000
Total:				$\$25,080,000$	

Source: Codiga Resource Recovery Center at Stanford

Industry experts employ an estimate of current new construction costs for a treatment plant with conventional activated sludge that ranges from $\$1,300$ to $\$2,600$ per m^3/d of treatment

capacity (\$5 to \$10/gallon per day), or \$60M to \$120M, for a new plant processing 12 MGD. Estimates of how individual unit processes contribute to total plant capital costs were derived from U.S. Environmental Protection Agency (USEPA) cost-estimating literature (USEPA, 1980). Assuming a mid-range total conventional aerobic plant cost of \$90M, cost estimates for individual unit processes for both water treatment and solids management are shown in Table 12.

Table 12: Unit Process Capital Costs for a Conventional Aerobic WWTP Processing 12 MGD (45,360 m³), Assuming a Total Plant Cost of \$90M

Water Treatment	% of Plant Cost	Unit Process Cost
Activated Sludge System	24%	\$21,920,000
Filtration	13%	\$11,290,000
Subtotal		\$33,210,000

Solids Management		
Solids Thickening	3%	\$2,580,000
Solids Anaerobic Digestion	19%	\$17,330,000
Subtotal		\$19,910,000

Source: Codiga Resource Recovery Center at Stanford

Although capital costs for an aerobic activated sludge system alone are likely to be lower than those for an SAF-MBR, the activated sludge system requires downstream filtration to achieve US secondary effluent standards for solids removal. The capital costs for wastewater treatment of a SAF-MBR are likely cost competitive with those of an activated sludge system, once filtration costs are accounted for.

Apart from the water treatment costs, an SAF-MBR would reasonably reduce the required size of solids management infrastructure, including solids thickening and digestion, by about one-third, yielding a capital cost savings in this analysis of about \$6M in solids management infrastructure.

2.4 Secondary Treatment Discussion

2.4.1 SAF-MBR Compared to Other AnMBR Configurations

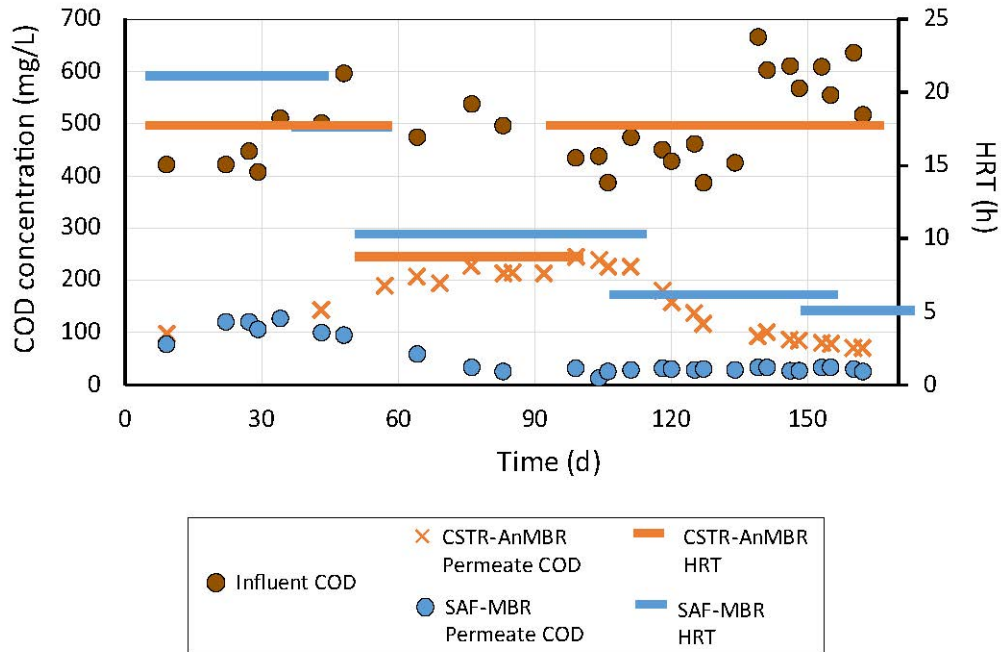
The SAF-MBR relies on a GAC biocarrier to retain anaerobic microbes in the biological reactor, decoupling the retention of microbes from the retention of dispersed solids (the solids retention time, SRT). To date, the most widely adopted AnMBR configuration, however, is the CSTR-AnMBR that disperses the anaerobic microbes within the bulk fluid of the reactor and relies on the membranes to retain the microbes, along with all other wastewater solids. Thus, whereas microbial retention and SRT are decoupled in the SAF-MBR, they are identical in the CSTR-AnMBR.

To compare the performance of a CSTR-AnMBR to the SAF-MBR, we started up and operated a pilot-scale CSTR-AnMBR (system volume = 5.5 m³ (1,450 gallons)) in parallel with the

SAF-MBR. The CSTR-AnMBR treated the same influent to the SAF-MBR under identical temperature conditions.

Influent COD and permeate COD concentrations from the CSTR-AnMBR and SAF-MBR during ~ 160 days of operation are shown in Figure 16, along with hydraulic loading rates (HRT) for each reactor.

Figure 16: Influent and Permeate COD Concentrations From CSTR-AnMBR and SAF-MBR



Source: Codiga Resource Recovery Center at Stanford

For the first 50 days of operation, the two reactors yielded similarly high permeate COD concentrations of around 100 mg/L, largely due to acetate concentration. Beginning around 70 days of operation, the SAF-MBR permeate COD concentration fell to around 30 mg/L, even as the loading rate of the system was increased and HRT was reduced. This rapid improvement indicated that the SAF-MBR startup was substantially complete in roughly 60 days. The CSTR-AnMBR permeate COD concentration, on the other hand, increased as the loading rate increased, indicating that system startup was not complete, and possibly also that the reduced HRT and associated reduction in SRT prevented adequate growth of anaerobic biomass and impaired treatment performance. Permeate quality in the CSTR-AnMBR began to improve only after hydraulic loading was reduced to increase the HRT and SRT. Even so, after 160 days of operation, permeate concentrations were about 90 mg/L at an HRT of 18 h and an SRT of 75 days. This comparison clearly demonstrates that the GAC biocarrier enables the SAF-MBR to complete startup much more rapidly than the CSTR-AnMBR.

The required SRT for CSTR-AnMBRs can be estimated with Equation 2.4.

$$SRT = \frac{SF}{(\hat{\mu} - b)} \quad (2.4)$$

where $\hat{\mu}$ is the maximum specific growth rate constant (1/d), b is the decay rate constant (1/d), and SF is a safety factor. $\hat{\mu}$ and b are temperature-dependent constants.

Because *Methanotrix* has the slowest growth rate within the community of microbes necessary to achieve anaerobic treatment, the SRT calculation needs to be based on the growth and decay rate of *Methanotrix* in an AnMBR $\hat{\mu} = 0.036$ 1/d and $b = 0.0023$ 1/d (Shin et al., 2021b), including an SF of 2.5.

Recommended SRT values for CSTR-AnMBRs to retain *Methanotrix* at various temperatures are summarized in Table 13.

Table 13: Required SRT to Retain *Methanotrix* at Various Temperatures

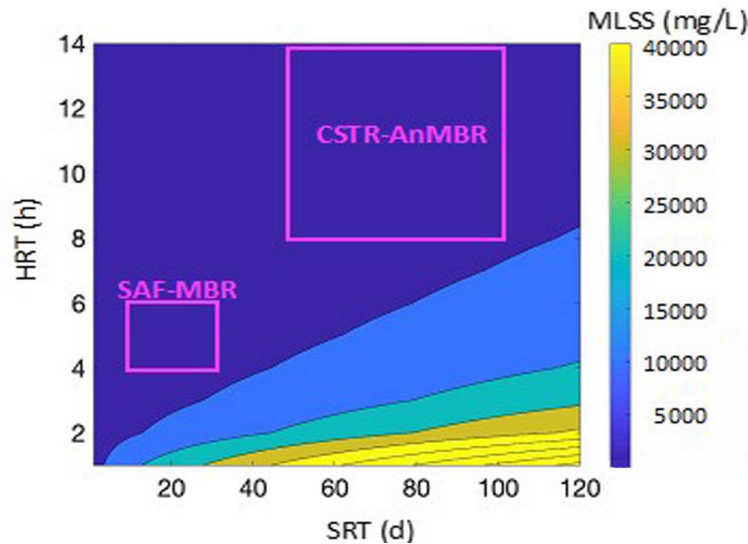
Temperature (°C)	SRT (d)
10	146
15	104
20	74
25	53
30	38

Source: Codiga Resource Recovery Center at Stanford

As shown in the table, CSTR-AnMBRs require long SRTs (53 ~ 104 days) at typical temperate climate water temperatures (15°C to 25°C) in the US (Evans et al., 2018). In the SAF-MBR, the GAC biocarrier retains the anaerobic organisms within the system regardless of bulk fluid SRT, freeing the SAF-MBR from this constraint. Thus, SAF-MBRs can operate at an SRT of about 20 days to achieve hydrolysis of particulate substrates.

The use of membranes in both system concentrates solids concentration (i.e., MLSS concentration) with a concentration factor of SRT/HRT. Thus, a longer SRT or a shorter HRT results in a greater MLSS concentration within the system. The membrane operations typically require MLSS concentrations lower than 10,000 mg/L to avoid unacceptably high membrane fouling rates. With the given SRT ranges of both systems and the threshold of the MLSS concentration, a color map with a simulation of MLSS concentration, depending upon SRT and HRT conditions, is shown in Figure 17.

Figure 17: Color Map of MLSS Concentration Depending on HRT and SRT



Source: Codiga Resource Recovery Center at Stanford

The CSTR-AnMBRs requiring long SRTs are limited to operate at minimum HRTs of 8 to 14h, which is similar or greater than the HRTs required in conventional aerobic secondary systems. By contrast, the SAF-MBR with a short SRT can operate at short HRTs, from 4 ~ 6 h. Thus, the SAF-MBR is the only anaerobic secondary treatment system to date that can provide the benefits of a reduced footprint compared to conventional systems.

2.4.2 Carbon Footprint Comparison: Conventional Aerobic WWTP Versus AnMBR

The SAF-MBR system has the potential to reduce the carbon footprint of wastewater treatment by reducing energy consumption and increasing production of renewable energy. The SAF-MBR also has the potential to reduce the carbon footprint by forgoing N₂O emissions from conventional aerobic systems (IPCC, 2019). The carbon footprint of the SAF-MBR, however, depends heavily on dissolved methane emissions through its effluent, fugitive emissions from the reactors via leaks, and the use of the chemicals having emission factors.

In a conventional wastewater treatment plant (WWTP), carbon footprints are largely driven by electricity use (0.3 kWh/m³) and N₂O emissions from the aeration tank. Aeration basins can emit 3.6×10⁻⁴ kgCO₂eq/kgN in a conventional activated sludge system, even without biological nitrogen removal (IPCC 2019). The mean influent total nitrogen concentration was 71 mgN/L, corresponding to a nitrous oxide production of about 8.0×10⁻⁵ kgN₂O/m³ or 0.024 kgCO₂eq/m³ of treated wastewater. The assumed carbon footprints associated with each end use are summarized in Table 14.

In the case of future WWTPs incorporating the SAF-MBR system, there is no carbon footprint associated with electricity use and N₂O emissions. Dissolved CH₄ in the SAF-MBR effluent was assumed to be treated with an air stripping tower that enables 98 percent dissolved CH₄ recovery. The mean dissolved CH₄ concentration in SAF-MBR was 20mgCH₄/L, and 2 percent of its concentration (0.4 mgCH₄/L) was included in the SAF-MBR carbon footprint calculation.

Calculations of the carbon footprint of chemicals used for membrane cleanings assume 1 MC/week and 1 RC/year, resulting in sodium hypochlorite use of 377 mgNaOCl/m³ (milligrams sodium hypochlorite per cubic meter) of treated wastewater and citric acid use of 1405 mgC₆H₈O₇/m³ of treated wastewater. The surplus electrical energy production from the SAF-MBR operation (Table 9) of 0.39 kWh/m³ (1,470 kWh/MG) can be exported to the grid and offset grid emissions (0.228 kgCO₂eq/kWh, per CEC [California Energy Commission], 2024). Fugitive emissions from leaks from the system are assumed to be zero. Although the demonstration-scale system was subject to gas leaks inherent to the smaller scale and temporary nature of the system, it is expected that a full-scale system would be completely sealed.

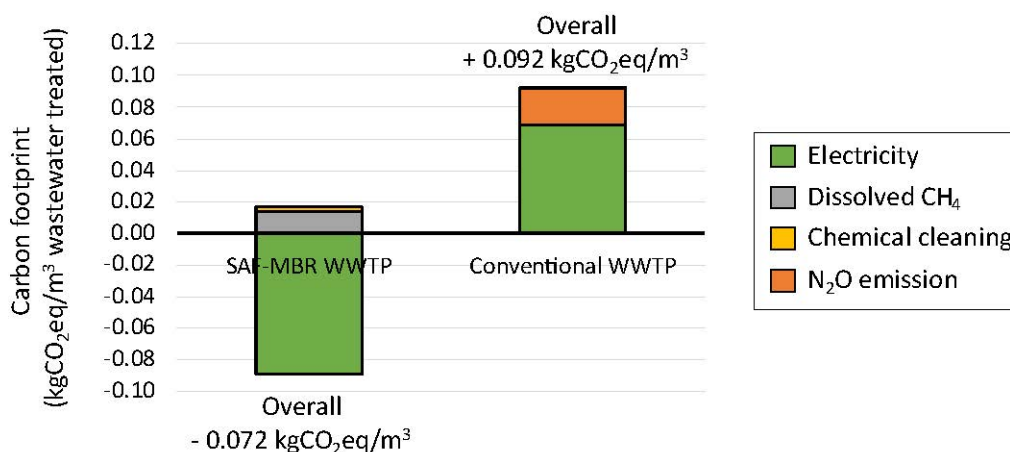
Table 14: Conversion Factor to Carbon Footprint (kgCO₂eq)

Content	Carbon Footprint	Unit
Electricity use	0.228	kgCO ₂ eq/kWh
Methane	34	kgCO ₂ eq/kgCH ₄
Nitrous Oxide	298	kgCO ₂ eq/kgN ₂ O
Sodium hypochlorite	6.13	kgCO ₂ eq/kgNaOCl
Citric acid	0.43	kgCO ₂ eq/kg C ₆ H ₈ O ₇

Source: Codiga Resource Recovery Center at Stanford

The carbon footprints of SAF-MBR-based WWTPs and conventional WWTPs are summarized in Figure 18.

Figure 18: Re Carbon Footprint (kgCO₂eq/m³) of an SAF-MBR-based WWTP and a Conventional WWTP



Source: Codiga Resource Recovery Center at Stanford

The SAF-MBR-based WWTP case has carbon footprints of 0.0138 kgCO₂eq/m³ for dissolved CH₄ and 0.0029 kgCO₂eq/m³ for chemical cleaning, for a total of 0.0167 kgCO₂eq/m³. This

carbon footprint is 82 percent smaller than that of the conventional WWTP case with 0.092 kgCO₂eq/m³ (0.068 kgCO₂eq/m³ for electricity use and 0.024 kgCO₂eq/m³ for N₂O emissions). Thus, the use of the SAF-MBR can save 82 percent of the carbon footprint in a conventional WWTP. The SAF-MBR, furthermore, produces surplus electricity that can prevent grid emissions, offsetting a carbon footprint of 0.089 kgCO₂eq/m³. The net carbon reduction potential of the SAF-MBR could enable WWTPs to eliminate 0.164 kgCO₂eq/m³ of current emissions.

The SAF-MBR does not remove nitrogen, which could limit the applicability of the SAF-MBR to plants with NPDES permits requiring nutrient removal. The ammonia in the SAF-MBR permeate, however, also presents an opportunity to recover valuable ammonia from wastewater and to further reduce the carbon footprint by preventing CO₂ emissions from ammonia synthesis due to the Haber-Bosch process (Shin et al., in preparation). Ammonia in the SAF-MBR permeate can be recovered by reverse osmosis (Shin et al., 2021c) while producing potable water (Szczuka et al., 2019). The ammonia concentrated in RO retentate can be recovered as ammonium sulfate through a conventional ammonia stripping system coupled with a sulfuric acid tank (Shin et al., 2021c).

CHAPTER 3:

Non-potable Reuse Process Performance

3.1 Non-potable Water Reuse Criteria and Challenges for Anaerobic Effluent

This section is a reformatted and lightly modified excerpt of a peer-reviewed publication (Szczyka et al., 2021) with open access licensed by Elsevier Ltd. under CC BY-NC-ND 4.0.

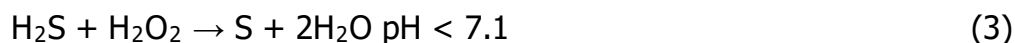
California's Title 22 Code of Regulations exemplifies standards for unrestricted non-potable applications. Key elements of Title 22 include use of an "oxidized" wastewater, filtration targeting < 0.2 nephelometric turbidity units (NTU), disinfection to achieve < 2.2 most probable number (MPN)/100 mL 7-day median total coliform concentrations, and maintenance of a chlorine or chloramine residual for distribution (CADPH, 2021). Non-potable reuse systems in the United States typically employ chloramines for disinfection (Furst et al., 2018). For systems treating oxidized, filtered wastewaters, Title 22 requires that processes provide a CT (product of total chlorine residual and contact time) value of 450 mg-min/L with a contact time of at least 90 minutes. Alternatively, systems must use spiking tests to demonstrate that the system can achieve 5-log inactivation of the virus surrogate, bacteriophage MS₂ (CADPH, 2021; Bae and Shin, 2016).

Showing that anaerobic membrane bioreactor effluent can be treated for unrestricted non-potable use is key for the adoption of anaerobic technologies. Anaerobic membrane bioreactors feature built-in membranes (Smith et al., 2012), thereby producing effluent that meets Title 22 filtration requirements. However, it is important to demonstrate that the disinfection system can achieve 5-log inactivation of spiked MS₂ bacteriophage and maintain a total chlorine residual for distribution. The high concentrations of sulfides and ammonia in anaerobic effluents render this difficult. Anaerobic biological sulfate reduction converts sulfate (SO₄²⁻) to sulfides (H₂S/ HS⁻) (Lens et al., 1998; Sarti et al., 2010). Sulfides are strong odorants, hindering public acceptance of non-potable reuse waters. Sulfides also rapidly quench both chlorine and chloramines, preventing the use of these disinfectants for pathogen inactivation and maintenance of a residual. Oxidation of sulfides requires four molar equivalents of total chlorine (Equation (1)) (Cadena and Peters, 1988). For an anaerobically-treated water containing 30 mg-S/L of sulfides (Lens et al., 1998), ~ 280 mg-Cl₂/L of total chlorine would be required. Even without sulfides, the high ammonia concentrations in anaerobic effluents (e.g., 50 mg-N/L [Szczyka et al., 2019]) react rapidly with free chlorine to form chloramines in situ (Equation (2)). Chloramines are less potent disinfectants than free chlorine (NRC, 2012; Furst et al., 2018), rendering it difficult to achieve pathogen inactivation goals. A 50 mg-N/L ammonia concentration would require impractically high free chlorine doses (> 400 mgCl₂/L) to exceed the breakpoint and achieve a free chlorine residual (Pressley et al., 1972). These

chlorine doses are far in excess of the ~ 10 mg-Cl₂/L typically employed to achieve the 450 mg-min/L CT value targeted by Title 22 (Furst et al., 2018).



Hydrogen peroxide (H₂O₂) is an alternative to chlorine for sulfide oxidation. Hydrogen peroxide has been used in conventional wastewater treatment to control sulfides, BOD₅, and foaming during and after aerobic biological wastewater treatment (Steiner and Gec, 1992; Ksibi, 2006). The products of sulfide oxidation are pH dependent (Equation (3) and Equation (4)) (Hoffman, 1977). Below the pK_a of hydrogen sulfide (pK_a = 7.1), elemental sulfur (S) formation is favored, while oxidation to sulfate is favored above the pK_a. Although lower H₂O₂ doses are required at pH < 7.1, filtration would be required to remove the particulate elemental sulfur. Even though sulfide oxidation to sulfate requires the same molar equivalents of H₂O₂ and chlorine, H₂O₂ is nearly half the cost of chlorine (Zhang et al., 2019; City of Oxnard, 2012). Chlorine addition after sulfide oxidation by H₂O₂ would form chloramines in situ. While this would provide a disinfectant residual, the ability to achieve sufficient MS₂ inactivation is unclear. UV disinfection offers an alternative route to MS₂ inactivation that should not be affected by interference from ammonia.



This study evaluated the feasibility of treating a sulfide-containing, filtered anaerobic effluent using a train based on: 1) H₂O₂ for sulfide oxidation, 2) UV disinfection to inactivate MS₂ bacteriophage, and 3) chlorine addition to provide a chloramine residual for distribution. In this study, we dosed H₂O₂ to pilot-scale SAF-MBR effluent spiked with sulfides. We evaluated reaction kinetics and oxidation products (e.g., sulfate) in this matrix as a function of pH. Sulfides and their oxidation products absorb light at 254 nm, the emission wavelength of the low-pressure mercury lamps typically used for UV disinfection. This study further characterized the effects of sulfides and their oxidation products on inactivation of MS₂ coliphage during subsequent UV disinfection. Finally, this study evaluated the chlorine dose required to achieve a chloramine residual for distribution after H₂O₂ and UV treatment. These results were used to develop a preliminary cost comparison between the H₂O₂/UV/chlorine treatment scheme for anaerobic effluents and the conventional application of chloramine disinfection of aerobic effluents.

3.2 Methods

3.2.1 Materials

This section is a reformatted and lightly modified excerpt of a peer-reviewed publication (Szczyka et al., 2021) with open access licensed by Elsevier Ltd. under CC BY-NC-ND 4.0.

Stock solutions of 30 percent H₂O₂ and 5.6 percent–6.5 percent sodium hypochlorite (NaOCl) were diluted with deionized water and standardized spectrophotometrically at 254 nm ($\epsilon_{254 \text{ nm}} = 18.6 \text{ M}^{-1} \text{ cm}^{-1}$ (Morgan et al., 1988)) and 292 nm ($\epsilon_{292 \text{ nm}} = 365 \text{ M}^{-1} \text{ cm}^{-1}$

(Feng et al., 2007)), respectively. Sulfide stocks were prepared daily by dissolving sodium sulfide nonahydrate in deoxygenated deionized water. Sulfide stocks were standardized by reacting the stock solution with a standardized free chlorine stock and measuring the chlorine demand based on a 4:1 NaOCl:sulfide stoichiometry for sulfide oxidation to sulfate. Thiosulfate, sulfite, and sulfate stock solutions were prepared in deoxygenated deionized water. MS₂ coliphage (ATTC 15597-B1) was propagated using E. coli (ATCC 700891) as the host organism, purified using methods previously described (King et al., 2020; Szczuka et al., 2020), and stored at -112°F (-80°C) prior to use.

3.2.2 Water Sample and Buffer Preparation

This section is a reformatted and lightly modified excerpt of a peer-reviewed publication (Szczuka et al., 2021) with open access licensed by Elsevier Ltd. under CC BY-NC-ND 4.0.

Anaerobically treated secondary effluent samples were collected from a pilot-scale SAF-MBR system treating micro-screened sewage from the Stanford University campus. The pilot reactor and operation have been described previously (Shin et al., 2021a). The Stanford system was started up prior to startup of the SAF-MBR at SVCW, enabling this study to proceed in parallel with the startup at SVCW. A 20 L sample of secondary effluent was collected from the reactor, filtered through 0.7- μ m glass fiber filters (Whatman), and stored at 39°F (4°C) before use. At the time of use, concentrations of all sulfur species of interest were below detection. Alternatively, phosphate buffer was prepared in deionized water and deoxygenated by boiling and sparging with nitrogen gas.

3.2.3 Kinetics Experiments

This section is a reformatted and lightly modified excerpt of a peer-reviewed publication (Szczuka et al., 2021) with open access licensed by Elsevier Ltd. under CC BY-NC-ND 4.0.

Samples (250 mL) of SAF-MBR effluent were spiked with sulfides. Hydrochloric acid or sodium hydroxide was used to adjust sample pH; pH was measured using a pH probe (Fisher Accumet). Once the target pH was reached, the 250 mL samples were aliquoted into 25 mL vials and capped headspace-free. Control experiments indicated that sulfide concentrations in each vial were within ~5 percent of each other, and sulfide concentrations did not decrease over the ~2 h time frame of the kinetics experiments. To initiate the reaction, H₂O₂ was injected into samples using a syringe. At each timepoint, 25 mL vials were sacrificed for immediate absorbance and total sulfide analysis. The remainder of each 25 mL vial was treated with 5 millimolar (mM) ZnCl₂ to precipitate ZnS; for low pH samples, NaOH was added to promote ZnS precipitation. H₂O₂ and sulfate concentrations were measured by colorimetric methods immediately after ZnCl₂ treatment. Samples were then treated with 2 mg/L catalase (250 units/mg) to degrade residual H₂O₂ and were saved for sulfite and thiosulfate analysis by ion chromatography. Control experiments showed that ZnCl₂ did not affect H₂O₂, sulfate, sulfite, and thiosulfate concentrations, and that quenching of H₂O₂ by catalase did not affect the analysis of sulfate, sulfite, and thiosulfate by ion chromatography. Experiments were conducted in duplicate.

3.2.4 UV Experiments

This section is a reformatted and lightly modified excerpt of a peer-reviewed publication (Szczyka et al., 2021) with open access licensed by Elsevier Ltd. under CC BY-NC-ND 4.0.

SAF-MBR or phosphate-buffered deionized water samples were placed in 5-cm depth open-top cylindrical dishes and spiked with sulfides, sulfate, sulfite, or thiosulfate under different conditions. Hydrochloric acid or sodium hydroxide was used to adjust sample pH. MS₂ was spiked into the samples targeting an initial concentration of $\sim 10^6$ PFU/mL. Hydrogen peroxide (H₂O₂) was spiked into some samples. Quartz lids were placed on each jar, and the samples were placed on a stir plate and exposed to 254 nm of light under a semi-collimated beam apparatus consisting of three 15 W Philips low pressure mercury lamps shining down onto the jars through a shutter. The SAF-MBR effluent samples had been filtered after collection to control turbidity. The incident UV fluence (mJ cm^{-2}) associated with specific illumination times was measured using iodide-iodate actinometry (Rahn et al., 2003). One objective of the study was to evaluate the extent to which sulfides and their oxidation products absorb UV light, thereby requiring higher incident UV fluence (and thus higher costs) to achieve the same level of disinfection. Therefore, we report the incident UV fluence rather than correcting the incident fluence for solution absorbance (i.e., the average UV fluence experienced by the solution). For perspective, the UV absorbance at 254 nm (UV₂₅₄) for the anaerobic effluent was 0.044 cm^{-1} (UV transmittance (UVT) = 90.4 percent) in the absence of sulfides. For a 5 cm depth of solution, the average UV fluence within the solution would be ~ 80 percent of the incident UV fluence (Jin et al., 2006). At desired intervals, subsamples for MS₂ analysis were taken from the jars, stored on ice, and plated within two hours of collection. Control experiments showed that (1) sulfide concentrations at the end of experiments remained within ~ 5 percent of the initial concentrations in dark controls in the absence of H₂O₂, and (2) MS₂ concentrations were not affected by H₂O₂, sulfides, thiosulfate, sulfite, or sulfate in dark controls. Experiments were conducted in duplicate or triplicate, except where noted. As an indication of the error associated with these experiments, the relative standard deviation of the pseudo-first order MS₂ inactivation rate constants fit to triplicate experiments involving MS₂ spiked into SAF-MBR effluent at pH 9.2 without sulfides (Figure 19) was 10.7 percent.

3.2.5 Analyses

This section is a reformatted and lightly modified excerpt of a peer-reviewed publication (Szczyka et al., 2021) with open access licensed by Elsevier Ltd. under CC BY-NC-ND 4.0.

UV₂₅₄ and UV absorbance spectra (200–400 nm) were measured using an Agilent Cary 60 UV–Vis spectrophotometer (minimum reporting level (MRL) = 0.01 cm^{-1}). H₂O₂ concentrations were measured by the peroxidase catalyzed oxidation of N,N– diethyl-p-phenylenediamine (DPD) (Bader et al., 1988). Hach colorimetric methods were used to measure sulfides (method 8131; MRL = 1.0 micromole [μM]), sulfate (method 8051; MRL = 2.0 μM), COD (method 8000; MRL = 1 mg/L), ammonia (method 10031; MRL = 0.4 mg-N/L), nitrate (method 10206; MRL = 0.2 mg-N/L), nitrite (method 10207; MRL = 0.02 mg- N/L), and monochloramine (method 10200; MRL = 0.05 mg- Cl₂/L). Sulfite (MRL = 2.0 μM) and thiosulfate (MRL = 5.0 μM) concentrations were determined using an ion chromatograph (IC; Dionex Integriion HPIC system) equipped with a Dionex IonPac AS19 column (Thermo Scientific), using a method

adapted from Zhang et al. (2020). Direct determination of sulfite via IC is a challenge due to oxidation of sulfite to sulfate in the eluent (Hansen et al., 1979) and poor separation of sulfite and sulfate peaks (Sunden et al., 1983). As such, sulfite concentrations were inferred by subtracting the sulfate concentration measured using Hach method 8051 and the coeluting sulfite and sulfate concentration measured on the IC. Coliphage MS₂ was enumerated using a double-agar layer assay (MRL = 10 plaque forming units [PFU]/mL), as described previously (Szczuka et al., 2020).

3.3 Non-potable Reuse Results and Discussion

3.3.1 General Water Quality

This section is a reformatted and lightly modified excerpt of a peer-reviewed publication (Szczuka et al., 2021) with open access licensed by Elsevier Ltd. under CC BY-NC-ND 4.0.

General water quality parameters for the Stanford pilot-scale SAF-MBR unit effluent are listed in Szczuka et al., 2021, Table S1. The COD (superset of BOD₅) of the effluent (25 mg/L) was < 30 mg/L, meeting discharge criteria. Ammonia (62.6 mg-N/L) was the only inorganic nitrogen species present in the effluent; inorganic nitrogen oxidation is not expected during anaerobic treatment. At the 62.6 mg-N/L ammonia concentration, a > 571 mg- Cl₂/L chlorine dose would be needed to achieve a free chlorine residual (1.8:1 chlorine: ammonia molar ratio). The effluent pH (7.2) and UV₂₅₄ absorbance (0.044 cm⁻¹) were similar to values previously reported for this pilot unit (Szczuka et al., 2019). The chloride concentration (51.5 mg/L) was < 70 mg/L, the most restrictive recommendation for non-potable water reuse (USEPA, 2012), and < 250 mg/L, the USEPA's Secondary Maximum Contaminant Level (MCL) established to avoid salt-associated taste issues in potable water (USEPA, 2024).

Since sulfate reduction to sulfides precedes methanogenesis (Lens et al., 1998), we expect nearly quantitative conversion of sulfate to sulfides in SAF-MBR effluent. Thus, sulfide concentrations ultimately depend on sulfate concentrations in the sewage influent. The drinking water supply serving the area contributing sewage to the SAF-MBR pilot facility is the Hetch Hetchy reservoir, a low-sulfate surface water overlaying granite bedrock. Sulfide concentrations in the SAF-MBR pilot effluent typically are ~2 mg-S/L (Szczuka et al., 2019), but total sulfides, sulfate, sulfite, and thiosulfate were below detection limits for the effluent employed for this study. This low-sulfate sewage enabled the isolation of the effect of sulfides by spiking sulfides into the SAF-MBR effluent.

Sewage at other facilities can feature higher sulfate concentrations resulting from minerals (e.g., gypsum) in groundwater-derived municipal drinking water supplies (e.g., 84 mg/L sulfate (880 μM) in well water from Dayton, Ohio (Snoeyink and Jenkins, 1980)). The sulfate levels within municipal drinking water are supplemented by 20 to 50 mg/L sulfate (~200 to 500 μM) from household and industrial discharges (Metcalf and Eddy, 1991). Lastly, saltwater infiltration into sewers can increase sulfate loads in coastal areas. While removal of sulfate prior to anaerobic treatment would avoid sulfide formation and enhance methane production, techniques such as ion exchange are challenging within a primary effluent matrix.

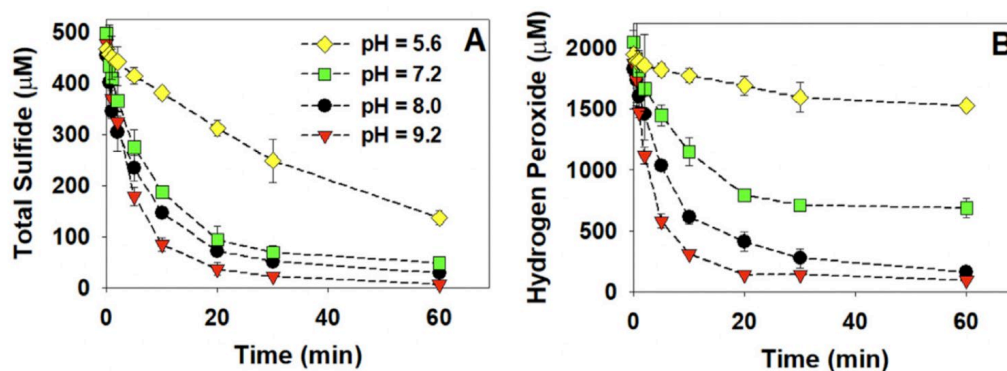
3.3.2 Timescale and Products of Sulfide Oxidation by H₂O₂

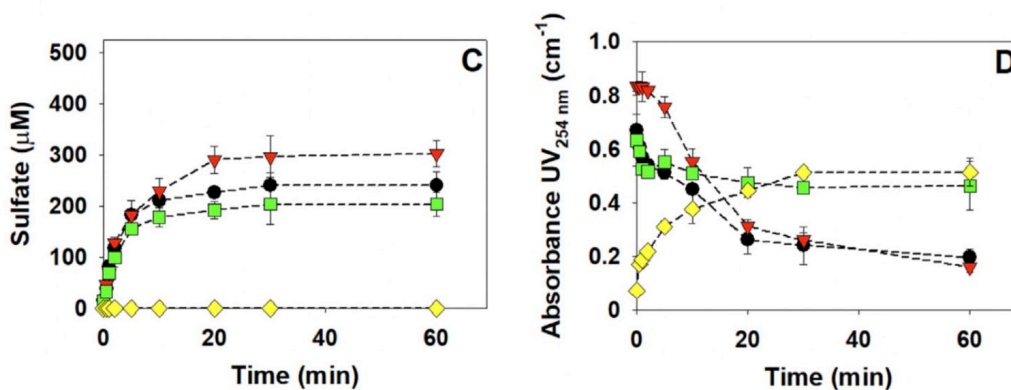
This section is a reformatted and lightly modified excerpt of a peer-reviewed publication (Szczuka et al., 2021) with open access licensed by Elsevier Ltd. under CC BY-NC-ND 4.0.

Previous research conducted in deionized water demonstrated that the stoichiometry, products, and kinetics of sulfide oxidation by H₂O₂ are pH-dependent Equations (3) and (4) (Hoffmann, 1977; Millero et al., 1989). At pH below the 7.1 pK_a of H₂S, H₂O₂ oxidation of H₂S favors elemental sulfur formation over timescales of hours ($k = 0.48 \text{ M}^{-1} \text{ min}^{-1}$ (Hoffmann, 1977)), consuming one molar equivalent of H₂O₂. At pH > 7.1, H₂O₂ oxidation of HS⁻ favors sulfate formation over timescales of minutes ($k = 29 \text{ M}^{-1} \text{ min}^{-1}$ (Hoffmann, 1977)), consuming four molar equivalents of H₂O₂. However, this previous research employed H₂O₂ at high molar excess (10–20-fold) and focused on low pH conditions (< 7 with limited experiments at pH ~8).

We evaluated H₂O₂ oxidation of 500 μM sulfides spiked into SAF-MBR effluent to mimic sulfide concentrations expected in SAF-MBR effluents at typical water reuse facilities (i.e., sewage sulfate concentrations ~50 mg/L). The first objective of these experiments was to evaluate the kinetics of sulfide oxidation, focusing on higher pH conditions within the range (5.6 to 9.2) feasible for pH adjustment during wastewater treatment, and on H₂O₂: sulfide molar ratios (1 to 10) closer to the expected stoichiometric requirements in order to limit reagent supply costs. Conducting these experiments within SAF-MBR effluent was important to incorporate the H₂O₂ demand of the SAF-MBR effluent matrix. The second objective was to evaluate product formation, with a particular focus on the extent to which H₂O₂ oxidation mitigates the negative impacts on UV disinfection associated with the absorption of germicidal UV light at 254 nm (UV₂₅₄) by sulfides. Figure 19 provides the loss of sulfides and H₂O₂, formation of sulfate, and change in UV₂₅₄ for application of 2 mM H₂O₂ (i.e., the 4:1 H₂O₂:sulfide molar ratio that is stoichiometric for oxidation to sulfate) at pH 5.6 (~3% HS⁻), pH 7.2 (~50% HS⁻), pH 8.0 (~89% HS⁻), and pH 9.2 (~99% HS⁻); Szczuka et al., 2021, Figure S1 provides the concentrations of sulfite and thiosulfate.

Figure 19: Concentration of (A) Total Sulfide, (B) Hydrogen Peroxide, (C) Sulfate, and (D) UV₂₅₄ When 500 μM Sulfide and 2000 μM Hydrogen Peroxide Were Spiked Into SAF-MBR Effluent Over a One-Hour Reaction Time. Error Bars Represent the Range of Experimental Duplicates.





Source: Codiga Resource Recovery Center at Stanford

Sulfide oxidation by H_2O_2 was slowest at pH 5.6 (Figure 19A), accompanied by consumption of only $\sim 360 \mu\text{M}$ H_2O_2 after 30 min (Figure 19B). At pH 5.6, the dominance of H_2S (~ 97 percent) would favor slow kinetics and the consumption of $\sim 360 \mu\text{M}$ H_2O_2 is close to the $500 \mu\text{M}$ expected for consumption of 1 molar equivalent of H_2O_2 to form elemental sulfur. No sulfate, thiosulfate or sulfite were observed (Figure 19C and Szczuka et al., 2021, S1). Attempts to measure elemental sulfur by high performance liquid chromatography (HPLC) with UV detection were not successful due to the low concentration ($< 500 \mu\text{M}$) involved. However, when the experiment was conducted in deionized water buffered at pH 5.6 with 2 mM phosphate buffer, the solution turned faintly cloudy, indicative of the formation of colloidal elemental sulfur. Szczuka et al., 2021, Figure S2 provides UV spectra for sulfides spiked into SAF-MBR effluent at each of the four pH values, demonstrating that sulfides absorb UV light at 254 nm. For reaction at pH 5.6, the UV_{254} increased significantly, leveling out after ~ 30 min in either SAF-MBR effluent (Figure 19D) or deionized water (Szczuka et al., 2021, Figure S3). We measured molar absorption coefficients at 254 nm of $85 \text{ M}^{-1} \text{ cm}^{-1}$ for H_2S and of $830 \text{ M}^{-1} \text{ cm}^{-1}$ for elemental sulfur on a molar S basis (Szczuka et al., 2021, Text S1), indicating that the conversion of H_2S to elemental sulfur would increase UV_{254} , as observed. The molar absorption coefficient of elemental sulfur was determined in 90 percent methanol and 10 percent deionized water due to the low solubility of elemental sulfur. Thus, a portion of elemental sulfur would form a separate colloidal phase in aqueous media, as observed in the deionized water experiment. If sulfide oxidation were followed by membrane-based treatment processes (e.g., microfiltration or reverse osmosis within a potable reuse train), colloidal sulfur would contribute to membrane clogging. Regardless, the slow H_2S oxidation kinetics and increase in UV_{254} at pH 5.6 are problematic for non-potable reuse treatment.

Sulfide oxidation by H_2O_2 was significantly faster at $\text{pH} \geq 7.2$ (Figure 19A), accompanied by H_2O_2 consumption after 30 min of $\sim 1330 \mu\text{M}$, $\sim 1550 \mu\text{M}$, and $\sim 1720 \mu\text{M}$ at pH 7.2, 8.0, and 9.6, respectively (Figure 19B). These findings align with expectations of a shift in reaction mechanism with the change in sulfide speciation. The predominance of HS^- above pH 7.1 favors faster kinetics, and the consumption of 1330–1720 μM H_2O_2 approaches the $2000 \mu\text{M}$ expected for consumption of 4 molar equivalents of H_2O_2 to form sulfate. For the 2 mM H_2O_2 dose in these experiments, the characteristic time for HS^- oxidation would be ~ 17 min based on the $29 \text{ M}^{-1} \text{ min}^{-1}$ rate constant provided by Hoffmann (1977), comparable to the timescale for sulfide degradation observed for $\text{pH} \geq 7.2$, where HS^- predominates. Thus, interference

with H₂O₂ oxidation of sulfides by the SAF-MBR matrix was not important. The lower H₂O₂ consumption at pH 7 than at pH 8.0 and 9.2 reflects the co-occurrence of H₂S and HS⁻ at this pH.

Support for the change in reaction mechanism with sulfide speciation is provided by the measured concentrations of sulfate, thiosulfate and sulfite (Figure 19C and Szczuka et al., 2021, S1). Sulfate formation was significant for pH ≥ 7.2, reaching ~200 μM at pH 7.2, ~220 μM at pH 8.0, and ~290 μM at pH 9.2 after 30 min (Figure 19C). However, complete oxidation to sulfate (S[+6]) did not occur. Concentrations of thiosulfate (S₂O₃²⁻ (S[+2])) reached ~50 μM at pH 7.2 and ~80 μM at pH 9.2 after 30 min (Szczuka et al., 2021, Figure S1A). Sulfite (SO₃²⁻ (S[+4])) was also observed at pH ≥ 7.2, but at lower concentrations (maximum ~10 μM) and declined to negligible levels after 30 min (Szczuka et al., 2021, Figure S1B). The detection of thiosulfate and sulfite demonstrate incomplete oxidation of sulfides, and concur with previous reports of thiosulfate formation during H₂O₂ oxidation of sulfides in deoxygenated deionized water at pH 9.0 (Takenaka et al., 2003).

Szczuka et al., 2021, Figure S2 provides UV spectra (200 to 400 nm) for 500 μM of sulfides, sulfate, thiosulfate or sulfite spiked into SAF-MBR effluent at each of the four pH values. Sulfides feature absorbance peaks with maxima near 230 nm but extending to 254 nm (Szczuka et al., 2021, Figure S2A). We calculated molar absorption coefficients at 230 nm and 254 nm for HS⁻ (Szczuka et al., 2021, Text S1). The 7570 M⁻¹cm⁻¹ value for the HS⁻ molar absorption coefficient at 230 nm agrees with the 8000 M⁻¹ cm⁻¹ value determined previously by Zuman and Szafranski (1976). Since the UV absorbance at 254 nm by HS⁻ (ε₂₅₄ = 950 M⁻¹ cm⁻¹) is stronger than by H₂S (ε₂₅₄ = 85 M⁻¹ cm⁻¹ (Szczuka et al., 2021, Text S1)), the UV₂₅₄ increases strongly as pH increases from 5.6 to 7.2, and then moderately for further pH increases, reaching ~2.5 cm⁻¹ at pH 9.2 (Szczuka et al., 2021, Figure S2A). While sulfate does not absorb UV light (Szczuka et al., 2021, Figure S2B), thiosulfate and sulfite both absorb UV at ~200 to 250 nm without pH dependence, although to a lesser degree than HS⁻ (Szczuka et al., 2021, Figures S2C and S2D). The molar absorption coefficients at 254 nm we calculated for thiosulfate and sulfite were 200 M⁻¹ cm⁻¹ and 20 M⁻¹ cm⁻¹, respectively (Szczuka et al., 2021, Table S2).

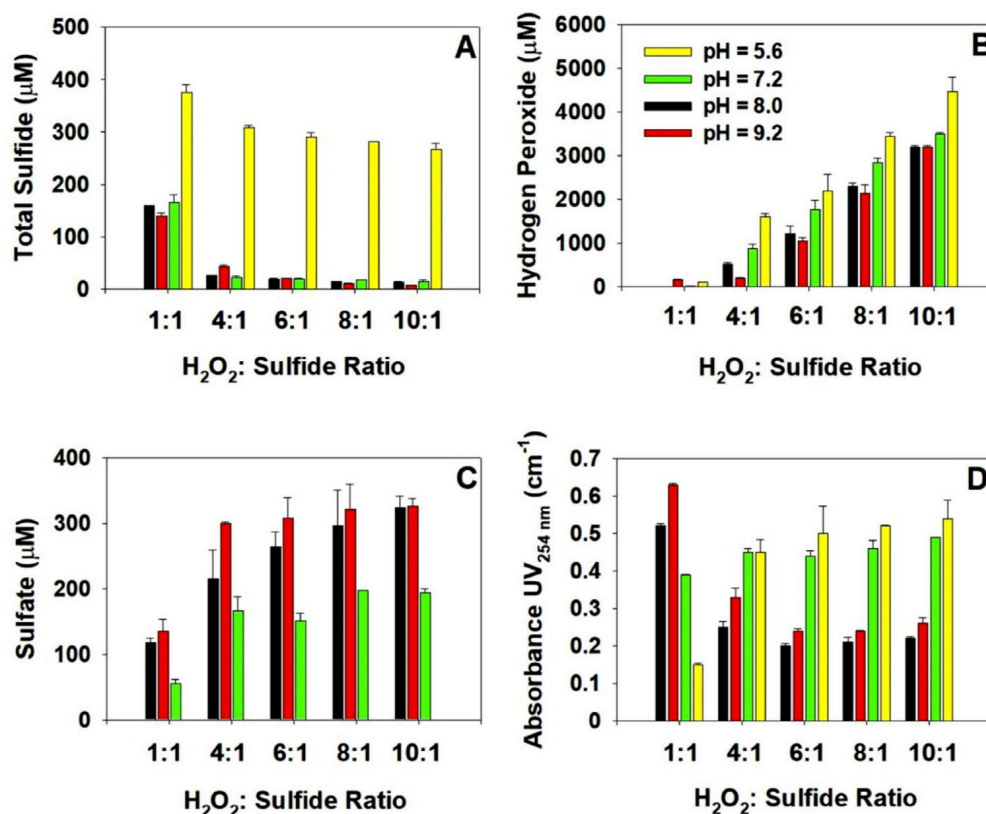
The SAF-MBR effluent exhibited ~0.044 cm⁻¹ (UVT = 90.4 percent) UV₂₅₄ background absorbance (i.e., without sulfides; Szczuka et al., 2021, Table S1). For the treatment of 500 μM sulfides in SAF-MBR effluent with 2000 μM H₂O₂, the initial UV₂₅₄ was highest (~0.8 cm⁻¹; UVT ~ 16 percent) at pH 9.2 (Figure 19D), reflecting the predominance of HS⁻. At pH 8.0 and 9.2, the UV₂₅₄ declined to ~0.25 cm⁻¹ (UVT = 56 percent) after 30 min. This decline reflects the conversion of HS⁻ to sulfate and thiosulfate, the latter contributing to the residual absorbance above the SAF-MBR background. At pH 7.2, where H₂S and HS⁻ co-occur, the UV₂₅₄ decreased from ~0.65 cm⁻¹ to ~0.5 cm⁻¹, reflecting the oxidation of H₂S to elemental sulfur and HS⁻ to sulfate and thiosulfate. Overall, the results indicate that pH adjustment to 8.0 would facilitate sulfide oxidation within 30 minutes while minimizing UV₂₅₄ for subsequent UV disinfection.

3.3.3 Effect of H₂O₂ Dose

This section is a reformatted and lightly modified excerpt of a peer-reviewed publication (Szczuka et al., 2021) with open access licensed by Elsevier Ltd. under CC BY-NC-ND 4.0.

For 500 μM sulfides spiked into SAF-MBR effluent, we tested the effect of H₂O₂:sulfide molar ratio (1–10) on the concentrations of reactants, products, and UV₂₅₄ after 30 min (Figure 20), the time at which reactant degradation and product formation leveled out for pH ≥ 7.2 (Figure 19). At pH = 5.6, $\sim 125 \mu\text{M}$ sulfides were consumed at a 1:1 molar ratio, leaving a low H₂O₂ residual (Figure 20). At a 4:1 molar ratio, sulfide consumption increased to $\sim 200 \mu\text{M}$, while consuming $\sim 360 \mu\text{M}$ H₂O₂. However, at higher molar ratios, each additional molar equivalent of H₂O₂ removed $\sim 12 \mu\text{M}$ sulfides, while leaving an additional $\sim 480 \mu\text{M}$ H₂O₂. No sulfate, thiosulfate or sulfite was observed (Figures 20 and Szczuka et al., 2021, S3). These results reflect the slow oxidation of H₂S to elemental sulfur by H₂O₂ oxidation, with no further significant oxidation of the elemental sulfur. Accordingly, additional H₂O₂ accumulates with some modest consumption by reaction with the SAF-MBR effluent matrix constituents. The increase in the UV₂₅₄ from 0.15 cm^{-1} at a 1:1 molar ratio to 0.45 cm^{-1} at a 4:1 molar ratio is associated with absorbance by elemental sulfur with only modest further increases in UV₂₅₄ at higher molar ratios (Figure 20D).

Figure 20: Concentrations of (A) Total Sulfide, (B) H₂O₂, (C) Sulfate, and (D) UV₂₅₄ Measured 30 Minutes After Addition of H₂O₂ at Various Molar Ratios Relative to 500 μM Sulfides Spiked Into SAF-MBR Effluent. Error Bars Represent the Range of Experimental Duplicates.



Source: Codiga Resource Recovery Center at Stanford

At pH 7.2, 8.0 and 9.2, sulfides were reduced to $\sim 150 \mu\text{M}$ at a 1:1 molar ratio, leaving negligible H_2O_2 residuals. At a 4:1 molar ratio, sulfides declined to $\sim 30 \mu\text{M}$, with residual H_2O_2 concentrations ranging from $\sim 200 \mu\text{M}$ at pH 9.2 to $\sim 800 \mu\text{M}$ at pH 7.2 (Figure 20B). Further increases in the molar ratio produced only modest further reductions in residual sulfide concentrations (down to $\sim 11 \mu\text{M}$ at a 10:1 molar ratio), but at a cost of $\sim 460 \mu\text{M}$ increase in residual H_2O_2 for each additional $500 \mu\text{M}$ H_2O_2 (i.e., each unit increase in the molar ratio). The $\sim 40 \mu\text{M}$ consumption of the additional H_2O_2 indicates reactions of H_2O_2 with other constituents of SAF-MBR effluent; H_2O_2 has been shown to readily react with organic matter in aerobically treated wastewater (Ksibi, 2006).

Both sulfate (Figure 20C) and thiosulfate (Szczuka et al., 2021, Figure S4) were observed. Complete oxidation of HS^- should form $\sim 500 \mu\text{M}$ sulfate. The detection of thiosulfate and the formation of sulfate at concentrations $< 500 \mu\text{M}$, even at a 10:1 molar ratio and pH 9.2, indicates that complete oxidation did not occur. Sulfate concentrations increased between molar ratios of 1 and 4, leveling out at higher molar ratios, with the highest concentrations ($\sim 300 \mu\text{M}$) observed for pH 8.0 and 9.2, but $\sim 200 \mu\text{M}$ at pH 7.2. Thiosulfate concentrations declined with increasing molar ratio from $\sim 120\text{--}150 \mu\text{M}$ at a 1:1 molar ratio to $\sim 40 \mu\text{M}$ at a 10:1 molar ratio. Thiosulfate is expected to form under alkaline conditions, but to decline when H_2O_2 is in stoichiometric excess (Takenaka et al., 2003). At the lowest molar ratios, the highest thiosulfate concentrations were observed at pH 7.2, concurring with expectations that the lower molar ratios and the slower kinetics associated with the mixture of H_2S and HS^- at this pH would favor the formation of this intermediate.

Given that elemental sulfur, thiosulfate and sulfides absorb UV light at 254 nm (Szczuka et al., 2021, Figure S2), UV_{254} was minimized ($\sim 0.2 \text{ cm}^{-1}$; UVT = 63 percent) at H_2O_2 :sulfide molar ratios ≥ 6 at pH ≥ 8.0 (Figure 20D). The higher UV_{254} observed at pH 7.2 ($\sim 0.45 \text{ cm}^{-1}$; UVT = 36 percent, similar to pH 5.6), despite concentrations of sulfides and thiosulfate comparable to those at pH 8.0 and 9.2 is attributable to elemental sulfur. Thus, a 6:1 molar ratio at pH 8.0 would minimize the reagent costs for pH adjustment and potentially minimize the UV fluence required for pathogen inactivation by minimizing UV_{254} . However, the UV_{254} at pH 8.0 and a 4:1 molar ratio was only 25 percent higher (0.25 cm^{-1} ; UVT = 56 percent) than at the 6:1 molar ratio. Thus, at pH 8.0, the lower cost of the H_2O_2 reagent at the 4:1 molar ratio must be weighed against the lower cost associated with UV fluence to achieve pathogen inactivation at the 6:1 molar ratio.

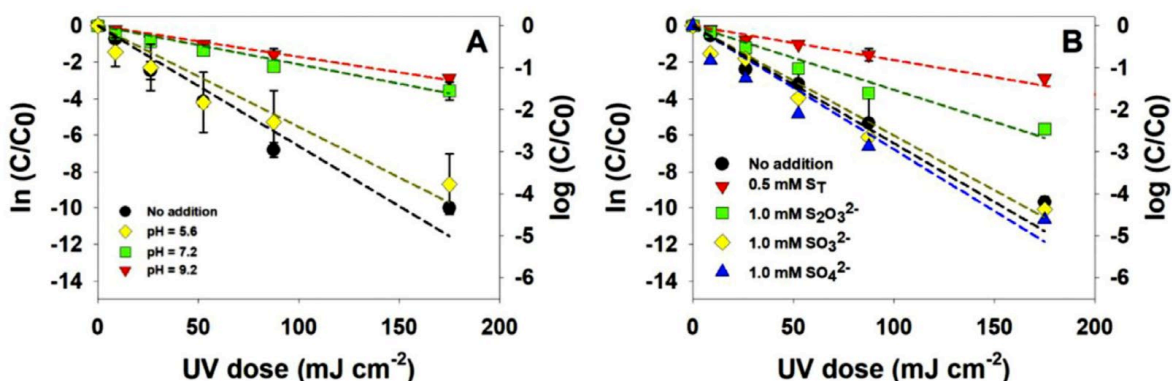
3.3.4 Effect of Sulfides on Log Inactivation of MS_2

This section is a reformatted and lightly modified excerpt of a peer-reviewed publication (Szczuka et al., 2021) with open access licensed by Elsevier Ltd. under CC BY-NC-ND 4.0.

Figure 21A shows that UV inactivation of bacteriophage MS_2 in phosphate buffer in the presence of $500 \mu\text{M}$ sulfides is pH dependent. In the absence of sulfides, a UV fluence of 175 mJ cm^{-2} achieved a 4.5-log removal value (LRV) of bacteriophage MS_2 , regardless of pH (data for pH 7.2 shown). In the presence of sulfides at pH = 5.6, MS_2 inactivation was similar to the no sulfide control. However, 175 mJ cm^{-2} UV fluence achieved only 1.5 and 1.3 MS_2 LRVs at pH

7.2 and 9.2, respectively. Approximating MS₂ inactivation by first order kinetics, UV fluence-based first order inactivation rate constants would be 0.055, 0.022, and 0.017 cm² mJ⁻¹ at pH 5.6, 7.2, and 9.2, respectively. The ~0.06 cm² mJ⁻¹ values measured in the absence of sulfides concurs with previous determinations for treatment of groundwater, among other water types (Templeton et al., 2006; Hinjen et al., 2006). Extrapolating from this data, UV doses of 530 and 670 mJ cm⁻² would be required to achieve a 5-log inactivation for bacteriophage MS₂ at pH 7.2 and 9.2, respectively. For comparison, the National Water Research Institute (NWRI) recommends that UV systems deliver a 90 mJ cm⁻² UV fluence for non-potable reuse of membrane-filtered municipal effluents treated by conventional, aerobic secondary biological treatment processes (NWRI, 2012).

Figure 21: Inactivation of Coliphage MS₂ in Phosphate Buffer by UV Light (A) in the Presence of 0.5 mM Sulfides at pH 5.6, 7.2, and 9.2 and (B) in the Presence of 0.5 mM Sulfides (S_T), 1 mM Thiosulfate (S₂O₃²⁻), 1 mM Sulfite (SO₃²⁻), or 1 mM Sulfate (SO₄²⁻) Buffered at pH 9.2.



The UV only control (no addition) in panel A was conducted at pH 7.2 and at pH 9.2 for panel B. In panel A, error bars represent the range of duplicate (pH 5.6, 7.2, no addition), and triplicate (pH 9.2) experimental measurements. In panel B, error bars represent the range of triplicate (0.5 mM sulfides, no addition) experimental replicates, and the range of duplicate analytical measurements for the thiosulfate, sulfite, or sulfate conditions.

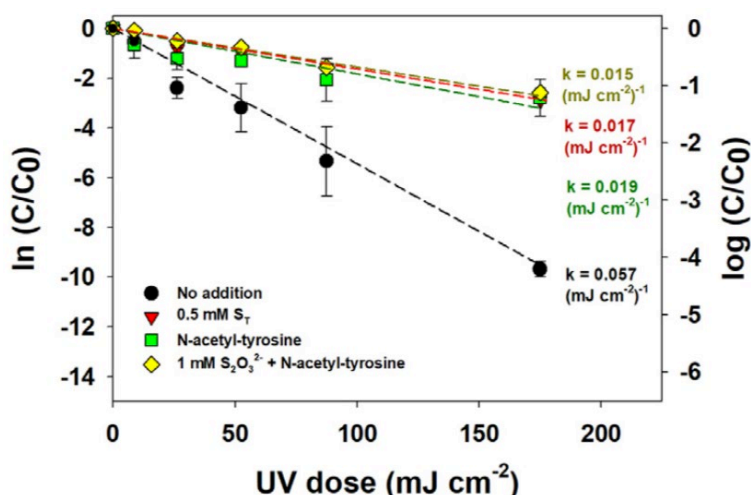
Source: Codiga Resource Recovery Center at Stanford

Figure 21B shows the effect of sulfides and sulfide oxidation products on UV inactivation of bacteriophage MS₂ in phosphate buffer at pH 9.2. MS₂ inactivation rates were within 18 percent for 1 mM sulfite (0.061 cm² mJ⁻¹), 1 mM sulfate (0.067 cm² mJ⁻¹), and the no addition control (0.057 cm² mJ⁻¹). However, the inactivation rate decreased to 0.035 cm² mJ⁻¹ for 1 mM thiosulfate, such that a 330 mJ cm⁻² UV fluence would be required to achieve 5-log inactivation of MS₂.

UV inactivation of MS₂ occurs predominantly by photooxidation of the genome, which absorbs UV light at 254 nm (Ye et al., 2018). The inhibition of bacteriophage MS₂ inactivation by UV in the presence of HS⁻ (i.e., sulfides at pH ≥ 7.2) and thiosulfate may relate to shielding of MS₂ by absorption of 254 nm light by HS⁻ and S₂O₃²⁻, or to reversal of the photo-oxidation reactions by these potent reductants. To test the importance of photon shielding, we supplemented samples with N-acetyl-tyrosine, which absorbs UV light at 254 nm but is not a potent reductant. Figure 22 shows UV inactivation of MS₂ in phosphate buffer at pH 9.2 in the pre-

sence and absence of 0.5 mM sulfides (predominantly HS^- at pH 9.2), 2.9 mM N-acetyl-tyrosine, and 1 mM thiosulfate with 2.0 mM N-acetyl-tyrosine. These solutions of N-acetyl-tyrosine, sulfides and thiosulfate mixed with N-acetyl-tyrosine exhibited a common UV absorbance ($\text{UV}_{254} = 0.8 \text{ cm}^{-1}$). The MS_2 inactivation rates in the presence of sulfides ($0.017 \text{ cm}^2 \text{ mJ}^{-1}$), N-acetyl-tyrosine ($0.019 \text{ cm}^2 \text{ mJ}^{-1}$), and the N-acetyl-tyrosine and thiosulfate mixture ($0.015 \text{ cm}^2 \text{ mJ}^{-1}$) were comparable and ~ 4 -fold lower than for the no-addition control. These results indicate that photon shielding is predominantly responsible for the reduction in UV inactivation rates by HS^- and thiosulfate. Overall, the results suggest the need to achieve complete oxidation of sulfides to sulfate to minimize the UV fluence needed to achieve 5-log inactivation of MS_2 .

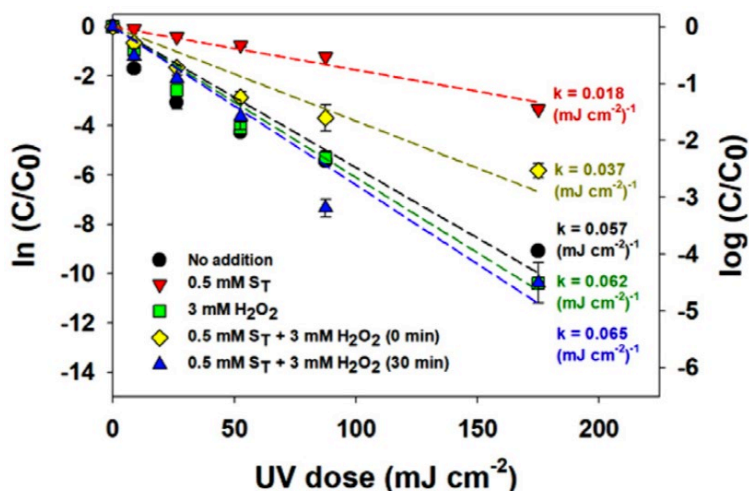
Figure 22: Inactivation of Coliphage MS_2 in Phosphate Buffer (pH 9.2) by UV Light in the Presence of 0.5 mM Sulfides (S_T), 2.9 mM N-acetyl-tyrosine, and 1 mM Thiosulfate with 2.0 mM N-acetyl-tyrosine



N-Acetyl-tyrosine was added at concentrations such that the total absorbances of solutions were equal at 0.8 cm^{-1} (except for the no addition control). Error bars represent the range of experimental triplicate (no addition, sulfide conditions) and duplicate (N-acetyl-tyrosine and thiosulfate + N-acetyl-tyrosine conditions) measurements.

Source: Codiga Resource Recovery Center at Stanford

Figure 23: Inactivation of Bacteriophage MS₂ in SAF-MBR Effluent by UV Light



Samples were spiked with 0.5 mM sulfide, 3 mM peroxide, or a combination 0.5 mM sulfide and 3 mM peroxide at pH 8.0. Samples treated with both sulfide and peroxide were treated with UV immediately (0 minutes) or held for 30 minutes prior to UV treatment. Error bars represent the range of experimental duplicates.

Source: Codiga Resource Recovery Center at Stanford

3.3.5 Effect of H₂O₂ Pre-treatment on MS₂ Inactivation

This section is a reformatted and lightly modified excerpt of a peer-reviewed publication (Szczuka et al., 2021) with open access licensed by Elsevier Ltd. under CC BY-NC-ND 4.0.

As can be seen in Figure 20, UV₂₅₄ of the SAF-MBR effluent spiked with 500 μM sulfides is minimized when the sample pH is adjusted to 8.0 and 3 mM H₂O₂ is added to achieve a 6:1 H₂O₂:sulfide molar ratio. At pH 8.0, the rate of MS₂ inactivation by UV ($k = 0.057 \text{ cm}^2 \text{ mJ}^{-1}$; Figure 23) in SAF-MBR effluent (UV₂₅₄ = 0.044 cm⁻¹; Szczuka et al., 2021, Table S1) was within the range of MS₂ inactivation in phosphate buffer ($k = 0.064 \text{ cm}^2 \text{ mJ}^{-1}$; data not shown) in the absence of sulfides or H₂O₂. For the addition of 3 mM H₂O₂ to the SAF-MBR effluent without sulfides, the rate of MS₂ inactivation ($0.062 \text{ cm}^2 \text{ mJ}^{-1}$) was similar to that in the absence of H₂O₂. These results indicate that neither direct reaction with H₂O₂ nor reactions with hydroxyl radical formed by UV photolysis of H₂O₂ are important for MS₂ inactivation. Although previous research indicated that hydroxyl radical production by UV photolysis of H₂O₂ can increase the rate of MS₂ inactivation during UV treatment, the importance of hydroxyl radical-mediated inactivation depends on the matrix. For example, Sun et al. (2016) showed that the addition of 0.3 mM H₂O₂ increased MS₂ inactivation by ~15-fold in phosphate buffer, but did not increase inactivation appreciably in wastewater, likely due to hydroxyl radical scavenging by dissolved organic matter.

We added 3 mM H₂O₂ to SAF-MBR effluent spiked with 0.5 mM sulfides and irradiated the sample with UV light either immediately after H₂O₂ addition or after a 30-minute reaction time to permit maximum oxidation of sulfides to products (Figures 1 and 2). When irradiated after a 30-minute reaction time, the MS₂ inactivation rate ($k = 0.065 \text{ cm}^2 \text{ mJ}^{-1}$) slightly exceeded the inactivation rate of the SAF-MBR effluent control containing neither sulfides nor H₂O₂ ($k = 0.057 \text{ cm}^2 \text{ mJ}^{-1}$). When irradiated immediately after the H₂O₂ addition to the sulfide-

containing effluent, the MS₂ inactivation rate was lower ($k = 0.037 \text{ cm}^2 \text{ mJ}^{-1}$), yet H₂O₂ addition nearly doubled the rate of MS₂ inactivation relative to the sulfides-containing effluent without H₂O₂ addition ($k = 0.018 \text{ cm}^2 \text{ mJ}^{-1}$). MS₂ concentrations did not change over the 30-minute reaction period prior to irradiation, indicating that direct reaction with H₂O₂ did not contribute to MS₂ inactivation. Rather, the increase in inactivation MS₂ rate can be attributed to H₂O₂ oxidizing sulfide to products with lower UV absorbance. In fact, the sulfide concentration after UV irradiation was lowest in the sample that was spiked with H₂O₂ and irradiated after a 30 min reaction time. In the sulfide-only control, ~420 μM sulfides were present after UV irradiation, compared to ~180 μM and ~5 μM when the samples were treated with H₂O₂ and irradiated with UV light immediately or after 30 minutes, respectively. For SAF-MBR effluent containing 0.5 mM sulfides, adjustment of the pH to 8.0 and pre-treatment with 3 mM H₂O₂ for 30 minutes would reduce the UV fluence needed to achieve 5-log inactivation of MS₂ from 640 mJ cm^{-2} to 180 mJ cm^{-2} , a reduction of 460 mJ cm^{-2} . When the SAF-MBR effluent containing 0.5 mM sulfides was treated with 2 mM H₂O₂ (i.e., a 4:1 H₂O₂:sulfide molar ratio) for 30 minutes at pH 8.0, the UV₂₅₄ was 0.25 cm^{-1} (Figure 20D), such that 5-log inactivation would require an applied UV fluence of 225 mJ cm^{-2} .

3.3.6 Free Chlorine Doses to Achieve Total Chlorine Residuals for Distribution

This section is a reformatted and lightly modified excerpt of a peer-reviewed publication (Szczuka et al., 2021) with open access licensed by Elsevier Ltd. under CC BY-NC-ND 4.0.

Lastly, we evaluated the free chlorine doses needed to attain 5 mg-Cl₂/L (70 μM) total chlorine residuals after 24 h to provide residuals for distribution; given the 62.6 mg-N/L (4.5 mM) ammonia concentration, the total chlorine residual consisted of chloramines. The SAF-MBR sample spiked with 0.5 mM sulfides was treated at pH 8.0 with 2 mM H₂O₂ (i.e., a 4:1 H₂O₂:sulfide molar ratio) for 30 minutes, and then with 225 mJ cm^{-2} UV fluence, the applied fluence needed to achieve 5-log MS₂ inactivation. The residual H₂O₂ concentration was 0.4 mM. The total chlorine residuals measured 24 h after application of 25 and 50 mg-Cl₂/L were 0.3 and 29 mg- Cl₂/L, respectively, suggesting that an ~30 mg- Cl₂/L applied free chlorine dose (0.42 mM) would leave an ~5 mg- Cl₂/L residual (Szczuka et al., 2021, Table S7). Similarly, the sulfide-spiked sample was treated with 3 mM H₂O₂ (i.e., a 6:1 H₂O₂:sulfide molar ratio) for 30 minutes, and then with the 180 mJ cm^{-2} applied UV fluence needed to achieve 5-log MS₂ inactivation. The residual H₂O₂ was 1.2 mM, and the free chlorine needed to achieve a 5 mg- Cl₂/L total chlorine residual was ~80 mg- Cl₂/L (1.1 mM) (Szczuka et al., 2021, Table S7).

For both H₂O₂:sulfide molar ratios, the applied chlorine dose needed to achieve the residual was lower than expected based upon the 1:1 stoichiometry (Eq. (5)) just to quench the residual H₂O₂. Additional experiments conducted in deionized water demonstrated that a portion of the free chlorine reacts with ammonia to form chloramines prior to being quenched by reaction with H₂O₂ (Szczuka et al., 2021, Text S₂). Chloramines are degraded by reaction with H₂O₂ more slowly than is free chlorine (Zhang et al., 2019), such that chloramine formation reduces consumption of the total chlorine residual via reactions with H₂O₂.



3.3.7 Comparison of Treatment Costs

This section is a reformatted and lightly modified excerpt of a peer-reviewed publication (Szczyka et al., 2021) with open access licensed by Elsevier Ltd. under CC BY-NC-ND 4.0.

The experimental results indicate that operating at a H₂O₂:sulfide molar ratio closer to 4 rather than 6 would reduce the cost of H₂O₂ supply and, by reducing the H₂O₂ residual, the cost of chlorine supply. However, these savings in reagent costs must be weighed against the increased energy cost associated with the higher UV fluence needed to achieve pathogen inactivation, since the UV₂₅₄ was higher at the 4:1 molar ratio (0.25 cm⁻¹) than at the 6:1 molar ratio (0.20 cm⁻¹) (Figure 20).

We conducted an initial comparison of the energy and chemical costs associated with H₂O₂/UV/chlorine treatment of SAF-MBR effluent (for both 4:1 and 6:1 H₂O₂:sulfide molar ratios) against the conventional treatment of aerobically-treated effluent by filtration (here microfiltration) and chlorine disinfection (Szczyka et al., 2021, Figure S6). Table 15 summarizes the results, while Szczyka et al., 2021, Text S3, details the cost estimates. For the conventional treatment of aerobic effluents, the estimate considered the energy costs associated with 1) activated sludge secondary treatment (\$0.039/m³), 2) microfiltration (\$0.052/m³), and 3) the cost for addition of chlorine for disinfection (\$0.017/m³), for a total cost of \$0.11/ m³. For H₂O₂ /UV/chlorine treatment of SAF-MBR effluent, the estimates considered 1) the energy cost associated with SAF-MBR treatment (energy-neutral or \$0.00/m³), 2) the cost of NaOH for adjusting the effluent to pH 8 (\$0.016/ m³), 3) the cost for H₂O₂ addition at 4:1 (\$0.122/ m³) and 6:1 (\$0.168/m³) H₂O₂:sulfide molar ratios, 4) the energy cost for an incident UV fluence of 225 mJ cm⁻² (\$0.0098/m³) for the 0.25 cm⁻¹ UV₂₅₄ associated with a 4:1 H₂O₂:sulfide molar ratio and 180 mJ cm⁻² (\$0.0078/m³) for the 0.20 cm⁻¹ UV₂₅₄ associated with a 6:1 H₂O₂:sulfide molar ratio, and 5) the cost to provide 30 mg/L as Cl₂ chlorine for the 4:1 H₂O₂:sulfide molar (\$0.052/m³) and 80 mg/L as Cl₂ chlorine for the 6:1 H₂O₂:sulfide molar (\$0.138/m³). The energy costs were modest relative to the chemical costs (Table 15). The overall energy and chemical cost to treat SAF-MBR effluent would be \$0.19/m³ for the 4:1 H₂O₂:sulfide molar ratio and \$0.33/m³ for the 6:1 H₂O₂:sulfide molar ratio. The reduction in chemical costs for H₂O₂ and chlorine associated with the 4:1 H₂O₂:sulfide molar ratio outweighed the higher energy cost for UV treatment needed to overcome the higher UV₂₅₄ for this molar ratio.

Table 15: Treatment Costs for Reuse of an Aerobically Treated Effluent or Anaerobically Treated Effluent Spiked with 500 μm Sulfide and Treated with H_2O_2 Dosed at Either a 6:1 or 4:1 H_2O_2 :sulfide Ratio

	Cost ($\text{\$ m}^{-3}$)		
	Conventional train	SAF-MBR based train	
		6:1 H_2O_2 : sulfide ratio	4:1 H_2O_2 : sulfide ratio
Conventional activated sludge	0.04	-	-
Microfiltration	0.05	-	-
SAF-MBR treatment	-	0	0
pH adjustment (NaOH)	-	0.02	0.02
H_2O_2 addition	-	0.17	0.11
UV treatment	-	0.01	0.01
Chlorine addition	0.02	0.14	0.05
Total	0.11	0.33	0.19

Source: Codiga Resource Recovery Center at Stanford

However, for treatment of wastewater featuring 0.5 mM sulfate (48 mg/L), which could form 0.5 mM sulfides in the anaerobic reactor, H_2O_2 /UV/chlorine treatment of SAF-MBR effluent at either H_2O_2 /sulfide molar ratio would not be cost-competitive with the conventional approach of treating wastewater by activated sludge followed by filtration and chlorine disinfection. However, the chemical and energy costs for H_2O_2 /UV/chlorine treatment of SAF-MBR effluent decrease with decreasing sulfide (and thus sewage sulfate) concentration. Further calculations (Szczuka et al., 2021, Text S3) indicate that the sulfide concentration at which H_2O_2 /UV/chlorine treatment of SAF-MBR effluent becomes cost-competitive with the conventional aerobic treatment train for non-potable reuse would be 285 μM (27 mg/L sewage sulfate) for the 4:1 H_2O_2 :sulfide molar ratio and 150 μM (14 mg/L sewage sulfate) for the 6:1 H_2O_2 :sulfide molar ratio.

3.3.8 Implications of Results for SVCW

This section is a reformatted and lightly modified excerpt of a peer-reviewed publication (Szczuka et al., 2021) with open access licensed by Elsevier Ltd. under CC BY-NC-ND 4.0.

Monitoring of the SAF-MBR influent at SVCW indicates that influent sulfate concentrations can range from 30-50 mg/L (310 μM – 510 μM) during dry weather flows. Effluent pH is typically 7.0-7.2. Assuming complete conversion of influent sulfate to sulfides, the most cost-effective scheme of proposed treatment scheme would require dosing of NaOH to adjust the pH to 8.0, 1.6 mM H_2O_2 for sulfide treatment with a 4:1 H_2O_2 :sulfide, an incident UV fluence of 225 mJ cm^{-2} for pathogen inactivation, and 30 mg/L as Cl_2 chlorine to maintain a residual. The cost of this treatment would total $\text{\$}0.15/\text{m}^3$, greater than the cost of conventional treatment as analyzed here. However, additional benefits associated with SAF-MBR treatment of wastewater would offset these costs. For example, the SAF-MBR presents the possibility of surplus energy generation ($\sim 0.4 \text{ kWh}/\text{m}^3$), with a value of $\text{\$}0.05/\text{m}^3$ that would offset the costs of non-potable treatment. The reduced costs for dewatering and hauling of biosolids due to anaerobic treatment would also offset costs for water reuse.

Influent sulfate concentrations at SVCW appear to follow a seasonal pattern, with concentrations increasing during winter wet weather months to up to 100 mg/L (1,000 µM). At these influent concentrations, treatment to Title 22 standards would likely be cost prohibitive. However, there is typically limited demand for Title 22 water in the wet months in Redwood City, such that treatment during periods of high influent sulfate concentrations may not be necessary.

There is also the potential that some influent sulfate in the SAF-MBR is not converted to sulfide. Incomplete sulfate conversion in earlier tests was observed once the microbial community had matured (Shin et al., 2014), with 15-20 percent of influent sulfate remaining unconverted, suggesting that the negative impacts of sulfide on water reuse costs may be lower than assumed in this analysis.

Finally, this analysis focused on meeting disinfection and residual requirements for Title 22, but another core requirement is that water qualify as "oxidized", signifying that organic matter in the water is "stabilized, is non-putrescible, and contains dissolved oxygen (CDPH 2021). The SAF-MBR readily achieves US Secondary Effluent Standards for removal of organic matter, such that the remaining organic matter should qualify as stabilize and non-putrescible. Although the SAF-MBR effluent is devoid of dissolved oxygen upon exiting the reactor, dissolved oxygen could be readily added to the water by several different methods, including running the SAF-MBR effluent through an air stripping column that would have the additional benefit of enabling removal and recovery of dissolved methane (Galdi and Luthy, 2021).

CHAPTER 4:

Potable Reuse Process Performance

This chapter is a reformatted and lightly modified version of a peer-reviewed publication adapted with permission from Szczuka, A.; Berglund-Brown, J.P.; Chen, H.K.; Quay, A.N.; and Mitch, W.A. 2019. *Evaluation of a Pilot Anaerobic Secondary Effluent for Potable Reuse: Impact of Different Disinfection Schemes on Organic Fouling of RO Membranes and DBP Formation*. Environ. Sci. Technol. 2019, 53, 6, 3166-3176. Copyright 2019 American Chemical Society.

4.1 Motivation for Potable Reuse of Anaerobic Effluent

Demonstrating the ability to link anaerobic secondary effluent to potable reuse trains is critical for fostering the adoption of anaerobic technologies by utilities that may need to pursue potable reuse in the future to meet water demands. Advanced treatment trains to purify wastewater for potable reuse typically employ the Full Advanced Treatment (FAT) train, consisting of microfiltration (MF), reverse osmosis (RO), and the UV/hydrogen peroxide advanced oxidation process (UV/H₂O₂ AOP) (Gerrity et al., 2013). Fouling of membranes, particularly RO membranes, can increase the cost of water production. For aerobically treated wastewaters, fouling by effluent organic matter and biofilm growth have been estimated to account for 26–52 percent (Tang et al., 2010) and up to 45 percent (Komlenic et al., 2010) of the total fouling, respectively. Chloramines, or more recently, ozone, have been applied upstream of membranes to control biofilm growth. However, reactions with these disinfectants alter the fouling behavior of organic matter by changing its chemical characteristics (Guo et al., 2012). For example, ozonation of surface water (Zeng et al., 2014) and aerobically treated wastewater (Stanford et al., 2011, Vatankhah et al., 2018) reduce fouling potential by rendering the organic matter more hydrophilic, but the effects of disinfectants on the fouling behavior of anaerobically treated wastewater have not been characterized.

A second important consideration for potable reuse trains is their ability to remove chemical contaminants (Drewes et al., 2013). Multiple studies have characterized contaminant removal during aerobic secondary treatment and associated potable reuse trains (Verlicchi et al., 2012; Yang et al., 2011; Drewes et al., 2002). The National Research Council has indicated that concentrations of disinfection byproducts (DBPs), particularly N-nitrosamines, in wastewater reuse systems are much closer to levels of public health concern than concentrations of pharmaceuticals (NRC, 2012). Low molecular weight, halogenated DBPs in disinfected aerobic secondary effluents are poorly removed by RO membranes and AOP treatment (Zeng et al., 2016a; Chuang et al., 2016). Some of the unregulated DBP classes, particularly haloacetonitriles, may be more important contributors to the DBP-associated toxicity of the final effluent than the N-nitrosamines, trihalomethanes (THMs) and haloacetic acids (HAAs) of current regulatory focus (Zeng et al., 2016a; Chuang et al., 2016). The few studies characterizing contaminant removal during anaerobic secondary treatment have focused on pharmaceutical removal (McCurry et al., 2014; Cheng et al., 2018; Huang et al., 2018). One study found that

a pilot-scale SAF-MBR system outperformed a full-scale aerobic secondary treatment system for removing N-nitrosamines and pharmaceuticals when treating a common primary effluent (McCurry et al., 2014). The fate of the DBPs associated with anaerobic effluents within potable reuse trains has not been evaluated.

The objective of this study was to characterize the impacts of different disinfection strategies on RO membrane fouling by dissolved organic compounds and DBP formation when applied to anaerobic secondary effluent from a pilot-scale SAF-MBR unit treating municipal primary effluent. The majority of the organic matter in aerobic effluents is believed to consist of soluble microbial products (SMPs), (Shon et al., 2006; Drewes et al., 1999; Rittmann et al., 1987) representing the biotransformation products of sewage constituents and biomolecules shed from bacteria. Because the metabolic pathways of anaerobic bacteria may differ fundamentally from those of aerobic bacteria, the tendency of the SMPs to foul membranes and generate DBPs might also differ. The disinfection strategies evaluated included various combinations of chloramination, ozonation, and biological activated carbon (BAC) filtration. This study evaluated whether the fouling behavior of the disinfectant-treated anaerobic effluent correlates with the hydrophobicity of the effluent organic matter, an important characteristic promoting membrane fouling (Zularisam et al., 2007). The formation of a range of regulated and unregulated DBPs was characterized. Lastly, the RO fouling behavior and DBP formation from anaerobic SMPs was isolated using SMPs generated from a laboratory-scale SAF-MBR system fed with a defined media.

4.2 Materials and Methods

4.2.1 Pilot- and Lab-Scale SAF-MBR Reactors

The pilot-scale SAF-MBR, located on the Stanford University campus, is as described previously (Shin et al., 2021a). The Stanford system was started up prior to startup of the SAF-MBR at SVCW, enabling this study to proceed in parallel with startup at SVCW. At the time of the experiments described here, the SAF-MBR treated ~ 0.2 m³/h with an ~ 12 h HRT. A 300 L sample of the effluent was collected ~ 6 months after startup. The sample was filtered using a prerinsed 1 μ m polypropylene cartridge filter (Culligan, Rosemont, IL) and 0.7 μ m glass fiber filters (Whatman GF/F), and stored at 39°F (4°C).

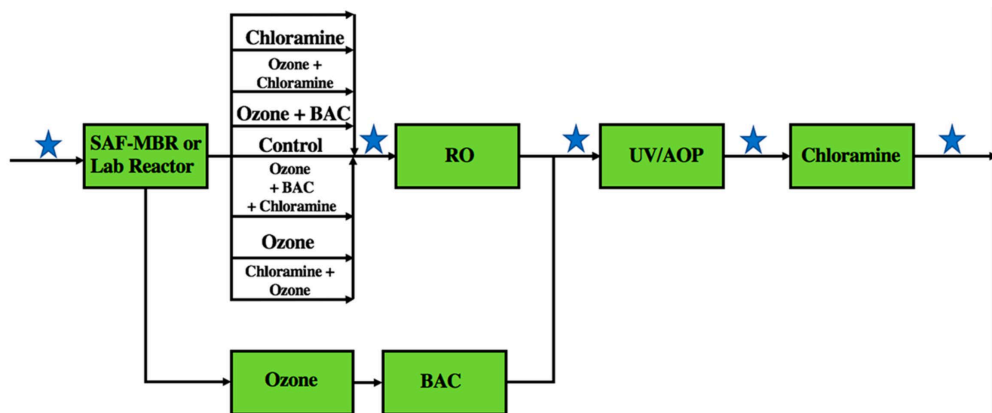
Two laboratory-scale FBR reactors were designed based on the pilot-scale FBR reactor; like the pilot-scale FBR reactor unit, the laboratory-scale units did not contain filters. Each reactor (1.7 L volume and 20 cm² cross-sectional area) was filled with 0.3 L of Filtrasorb 400 GAC and fluidized to achieve ~ 20 – 30 percent bed volume expansion (16 m/h upflow velocity). Each reactor was fed tap water containing 125 mg/L (as COD) acetate, 125 mg/L (as COD) propionate, 57 mg-N/L ammonium chloride and 5 percent by volume supernatant from an anaerobic digester at a local wastewater treatment plant, adapted from Yoo et al. (Yoo et al., 2014). At a 1 mL/min flow rate, the HRT was 6 h based on the expanded GAC bed volume. One year after startup of the reactors, samples of the treated effluent were collected, filtered through glass fiber filters, and stored at 39°F (4 °C). The effluent COD after filtration was <30 mg/L, demonstrating >88 percent COD removal across the units. Reflecting the activity of methanogens, the gas in the headspace of the reactor consisted of 5 to 20 percent methane

with balance nitrogen over the course of sampling. Given the low flow rate of the reactors and concerns over the stability of the organics during storage, it was not possible to collect and accumulate large quantities of effluent. Smaller batches (40 L) were collected and stored for less than 5 days at 39°F (4°C), and separate controls were run for each batch.

4.2.2 Sample Pretreatment

Samples were ozonated, chloraminated, or treated with BAC in the different combinations shown in Figure 24 prior to RO treatment. Ozone/BAC treatment alone was also evaluated as an alternative to RO treatment. Ozone stock solutions were generated by passing oxygen gas (>99 percent) through a Triogen ozone generator (East Kilbride, Scotland) and bubbling the effluent through deionized water in a chilled ice bath. Ozone stocks (~40 mg/L) were standardized by measuring UV absorbance at 260 nm ($\epsilon_{260} = 3200 \text{ M}^{-1}\text{cm}^{-1}$) (von Sonntag e. al., 2012). Ozone was applied to samples at 0.8 mg O₃/mg dissolved organic carbon (DOC). Because ozone addition diluted the samples, samples for other treatments were diluted with deionized water to the same degree to maintain a consistent DOC. Samples were chloraminated by adding sodium hypochlorite (5.65 to 6 percent, Fisher Scientific) directly to the samples to form chloramines in situ, since the samples contained substantial ammonia concentrations (~40 to 60 mg- N/L). At the highest chloramine dosage employed (5 mg/L as Cl₂), there was an ~50-fold molar excess of ammonia. RO treatment reduced the ammonia concentration to ~3 mg-N/L. Hypochlorite stocks were standardized by measuring UV absorbance at 292 nm ($\epsilon_{292} = 362 \text{ M}^{-1}\text{cm}^{-1}$) (Furman et al., 1998). BAC treatment was conducted by passing samples through a ~5 cm² cross-sectional area column containing 58 mL of Filtrasorb 400 GAC with a 30-minute empty bed contact time (EBCT), as detailed previously (Chuang et al., 2017). Before and after sample treatment, a 20 mg/L as COD solution of acetate was passed through the BAC column; the removal of >80 percent of the COD validated the biological activity.

Figure 24: Laboratory-scale Advanced Treatment Train Options for Treating Pilot-scale SAF-MBR or Laboratory-scale FBR Effluents



Various combinations of ozone, chloramines and BAC treatment were applied upstream of RO treatment. O₃/BAC treatment alone was evaluated as an alternative to RO treatment. RO and O₃/BAC effluents were treated by the UV/hydrogen peroxide AOP and then chloramination under conditions reflecting those used to maintain a distribution system disinfectant residual. Blue stars indicate sample locations.

Source: Codiga Resource Recovery Center at Stanford

4.2.3 RO Flux Decline Measurements

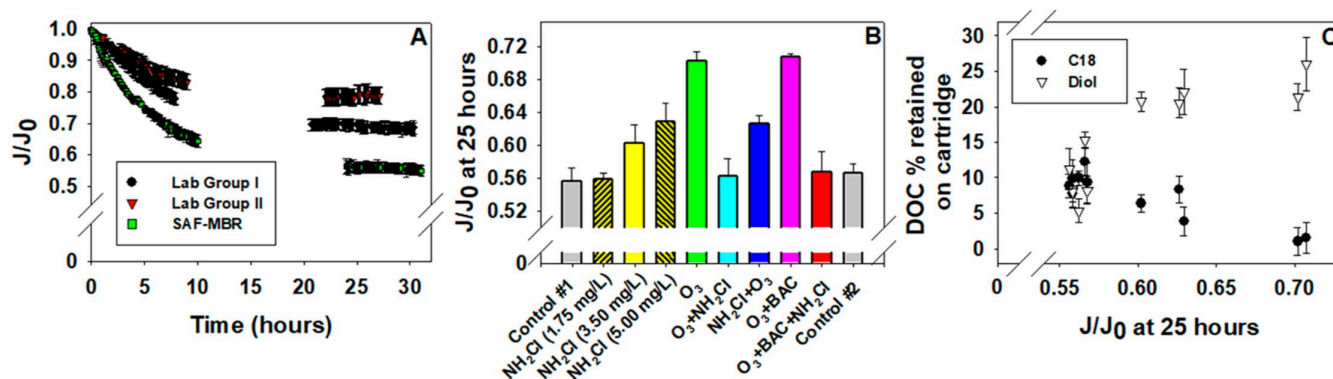
Flux decline was measured using a laboratory-scale crossflow RO test unit with three plate-and-frame membrane cell units operated in parallel, as described previously (Steinle-Darling et al., 2007). Each unit housed a 92 mm × 145 mm flat-sheet ESPA-DHR RO membrane coupon (Hydranautics, Oceanside, CA); this membrane was recommended by Hydranautics for use in potable reuse trains fed with aerobically treated secondary effluent. Permeate and retentate were recirculated into a temperature-controlled feed tank (68°F [20°C]) to maintain a 15 L feed volume and consistent composition throughout each run. New membranes were used for each experiment. The membrane pretreatment protocol was adapted from Ang et al. (2006). Membranes were soaked in deionized water, and then were compacted within the crossflow test unit by applying deionized water for 6 h at 250 psi and a 2.4 L/min flow rate. A 15-h period of stabilization and equilibration followed using foulant-free electrolyte solutions mimicking the constitutions of the laboratory reactor effluent (150 mg/L NaCl, 40 mg-N/L NH₄Cl, and 200 mg/L as CaCO₃ alkalinity) or the pilot-scale SAF-MBR reactor effluent (200 mg/L NaCl, 60 mg-N/L NH₄Cl, and 200 mg/L as CaCO₃ alkalinity). Feed pressure was maintained at 225 (±5) psi, and the influent flow rate was constant at 1.0 (±0.1) L/min, corresponding to an 8.5 cm/s crossflow velocity.

After pretreating the membranes, fouling experiments were carried out by running the samples under the same operating conditions employed for stabilization and equilibration for ~30 h. The permeate was collected in flasks placed on scales. The cumulative permeate weight in each flask was periodically measured and used to calculate the permeate flow rate. The permeate flow rate declined from an initial value of 1.0 L/h over the course of an experiment; the initial permeate flow rate corresponds to a permeate flux of 85 L m⁻²h⁻¹. The three parallel membrane units permitted the fouling experiments to be conducted in triplicate. The RO unit was cleaned after every run, and select runs were repeated throughout to demonstrate stable system operation. As validation, the flux decline profile observed during treatment of a 300 mg/L bovine serum albumin solution was similar to that observed by Ang and Eimelech during treatment of the same solution at an 8.1 cm/s crossflow velocity (Ang et al., 2007).

Note that the results from these fouling experiments are not expected to predict fouling rates that would be observed under full-scale operations. Full-scale RO systems typically operate under conditions of constant RO permeate flux, wherein fouling necessitates a higher feed pressure to maintain a constant RO permeate flux. Fouling by dissolved organics is important over short time scales, but biofouling contributes to fouling over longer time scales, even when disinfectants are added as pretreatments to control biofouling. The purpose of these experiments was to compare the efficacy of different pretreatments for mitigating fouling by dissolved organics. This mitigation could occur by chemical alterations to the dissolved organics resulting from reactions with oxidants (e.g., ozone) or removal of dissolved organics (e.g., BAC). Under the experimental conditions, RO permeate flux declined rapidly over the first 5 h, but eventually stabilized within 25 h (Figure 25A). Mitigation of RO fouling by dissolved organics was indicated by a slower decline in RO permeate flux, and a higher RO permeate flux after stabilization of the flux had been achieved. The initial RO permeate flux in these experiments (85 L m⁻²h⁻¹) was higher than those employed at full-scale. This was

necessary to enable significant fouling to be observed within the 25 h time scale. A long-term pilot-scale evaluation of RO fouling under constant-flux conditions, encompassing fouling by both dissolved organics and biofouling, is needed to characterize the fouling that would occur under full-scale conditions. The purpose of these experiments was to screen different pretreatment strategies regarding their efficacy for controlling dissolved organics, facilitating the selection of a more limited array of pretreatments to evaluate in future long-term pilot-scale testing. Although not predictive of the absolute fouling rates that would be observed at full-scale, the experimental procedure has been used in many previous studies to compare fouling rates by dissolved organics (Ang et al., 2006; Ang et al., 2007; Ang et al., 2011; Lee et al., 2006a; Lee et al., 2004; Lee et al., 2006b).

Figure 25: (A) Normalized RO Flux (J/J_0) Over Time for Representative Untreated Controls of Pilot-scale SAF-MBR and Lab-scale FBR (Groups I and II) Effluents. (B) Normalized RO Flux (J/J_0) After 25 h for Pilot-scale SAF-MBR Effluent Treated With Different Doses of Chloramines and Different Combinations of Chloramines (3.5 mg/L as Cl_2), Ozone (0.8 mg O_3 /mg DOC) and BAC (30 min EBCT). (C) Relationship Between the Fraction of DOC Retained on C18 or Diol SPE Cartridges and the Normalized RO Flux Measured After 25 h for Samples of RO Influent From the Pretreated and Control SAF-MBR Effluent Samples From Panel B. Error Bars Represent the Standard Deviations of Triplicate (A, B) or Duplicate (C) Measurements.



Source: Codiga Resource Recovery Center at Stanford

4.2.4 Polarity Rapid Assessment Method (PRAM)

The polarity of the RO influent samples after disinfectant pretreatment was assessed using a modified PRAM protocol, as described previously (Rosario-Ortiz et al., 2007a; Rosario-Ortiz et al., 2007b). This method characterizes the DOC by its retention on solid phase extraction (SPE) cartridges containing media targeting different chemical characteristics. We used 3 mL Supelco C18 and Diol SPE cartridges (200 mg media, 8 mg carbon capacity) to evaluate the hydrophobicity and hydrophilicity of the DOC, respectively. SPE cartridges were cleaned with 10 mL HPLC grade methanol, followed by 150 mL of ultrapure water generated from a Millipore system with a Q-Gard 1 purification cartridge. After this water rinse, there was no detectable DOC in the SPE effluent. A 50 mL sample was passed through the cartridge, and the final 15 mL was analyzed for DOC. For example, a greater difference between the influent

and effluent DOC measured across a C18 SPE cartridge would indicate that the DOC exhibited higher hydrophobicity.

4.2.5 Post-Treatment of RO and O₃/BAC Effluents

The RO or alternative O₃/BAC effluents were treated by the UV/H₂O₂ AOP and chloramines to characterize DBP formation under conditions mimicking advanced treatment for potable reuse. Hydrogen peroxide stocks (30 percent v/v, Fisher Scientific) were standardized by UV absorbance at 240 nm ($\epsilon = 40 \text{ M}^{-1} \text{ cm}^{-1}$) (Nelson et al., 1972). Hydrogen peroxide was added to samples at 3 mg/L. UV irradiation was conducted using a semi-collimated beam apparatus containing three 15 W Philips low pressure mercury lamps emitting at 254 nm, as detailed previously (Chuang et al., 2016). UV light shone down through a shutter onto a 750 mL crystallization dish, which was stirred by a magnetic stir bar. Incident irradiance (0.60 mW cm^{-2}) was determined by iodide–iodate actinometry (Bolton et al., 2011; Goldstein et al., 2008). A fluence of 700 mJ/c m² was targeted.

The AOP effluent samples were chloraminated under Uniform Formation Conditions (UFC) mimicking conditions relevant to chloraminated distribution systems. The pH of the AOP effluent was adjusted to ~8 with 4 mM borate buffer and treated with 5 mg/L of preformed monochloramine. Monochloramine stocks were prepared daily by adding sodium hypochlorite dropwise to an ammonium chloride solution (1:1.2 molar ratio at pH 8.5), and standardized by measuring UV absorbance at 245 and 295 nm, as described previously (Schreiber et al., 2005). The chloraminated samples were maintained in the dark for 3 days at room temperature (68°F [20°C] to 70°F [21°C]), leaving a > 1 mg/L as Cl₂ total chlorine residual. The total chlorine residual was quenched with 33 mg/L ascorbic acid, and samples were extracted within 4 h for DBP analysis.

4.2.6 Analyses and Toxicity Calculation

Analytical methods for basic water quality parameters applied to filtered water samples are provided in Szczuka et al. (2019), Supporting Information (SI) Text S1. Forty-three compounds were measured in samples collected from the sample points indicated in Figure 24 using gas chromatography and mass spectrometry-based modified USEPA Methods described previously (Zeng et al., 2016b) and summarized in Szczuka et al. (2019), SI Text S2. Thirty-five halogenated DBPs, including 4 regulated THMs, 6 iodinated THMs (I-THMs), 10 HAAs (including iodoacetic acid), 4 haloacetonitriles, 4 haloacetamides, 4 haloacetaldehydes, 2 halo ketones and chloropicrin were measured in triplicate with ~0.2 µg/L method reporting limits (MRLs). Eight N-nitrosamines were measured in duplicate with ~2 ng/L MRLs.

The contribution of a DBP to the toxicity of a disinfected water is a function of both its concentration and its toxic potency. Measured DBP concentrations were divided by metrics of toxic potency to evaluate their contribution to the DBP-associated toxicity of the disinfected waters. The metrics of toxic potency focused on DBP concentrations associated with a 50 percent reduction in the growth of Chinese hamster ovary (CHO) cells compared to untreated controls (i.e., LC50 cytotoxicity values) for halogenated DBPs. Concentrations associated with a 50 percent lifetime excess cancer risk (i.e., LECR50 values) were used for N-nitrosamines, because these values are lower than LC50 cytotoxicity values (see Szczuka et al. (2019), SI

Text S3 for further discussion). The purpose was not to estimate an absolute risk, but to estimate the relative importance of the individual DBPs for the DBP-associated toxicity. The toxicity-weighting procedure, and the same toxic potency metrics, have been employed previously (Zeng et al., 2016a; Chuang et al., 2017; Zeng et al., 2016b; Li et al., 2018; Furst et al., 2018; Szczuka et al., 2017).

4.3 Results and Discussion

4.3.1 Water Quality

Szczuka et al. (2019), SI Table S1, provides the basic water quality parameters for the untreated effluents of the SAF-MBR and the lab-scale FBR reactors. The bromide concentration was higher in the SAF-MBR effluent (227 µg/L) than the lab-scale FBR effluents (~50 µg/L). DOC, the other major difference between the effluents, was 3.5 mg/L for the SAF-MBR effluent. The batches of effluent collected from the FBRs fell into two groups, with effluents used for ozonation, chloramination, and ozonation/chloramination experiments (Group I) featuring 2.2 mg/L DOC and samples used for ozonation/BAC and ozonation/BAC/chloramination experiments (Group II) containing 1.6 mg/L DOC. Because the DOC concentration should impact RO fouling, each fouling experiment with FBR effluent compared pretreated effluent to a concurrent untreated control. The SAF-MBR treated filtered sewage with a higher strength (600 mg-COD/L) than the acetate and propionate-based synthetic sewage (250 mg-COD/L) supplied to the FBRs. The higher DOC concentration in the SAF-MBR effluent may reflect the higher influent COD and the occurrence of nonbiodegradable organics in the sewage. Regardless, all of the reactors achieved ~20 mg-COD/L in the effluent (≥90 percent removal).

At 44–62 mg-N/L, ammonia was the main inorganic nitrogen species, as expected for the anaerobic effluent. The effluent pH ranged from 6.9 to 7.1 upon sample collection, but increased within 5 h to pH 8.0, likely due to off-gassing of carbon dioxide. While pH has been shown to affect RO membrane fouling, (Ang et al., 2006; Ang et al., 2007) back-titrating the pH to 7.0 with HCl showed that the difference in pH did not affect membrane fouling (Szczuka et al., 2019, SI Figure S1).

The carbohydrate and protein concentrations measured in a filtered pilot-scale FBR sample were 13.8 (±1.1) mg-glucose/L and 12.6 (±1.3) mg-BSA/L, respectively. The carbohydrate concentration was comparable to the 4.9–12.3 mg-glucose/L levels measured in aerobic MBR effluents, while the protein concentration was higher than the 1.0–4.3 mg-BSA/L levels measured in aerobic MBR effluents (Liang et al., 2007, Juang et al., 2013). In the FBR influent, 6.0 (±0.1) mg-S/L sulfate and <5 µg-S/L sulfides were detected, while <0.7 mg-S/L sulfate and 2.1 (±0.01) mg-S/L sulfides were detected in the FBR effluent. The results indicate the presence of sulfate-reducing bacteria, with some of the sulfides likely lost to volatilization together with the methane.

4.3.2 RO Membrane Fouling

The RO permeate flux (J) values were initially 80 to 85 L m⁻²h⁻¹. Figure 25A provides example plots of the fluxes over time normalized by the initial flux (i.e., J/J₀) for untreated controls representative of the pilot-scale SAF-MBR effluent and the two Groups of lab-scale FBR

effluents. The normalized flux values declined over the initial ~5 h, but stabilized within 25 h. The normalized flux values measured at 25 h, hereafter referred to as the post-stabilization normalized flux values, ranged from 0.56 for the SAF-MBR effluent to 0.80 for the Group II FBR effluent. These post-stabilization normalized flux values are within the 0.50 to 0.95 range observed for RO treatment of 25–50 mg/L solutions of model proteins and polysaccharides under similar RO operating conditions (i.e., ~ 80 L m⁻²h⁻¹ initial flux) (Lee et al., 2006a; Li et al., 2007). The flux decline broadly correlated with the DOC (Szcuka et. al. (2019) SI Figure S2). Any differences in the pilot-scale SAF-MBR and lab-scale FBR effluents driven by differences in their influents (i.e., nonbiodegradable sewage constituents versus SMPs generated from synthetic sewage) appeared to be of lower importance than the bulk DOC.

Disinfected effluents followed similar patterns in terms of flux decline trends, with relatively rapid declines within 10 h, but with the normalized flux stabilizing within 24 h. Figure 25B compares the post-stabilization normalized flux for the SAF-MBR effluent after pretreatment with different combinations of chloramines (1.75 to 5.0 mg/L as Cl₂ for a 30 min contact time prior to RO treatment), ozone (0.8 mg O₃/mg DOC) and BAC (30 min empty bed contact time). The consistency of the post-stabilization normalized flux for untreated controls run at the beginning and end of the experiments demonstrated the stability of the RO system operation. The post-stabilization normalized flux increased modestly from 0.56 to 0.63 when the chloramine dose was increased to 5 mg/L as Cl₂, covering the range typically applied to control biofouling upstream of RO systems receiving aerobically treated wastewater. Biofouling should not be significant over the 25-h time scale of the experiment. Instead, dissolved organics should dominate fouling over the 25-h experimental time scale, and the changes induced by chloramine pretreatment reflect alterations in the dissolved organics resulting from reactions with chloramines (see the discussion in the following section). After ozonation, samples were held for 30 min prior to chloramination, BAC treatment or RO treatment to permit the decay of the ozone residual and thereby prevent membrane damage. Ozonation alone reduced the flux decline significantly, achieving a post-stabilization normalized flux of 0.70; rationales for the effects of disinfectants on flux decline are provided in the next section. Because the ozone residual must dissipate upstream of membranes to prevent membrane degradation, ozone typically must be paired with chloramines to inhibit biofilm growth on membranes (Ridgway et al., 1984; Xu et al., 2010); if properly applied, chloramines can mitigate biofouling, leaving fouling by dissolved organics as a dominant driver of membrane fouling. Although either order of chloramine and ozone addition increased the flux decline relative to ozonation alone, a lower flux decline was observed when ozone was added after chloramines. BAC treatment after ozonation did not affect flux decline relative to ozonation alone, nor did BAC treatment between ozonation and chloramination affect the flux decline relative to ozonation and chloramination alone; however, BAC treatment may aid treatment by quenching ozone residuals prior to RO treatment. BAC treatment was expected to reduce the flux decline by removing DOC, but the DOC removal was at most 14 percent. The low DOC removal may reflect the prior removal of the most biodegradable fractions of DOC within the SAF-MBR, which also contains biofilm-coated activated carbon, albeit with anaerobic bacteria. The similarity of the results for the SMPs in the lab-scale FBR effluents (Szcuka et al., 2019, SI Figure S3) suggests that SMPs may contribute significantly to the behavior of the DOC in

the pilot-scale SAF-MBR effluent. The one exception was for chloramination alone, where chloramination increased the flux decline when applied to the lab-scale FBR effluent.

The positive impact of ozonation for mitigating fouling concurs with previous research where ozonation of aerobic MBR effluent reduced RO fouling (Stanford et al., 2011) and ozonation of an aerobic sequencing batch reactor effluent decreased nano-filtration membrane fouling (Vatankhah et al., 2018). To provide some comparison of the effects of pretreatments on RO flux decline with aerobically treated wastewater effluents using the same experimental apparatus, experiments were conducted using a nitrified secondary activated sludge effluent (pH 8.0, 7.1 mg/L DOC). The post-stabilization normalized RO flux in an untreated control was 0.38 (Szcuka et al., 2019, SI Figure S4), lower than the 0.56 value observed with the SAF-MBR effluent. Treatment of the aerobic effluent with 0.8 mg O₃/mg DOC or 5 mg/L as Cl₂ chloramines increased the post-stabilization normalized flux to 0.54 and 0.50, respectively. Similar to the SAF-MBR effluent, both ozonation and chloramination of the aerobic effluent mitigated flux decline, but the differences in the performance between ozonation and chloramination were not significant ($p < 0.05$ by a paired t-test relative to their respective controls). Thus, the fouling behavior of the SAF-MBR and aerobic effluents were qualitatively similar, although the flux decline was lower overall for the SAF-MBR, likely due to its lower DOC (3.5 mg/L); the DOC of this aerobic effluent was at the low end of the 8.7 to 14.9 range observed in aerobic secondary effluents feeding potable reuse trains (Zeng et al., 2016a).

4.3.3 Correlation of Flux Decline with DOC Hydrophobicity

It was hypothesized that flux decline should increase with the prevalence of hydrophobic moieties in DOC that would adhere to the polymeric membrane surface. The prevalence of hydrophobic and hydrophilic moieties in the SAF-MBR effluent DOC before and after various pretreatments was assessed using the PRAM technique by measuring the retention of DOC on hydrophobic C18 and hydrophilic Diol SPE cartridges. For samples of RO influent collected after pretreatment of SAF-MBR effluent (Figure 25C), the maximum DOC retention on the hydrophobic C18 SPE cartridge was 12 percent for an untreated control, while the maximum DOC retention on the hydrophilic Diol SPE cartridge was 26 percent after treatment by ozone and BAC (Szcuka et al., 2019, SI Table S2). The DOC retention on these cartridges indicated a clear correlation between the post-stabilization normalized RO flux and increasing hydrophobicity and decreasing hydrophilicity (Figure 25C).

Similar trends were observed for the Group I lab-scale FBR effluents (Szcuka et al., 2019, SI Figure S5), although the error in the DOC measurements was larger (Szcuka et al., 2019, SI Table S3) due to the lower DOC values. The similarity of the trends again suggests that the behavior of SMPs correlates with that of the broader DOC. For the Group II FBR effluents, which featured the lowest DOC concentrations (1.6 mg/L in the controls), the error in the DOC measurements was too high to draw any conclusions.

The PRAM results indicate that ozonation reduced fouling by rendering the DOC more hydrophilic. Previous research has demonstrated that ozonation of surface water or wastewater NOM renders it more hydrophilic, by degrading aromatic functional groups and generating carboxylic acids (Song et al., 2010; Świetlik et al., 2004; Van Geluwe et al., 2011a; Van Geluwe et al., 2011b). Zeng et al. (2014) demonstrated that treatment of model proteins, fatty

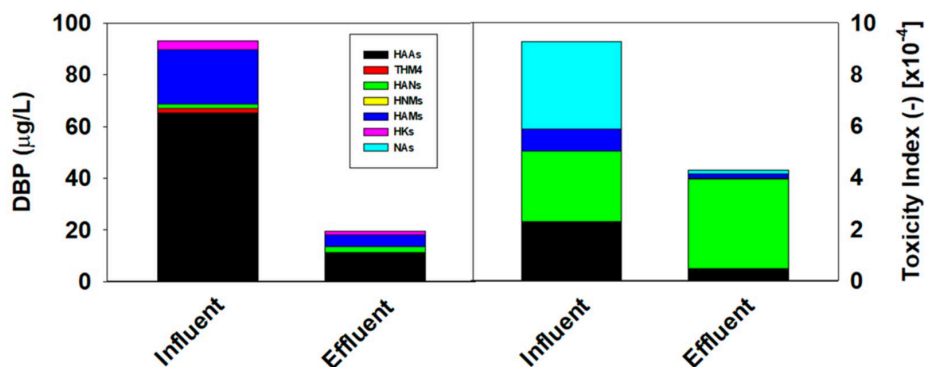
acids, polysaccharides, humic substances, and surface waters at similar ozone doses decreases the attachment efficiency of the organic matter to a model hydrophobic surface.

Chloramination of the lab-scale FBR effluent increased the hydrophobic character of the SMPs and RO flux decline (Szczyka et al., 2019, SI Figures S3 and S5), while chloramination of the pilot-scale SAF-MBR effluent increased the hydrophilic character of the effluent DOC and increased the post-stabilization normalized RO flux (Figure 25). Although chloramination was not evaluated, Zeng et al. (2014) demonstrated that increasing the free chlorine dosed to model compounds and surface waters first increased their attachment efficiency to a hydrophobic surface, likely by forming hydrophobic chlorine-containing byproducts. However, at higher doses the attachment efficiency began to decrease, and in some cases was lower than for untreated controls, likely because oxidation reactions produced lower molecular weight, hydrophilic products. At the total chlorine to DOC ratios employed in the current study (i.e., 0.17 mmol oxidant/mmol carbon for application of 3.5 mg/L as Cl₂ chloramines to 3.5 mg/L DOC), Zeng et al. (2014) observed a net increase in attachment efficiency, concurring with the results from chloramination of the SMPs from the lab-scale FBR. The opposite behavior observed during chloramination of the SAF-MBR effluent may suggest that chloramine reactions with the non-SMP components of the SAF-MBR DOC are more likely to lead to oxidation than chlorine addition. Over the short-term, fouling by dissolved organics should dominate over biofouling due to the application of disinfectants, such as chloramines. Over the longer term, biofouling could contribute to fouling and necessitate membrane cleaning.

4.3.4 DBP Formation Along Potable Reuse Trains

Figure 26 provides the concentrations of DBPs on a mass or toxicity-weighted basis measured in the pilot-scale SAF-MBR influent and effluent after application of the chloramine UFC protocol. SAF-MBR treatment reduced the total concentration of DBPs measured post-chloramination by ~ 80 percent such that the total concentration of DBPs remained ≤20 µg/L. HAAs were the dominant DBP class on a mass basis, followed by haloacetamides. THMs and HAAs in the chloraminated SAF-MBR effluent remained well below their 80 µg/L and 60 µg/L Maximum Contaminant Levels (MCLs). The only N-nitrosamines measured in the chloraminated SAF-MBR effluent were N-nitrosodimethylamine (NDMA, 5.7 ng/L) and N-nitrosopyrrolidine (6.7 ng/L). On a toxicity-weighted basis, SAF-MBR treatment reduced the total post-chloramination DBP-associated toxicity by 55 percent to 4×10^{-4} . Haloacetonitriles were the dominant contributors to toxicity in the chloraminated effluent.

Figure 26: DBPs Measured in the Pilot-scale SAF-MBR Influent and Effluent After Chloramine UFC Treatment on a Mass and Toxicity-weighted Basis.



THM4 = four regulated trihalomethanes. HANs = haloacetonitriles. HNM4 = halonitromethanes. HAMs = haloacetamides. HKs = halo ketones. Nas = nitrosamines

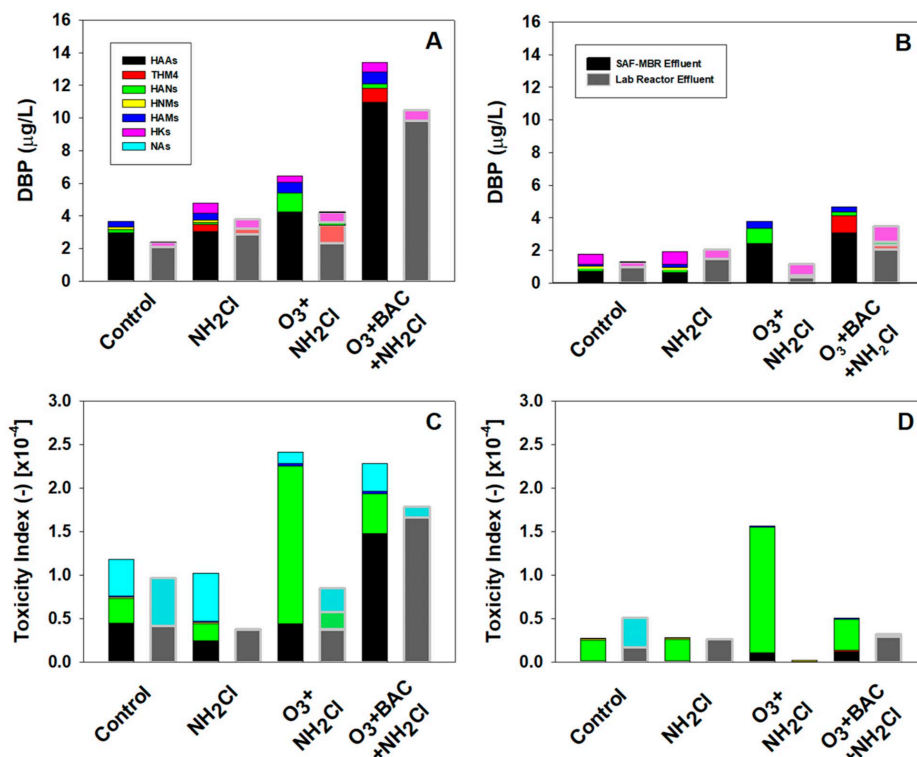
Source: Codiga Resource Recovery Center at Stanford

Figure 27A and C provide the mass-based and toxicity-weighted concentrations of DBPs measured directly in the pilot-scale SAF-MBR and lab-scale FBR effluents or after pretreatment by chloramination (NH_2Cl), ozonation followed by chloramination ($\text{O}_3/\text{NH}_2\text{Cl}$), or ozonation followed by BAC and then chloramination ($\text{O}_3/\text{BAC}/\text{NH}_2\text{Cl}$); all were measured without post-chloramination using the UFC protocol. The ozone residual was allowed to decay prior to chloramination or BAC treatment and the chloramine contact time was 30 min before halting for DBP analysis. The highest total DBP concentration was only $\sim 14 \mu\text{g/L}$ in the SAF-MBR effluent treated by $\text{O}_3/\text{BAC}/\text{NH}_2\text{Cl}$. Total DBP concentrations measured in the lab-scale FBR effluent after the same pretreatments were typically ~ 25 percent lower than for the SAF-MBR effluent, suggesting an important contribution of SMPs to DBP formation in the SAF-MBR effluent. HAAs were the dominant DBP class on a mass basis in all cases. The highest N-nitrosamine concentrations were detected in the SAF-MBR effluent treated by $\text{O}_3/\text{BAC}/\text{NH}_2\text{Cl}$, where 7.7 ng/L NDMA and 9.9 ng/L N-nitrosomorpholine were detected. The total toxicity-weighted DBP concentrations ranged from $\sim 1.0\text{--}2.5 \times 10^{-4}$ for the SAF-MBR effluent, with the higher values associated with ozone pretreatment. HAAs, haloacetonitriles and N-nitrosamines were the main contributors to the DBP-associated toxicity.

A similar total concentration of DBPs was measured after $\text{O}_3/\text{BAC}/\text{NH}_2\text{Cl}$ treatment upstream of RO treatment at a potable reuse facility receiving aerobically treated municipal wastewater, although THMs were the dominant DBPs on a mass basis (Zeng et al., 2016a). Much higher total DBP concentrations ($\geq 60 \mu\text{g/L}$) were observed in the RO influents at other facilities receiving aerobically treated municipal effluent that employed NH_2Cl or $\text{O}_3/\text{NH}_2\text{Cl}$ as pretreatments, (Zeng et al., 2016a) and again THMs were the dominant DBP class. The total toxicity-weighted DBP concentrations determined for these RO influents ranged from $\sim 5\text{--}14 \times 10^{-3}$, with haloacetonitriles, haloacetamides, and haloacetaldehydes typically the dominant contributors to the DBP-associated toxicity (Zeng et al., 2016a). Thus, regardless of the pretreatment strategy, the RO influent associated with the SAF-MBR effluent featured total toxicity-weighted DBP concentrations that were at least an order of magnitude lower than observed in RO influents at facilities receiving aerobically treated secondary effluents.

Figure 27B and D provide the mass-based and toxicity-weighted concentrations of DBPs measured after pretreatment of the SAF-MBR effluent, passage through RO, treatment by the UV/H₂O₂ AOP and then chloramination for 3 days under UFC conditions. Compared to the RO influents without post-chloramination (Figures 4.4A and 4.4C), the total concentrations of DBPs were reduced by at least 50 percent even though the final effluent was chloraminated for 3 days. The highest total concentration was only ~5 µg/L for pretreatment by O₃/BAC/NH₂Cl. The total toxicity-weighted concentrations of DBPs in the final effluents following post-chloramination ranged from ~0.25–1.6 × 10⁻⁴. Haloacetonitriles were the dominant contributors to the DBP-associated toxicity. Note the similarity between the haloacetonitrile concentrations in the RO influent (Figures 4.4A and 4.4C) and the final effluent post-chloramination (Figures 4.4B and 4.4D), reflecting their low rejection by RO (Zeng et al., 2016a) and poor removal by the UV/H₂O₂ AOP (Chuang et al., 2016). For pilot- or full-scale reuse facilities receiving aerobic secondary effluents, the total DBP concentrations after pretreatment by NH₂Cl upstream of microfiltration and then treatment by RO, the UV/H₂O₂ AOP, and the chloramine UFC protocol were ~15–30 µg/L. Furthermore, the total toxicity-weighted DBP concentrations in the chloraminated final effluents of these aerobic-related facilities were ~ (4–8) × 10⁻⁴ (Zeng et al., 2016a), at least 4-fold higher than for the anaerobic-related samples in this study.

Figure 27: DBPs Measured After Various Pretreatments on a Mass and Toxicity-weighted Basis Directly in the RO Influent Without Post-chloramination (A, C) and in the Final Effluent After Treatment by RO, the UV/H₂O₂ AOP and Post-chloramination Using the Chloramine UFC Protocol (B, D)

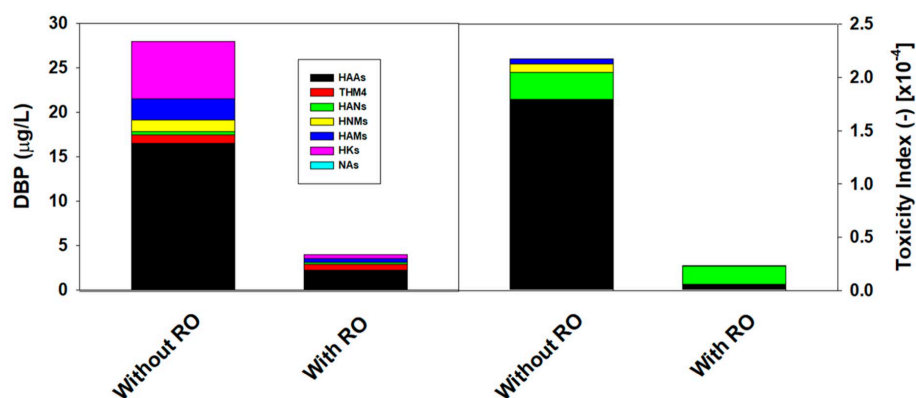


Solid bars represent pilot-scale SAF-MBR effluent. Shaded bars represent lab-scale FBR effluent.

Source: Codiga Resource Recovery Center at Stanford

Lastly, O₃/BAC without RO is being considered as an alternative treatment train to MF/RO systems for potable reuse. Figure 28 compares the DBP concentrations on a mass and toxicity-weighted basis for the SAF-MBR effluent treated by O₃/BAC, the UV/H₂O₂ AOP and the chloramine UFC protocol without and with RO treatment between the BAC and UV/H₂O₂ AOP. At ~28 µg/L, the total concentration of DBPs was ~7-fold higher without RO treatment. The total toxicity-weighted DBP concentration was ~9-fold higher without RO treatment at 4.5 × 10⁻⁴. HAAs were the dominant DBP class on a mass basis for both effluents. While HAAs dominated the DBP-associated toxicity for the effluent without RO treatment, haloacetonitriles dominated the DBP-associated toxicity for the final effluent receiving RO treatment.

Figure 28: DBPs Measured on a Mass and Toxicity-weighted Basis After Treatment of the Pilot-scale SAF-MBR Effluent by O₃/BAC, the UV/H₂O₂ AOP and Post-chloramination Using the Chloramine UFC Protocol Without and With RO Treatment Between the BAC and the UV/H₂O₂ AOP



Source: Codiga Resource Recovery Center at Stanford

4.3.5 Environmental Implications

For utilities in arid regions considering switching to this anaerobic secondary treatment technology, the compatibility of the SAF-MBR effluent with potable reuse trains is a key consideration. Our results indicate that the effects of disinfectant pretreatments on the fouling behavior of the SAF-MBR effluent were qualitatively similar to that of aerobic effluents, although the flux decline can be lower, likely due to the low DOC achieved by SAF-MBR treatment. Ozonation was most effective for mitigating flux decline by rendering the DOC more hydrophilic. If combined with chloramination, ozonation should be added after chloramines to minimize flux decline. BAC treatment had little effect in terms of DOC removal and mitigating flux decline.

The ~5 µg/L highest total concentration of DBPs measured for SAF-MBR effluent following treatment by different disinfectant pretreatments, RO, the UV/H₂O₂ AOP and post-chloramination was significantly lower than the ~15–30 µg/L range measured in full-scale RO-based potable reuse trains receiving aerobic effluents (Zeng et al., 2016a). The total toxicity-weighted DBP concentrations in these final effluents were at least 4-fold lower for the SAF-MBR effluents than for the aerobic effluents. Haloacetonitriles typically dominated the DBP-associated toxicity for both effluents (Zeng et al. 2016a). These metrics indicate the high

quality of the SAF-MBR effluent. Indeed, the total DBP concentration for SAF-MBR effluent treated only by O₃/BAC, the UV/H₂O₂ AOP and post-chloramination without RO was comparable on a mass- or toxicity-weighted basis to that for aerobic effluents receiving various pretreatments, and then treatment by RO, the UV/H₂O₂ AOP and post-chloramination. These results suggest the possibility of avoiding RO treatment, and its associated issues with energy consumption and concentrate disposal.

Given the qualitative similarities in the behavior of the SAF-MBR and aerobic effluents in terms of RO fouling behavior and DBP formation, the lower DOC achieved by SAF-MBR treatment may account for a significant fraction of its advantages. The qualitative similarity with regard to RO fouling and DBP formation between the SAF-MBR effluent and the SMPs emitted from lab-scale FBR reactors suggests that SMPs contribute significantly to the DOC in the SAF-MBR effluent. However, further research is needed to characterize the SAF-MBR effluent, as some differences with aerobic effluents were noted, such as the predominance of HAA formation in the SAF-MBR effluent compared to THMs in aerobic effluents.

Additional research is needed before anaerobic secondary effluent can be successfully linked to potable reuse. An evaluation is needed of pathogen removal within the SAF-MBR, for comparison to current aerobic biological treatment systems. Methods are needed to remove nutrients. The elevated ammonia concentrations in the SAF-MBR effluent (~50 mg-N/L) could affect potable water quality. The incorporation of RO treatment in the reuse train was beneficial in this regard, as RO treatment reduced the ammonia concentration to ~3 mg-N/L. Additionally, the sewage in this study featured low sulfate concentrations (6.0 mg-S/L). For sewage containing high sulfate concentrations, one area that needs further research regards technologies to mitigate sulfide production by biological sulfate reduction. In addition to reducing the energy recoverable as methane, sulfides are potent odorants, and scavenge chemical oxidants (e.g., ozone and chloramines) added to control pathogens and mitigate RO membrane fouling. High sulfate concentrations should also promote the conversion of the microbial community from methanogens to sulfate-reducers. Whether the characteristics of the SMPs emitted by sulfate-reducers differ with respect to RO fouling behavior and DBP production requires further research. While DBPs are regulated and may occur at concentrations closer to levels of public health concern than other contaminants (NRC, 2012), such as pharmaceuticals, these other contaminants raise concerns for public acceptance. A previous study demonstrated superior removal of pharmaceuticals by a pilot-scale SAF-MBR unit compared to a parallel activated sludge process (McCurry et al., 2014). However, whether conversion of the microbial community toward sulfate-reducers affects the removal of pharmaceuticals and other chemical contaminants in sewage also requires further research.

CHAPTER 5: Technology Transfer

5.1 Technology/Knowledge Dissemination Target Audience

In addition to the general public, the project team targeted several overlapping audiences within the water and wastewater sector with the results of this project. Specific stakeholder groups, and the use for which they will employ project results, are summarized in Table 16:

Table 16: Users and Uses of Project Results

User	Use
Regulators	Verify capability of technology to achieve target water quality standards; use data as basis to authorize further and larger-scale deployment of the technology.
Utilities	Determine if the SAF-MBR would be viable and beneficial in their service area; evaluate potential costs and benefits.
Consulting Engineers	Learn performance benchmarks and some modeling parameters useful in anticipating system performance in new contexts, and for designing other SAF-MBRs,
Researchers/Academia	Identify key knowledge gaps to guide basic research for further improving performance of the SAF-MBR,

Source: Codiga Resource Recovery Center at Stanford

5.2 Technology/Knowledge Dissemination Activities

The results from this work were disseminated using various channels intended to reach the diverse target audiences of this project, as summarized in Table 17.

Table 17: Activities and Target Audience for Technology/Knowledge Dissemination

Activity	Target Audience
Publication of results in peer-reviewed publications accessible to the public	Regulators Consulting Engineers Researchers/Academia
Direct communication with directors of utilities, regulatory agencies, and associations like the Bay Area Clean Water Agencies (BACWA) and the California Association of Sanitation Agencies (CASA)	Regulators Utilities
Presentation of results at annual convenings of ReNUWIt, the NSF Engineering Research Center for Reinventing the Nation's Urban Water Infrastructure	Regulators Consulting Engineers Researchers/Academia Utilities

Activity	Target Audience
Presentation in at least two conferences such as WaterReuse California (WRCA), American Water Works Association (AWWA), California Water Environment Association (CWEA) annual conference, or Water Environment Federation (WEFTEC) annual conference	Regulators Consulting Engineers Utilities
Presentation at CEC EPIC workshops and events	Regulators Consulting Engineers Researchers/Academia Utilities
Host an open house on site to demonstrate system	Regulators Consulting Engineers Utilities
Issue project updates in trade publications like <i>Civil Engineering</i> , <i>AWWA and CWEA Publications</i> , as well as news outlets like the <i>Stanford Report</i>	Regulators Consulting Engineers Researchers/Academia Utilities
Publicizing project information on a publicly accessible website	Regulators Consulting Engineers Researchers/Academia Utilities

Source: Codiga Resource Recovery Center at Stanford

5.2.1 Activities to Date:

The following activities have been conducted to date:

- Publication of news articles on the CEC-funded SAF-MBR project in Civil Engineering (September 2018) and on the Stanford News Service (May 2018, <https://news.stanford.edu/2018/05/10/new-plant-tests-energy-saving-way-treat-wastewater/>)
- Hosting a project launch meeting with regional utility stakeholders, consulting engineers, regulators, and academics, as documented on the California Water Environment Association website (<https://www.cwea.org/news/svcw-set-to-launch-largest-pilot-ever-for-anaerobic-secondary-treatment/>, last accessed 4/13/22)
- Presentation of SAF-MBR technology and potential benefits at California Water Environment Association annual meeting, April 18 2018, "The Future of Water Treatment and Resource Recovery," and to webinars sponsored by the US Department of Energy and others
- Highlighting the SAF-MBR as a technology of interest on the Leaders Innovation Forum for Technology (LIFT) web portal hosted by the Water Research Foundation (WERF) (<https://www.cwea.org/news/svcw-featured-as-lift-research-partner/>, last accessed 4/13/22)

- Presentation of SAF-MBR technology and project at California Energy Commission EPIC Symposium, February 19, 2019, on a panel entitled “Enabling Localized Clean Energy Portfolios”
- Publication of a peer-reviewed journal article on processing of SAF-MBR effluent using reverse osmosis (RO) and implications for potable water reuse in February 2019, written by Aleksandra Szczuka, Juliana P. Berglund-Brown, Hannah K. Chen, Amanda N. Quay, and William A. Mitch (2019). “Evaluation of a Pilot Anaerobic Secondary Effluent for Potable Reuse: Impact of Different Disinfection Schemes on Organic Fouling of RO Membranes and DBP Formation.” *Environmental Science & Technology*, 53 (6), 3166-3176. DOI: 10.1021/acs.est.8b05473. (pubs.acs.org/doi/10.1021/acs.est.8b05473)
- Publication of a peer-reviewed journal article on processing of SAF-MBR effluent for non-potable water reuse in March 2021 Written by Aleksandra Szczuka, Juliana P. Berglund-Brown, Jessica A. MacDonald, and William A. Mitch (2021). “Control of sulfides and coliphage MS₂ using hydrogen peroxide and UV disinfection for non-potable reuse of pilot-scale anaerobic membrane bioreactor effluent.” *Water Research*, X 11, 100097. DOI: <https://doi.org/10.1016/j.wroa.2021.100097>
- Featuring the SAF-MBR on SVCW’s website (<https://svcw.org/sustainability/innovation/new-technology/>, last accessed 4/13/22)

While it is not possible to list all participants or stakeholders that have been engaged with our various knowledge transfer activities, a non-exhaustive sample of the various groups we have engaged is provided in Table 18.

Table 18: Partial List of Stakeholders Engaged in Technology/Knowledge Dissemination Activities

Stakeholder Type	Partial List of Engaged Stakeholders
Regulators/Government	California State Water Resources Control Board San Francisco Bay Regional Water Quality Control Board US Environmental Protection Agency California Water Boards, Division of Drinking Water CA State Senator Scott Wiener
Utilities	SVCW City of Palo Alto Valley Water San Francisco Public Utilities Commission BACWA BAWSCA (Bay Area Water Supply and Conservation Agency) Linda County Water District CASA

Stakeholder Type	Partial List of Engaged Stakeholders
Consulting Engineers	Kennedy/Jenks Consultants Brown and Caldwell West Yost Lee + Ro Sherwood Design Engineers
Researchers/Academia	Lawrence Berkeley National Laboratory ReNUWIit (includes UC Berkeley, Colorado School of Mines, Stanford, New Mexico State University)
Equipment Providers	Suez Endress & Hauser Ovivo LG NanoH2O Trojan Technologies Sulzer Flo-Line Technology

Source: Codiga Resource Recovery Center at Stanford

5.3 Policy Development Activities

A key aspect of this project is sharing project results with key regulatory authorities who will be responsible for certifying the SAF-MBR as a technology suitable for potable and non-potable water reuse. We have shared results through project Technical Advisory Committee meetings with the Division of Drinking Water (DDW) at the California Water Boards, as well as through regional partnership workshops.

SVCW is one of the lead agencies in a regional partnership preparing local agencies, regulators, and the public for the future deployment of potable water reuse systems in the San Francisco Bay Area. This partnership convenes key partners, including the State Water Resources Control Boards and the San Francisco Bay Regional Water Quality Control Board. This CEC-funded project is enabling SVCW to introduce the concept of anaerobic secondary treatment as a possible alternative technology to be used in combination with post-treatment systems to meet required water quality objectives, with lower energy requirements, and other contaminant reduction benefits. Some of the regulators engaged in this process are listed in Table 18.

Future engagement with regulators will focus on engaging DDW, as well as the San Francisco Bay Regional Water Quality Control Board. The former is responsible for granting Title 22 certifications for water reuse systems and thus is critical to enabling wider adoption of the SAF-MBR. Key requisites for Title 22 approval include obtaining DDW determination of the conditions under which SAF-MBR effluent qualifies as fully oxidized and obtaining DDW approval of full treatment trains that further purify SAF-MBR effluent to meet potable and non-potable standards. The ongoing pilot tests funded by the US Bureau of Reclamation and the California State Water Resources Control Boards – Prop 1, which are discussed in Section 6.1, should yield the operation data needed to achieve this milestone.

CHAPTER 6:

Future Work to Commercialize Technology

Through this project at SVCW, the SAF-MBR proved to be a viable technology to achieve secondary effluent standards for wastewater treatment while generating a surplus of renewable energy. The performance of the system was demonstrated at a scale of 24,000 gallons per day (gpd). Further, strategies to further treat SAF-MBR effluent to achieve both potable and non-potable water reuse standards indicate a complete process based on anaerobic secondary treatment is a competitive alternative to conventional aerobic-based paradigms.

Several areas of work remain to foster scale-up and adoption of this promising technology. First, water reuse trains downstream of the SAF-MBR must be demonstrated at pilot scale, as prospective technology adopters in California are almost certain to want the option to economically reuse water. Additionally, modeling tools are needed to allow simulation and prediction of SAF-MBR performance in different contexts. Finally, retrofit strategies must be developed for existing plants to transition to an anaerobic paradigm. Progress and planned work on these areas are discussed below.

6.1 Demonstration of Water Reuse Trains at Pilot Scale

The present effort has identified strategies to treat SAF-MBR effluent to meet California standards for non-potable and potable reuse. These strategies must now be further evaluated and demonstrated at pilot scale. The research team has secured two follow-on grants from the California State Water Resources Control Board Proposition 1 funding and from the US Bureau of Reclamation to conduct this demonstration over the course of two years. Successful demonstration of downstream water reuse systems at pilot scale is a pre-requisite to facilitate further scale-up of the system as discussed in Section 6.3. The research team will operate a combination of the following unit processes downstream of the SAF-MBR to achieve the desired water qualities: a chemical contactor for water oxidation by hydrogen peroxide and/or chlorine disinfection; a membrane aerated biofilm reactor for sulfide and ammonia management; reverse osmosis; and ultraviolet advanced oxidation (UV/AOP) for final oxidation of trace organic materials.

This additional effort will validate and improve the strategies identified in this project, yielding more robust operational and cost data needed to assess scale-up viability. Construction on this project is underway, with operations expected to commence early 2022. A discussion of future options for further scale-up of the SAF-MBR for commercialization is included in Section 6.2.

6.2 Modeling Platform to Predict SAF-MBR Performance in Different Contexts

The different performance of various anaerobic membrane bioreactors (AnMBRs) in diverse contexts prompted the research team to investigate fundamental processes driving treatment performance. In separate work, the team has identified a subset of influent COD that

determines effluent water quality. The portion of COD that is smaller than the pore size of typical ultrafiltration membranes used in MBRs (0.04 μm) yet large enough to require hydrolysis, is a critical design parameter needed to predict treatment outcomes. This fraction of COD, referred to as ultra-fine COD (UFCOD), is not retained by membranes and its removal rate in AnMBRs is determined primarily by water temperature and reactor HRT. In contexts in which influent UFCOD is low, such as at SVCW, the existing SAF-MBR system is a highly attractive alternative to conventional aerobic treatment. In contexts with high influent UFCOD, different membranes with smaller pore sizes may improve reactor performance and enable similar results as achieved in SVCW with conventional membranes. A provisional patent was filed for this new reactor configuration, and it will be tested and further developed at Stanford in 2022.

Existing tools for anaerobic process modeling have focused on high-strength wastes, and do not accurately predict behavior of anaerobic systems treating dilute wastewater such as sewage (Shin et al., 2021b). The research team developed a modeling platform based on fundamental kinetics to simulate the performance of an anaerobic MBR based on key contextual variables. These variables include water temperature, influent COD, UFCOD, HRT, and bulk fluid wasting rate. Model outputs include "effluent (=permeate) characteristics (i.e., acetate, propionate, COD, dissolved methane); gas composition and production rates (N_2 , CH_4 , CO_2); and predicted concentrations of mixed liquid suspended solids (MLSS), and recirculated bulk COD" (Shin et al., 2021b). These output parameters constitute the key design parameters necessary to anticipate system viability in different contexts.

Future work for this effort includes publicizing the model platform, and further developing it into a user-friendly tool to be added to existing process engineering modeling software.

6.3 Pathway for System Scale-up and Adoption

A viable approach is needed to further scale up the SAF-MBR design from 24,000 gpd to a capacity of millions of gallons per day. One possible approach is to convert existing anaerobic digesters into FBRs, the biological process reactor of the SAF-MBR. Many wastewater treatment plants in California have excess digester capacity (SWRCB, 2019), such that these unused or under-used assets could be converted to a new function without disrupting ongoing daily process operations. Existing digesters have the additional advantage that much of the required biogas management infrastructure is already in place for these systems, potentially allowing for a simpler retrofit than for aeration basins. Following successful pilot-scale tests of water reuse systems as discussed in Section 6.1, the project team will develop a list of facilities with excess capacity that would be optimal candidates to conduct this scale-up.

One such potential candidate is SVCW itself, as 1 of SVCW's 3 digesters is idle. This digester has an inside diameter of 96' and a design water depth of 30'. Under similar operating conditions to the existing demonstration, this digester could provide secondary treatment for approximately 6.75 MGD, or about half of SVCW's typical dry weather flow. An additional reactor to house the membranes would be necessary, occupying approximately an additional 1,250 square feet of footprint. A detailed design would be required to estimate additional footprint for ancillary equipment as well as costs of a retrofit. The research team is conducting a preliminary analysis of this option.

CHAPTER 7:

Conclusion

The SAF-MBR system at SVCW demonstrated that this new technology is a technically feasible approach to eliminate the energy-intensive practice of aeration for secondary treatment. The SAF-MBR also offers operational and potential capital cost savings over conventional systems. The SAF-MBR provides opportunities for energy savings, increased energy production, and reduced production of biosolids. Effluent from the SAF-MBR can be further processed for non-potable and potable water reuse.

The SAF-MBR Achieves US Secondary Effluent Standards for Solids and Organics in a Compact Footprint

Mean influent COD at steady state was 550 mg/L. After about 76 days, mean effluent COD stabilized, with steady state value of 36 mg/L, yielding a COD removal rate of 94 percent. Mean permeate BOD₅ (16 mg/L) and TSS (1 mg/L) confirm that the SAF-MBR is achieving US secondary effluent standards. This treatment performance was achieved while operating the system at a HRT of 5.2 hours, lower than the 6-10 hours that are typical for conventional activated sludge systems (aeration basin plus secondary clarifier).

The SAF-MBR Enables Energy-positive Secondary Treatment, and Renewable Electricity Export

Energy required to operate the system during testing was approximately 0.25 kWh/m³ (950 kWh/MG), of which about 80 percent (0.2 kWh/m³ or 760 kWh/MG) is required for GAC fluidization. The project team estimates that the fluidization system could be hydraulically optimized to reduce energy consumption by 0.1 kWh/m³ (380 kWh/MG). When capturing biogas and the dissolved methane from the permeate and assuming typical energy conversion efficiencies from a combined heat and power plant, the total energy production potential of the system is about 0.60 kWh/m³ (2,270 kWh/MG) of electricity and 0.67 kWh/m³ (2,530 btu/MG) of heat. This energy generation potential would enable energy-positive secondary treatment, with a power surplus of about 0.35 kWh/m³ (1,320 kWh/MG). The power surplus can be greater if the energy production potential from primary solids were considered. Thus, a full-scale wastewater treatment process employing a SAF-MBR for secondary treatment could produce a renewable energy surplus of 0.4 kWh/m³ (1,560 kWh/MG) for export to the grid. At SVCW, this would be equivalent to a whole-plant renewable power surplus of about 760 kW.

The SAF-MBR Reduces Biosolids Production from Wastewater Treatment

The biosolids production rate of the SAF-MBR is approximately 0.02 gVSS/gCOD_{removed}, about a 92 percent reduction in secondary solids production compared to the 0.218 gVSS/gCOD_{removed} of conventional aerobic secondary treatment processes.

The SAF-MBR Can Enable Operating and Capital Cost Savings

Eliminating energy use and reducing disposal of biosolids production at a full-scale treatment plant would eliminate approximately 35 percent of operating expenses at typical wastewater treatment plants. Capital costs could also be reduced due to smaller required reactor volumes and reduced solids management infrastructure, although further modeling for scaled-up construction costs is necessary.

Effluent From the SAF-MBR Can Be Further Treated for Non-Potable Water Reuse, but Sulfide Concentrations Impact Costs

A treatment process consisting of sulfide oxidation by H_2O_2 , pathogen inactivation by UV irradiation, and residual formation by chlorine addition to form chloramines enables achievement of Title 22 disinfection requirements. Sulfide oxidation proceeded favorably in approximately 30 minutes using a 4:1 H_2O_2 :sulfide stoichiometry at $pH \geq 8$. At an initial sulfide concentration of 0.5 mM, effluent pretreated at this ratio would require a UV fluence of 225 mJ cm^{-2} to achieve the required 5-log (99.999 percent) inactivation of MS_2 phage.

Costs for treating SAF-MBR effluent with 0.5mM sulfides would be approximately $\$0.19/\text{m}^3$ ($\$720/\text{MG}$), nominally more than the cost of chemicals and energy consumption for conventional aerobic wastewater liquids treatment and disinfection. However, the SAF-MBR presents additional benefits that can offset the more elevated costs of sulfide management. Specifically, surplus energy production and reduced solids handling costs can make anaerobic-based achievement of Title 22 water for non-potable reuse cost competitive with the conventional paradigm.

Effluent From the SAF-MBR Can Be Further Treated for Potable Water Reuse, With Potential Benefits for RO Flux Decline and Toxicity From Disinfection Byproducts

Chloramination prior to application of ozone yielded a lower flux decline than when ozonation preceded chloramination. The flux decline was comparable to or slower than flux declines for aerobic wastewater effluents. Under all pretreatment scenarios investigated, total concentration of DBPs was below $14 \mu\text{g/L}$ prior to RO. Following RO and the remainder of the FAT train, total DBPs were below $5 \mu\text{g/L}$. The total calculated DBP toxicity was a quarter of that typically observed at full scale potable reuse facilities processing aerobic secondary effluent.

The above advantages compound with previously observed superior removal of pharmaceutical compounds in SAF-MBR systems. However, further testing to ensure proper management of sulfides and evaluate the impact of seasonal sulfide variations is necessary.

The SAF-MBR Offers Benefits for California Statutory Objectives and for Ratepayers

Adoption of the SAF-MBR at wastewater treatment systems would advance the State's statutory goals as expressed in Senate Bill 350 to increase electricity and natural gas efficiency (the SAF-MBR reduces use of electricity and offsets use of natural gas). By reducing NO_x

emissions from secondary treatment and energy needs for electricity and biosolids transport, they also directly address AB-32. Ratepayers would also potentially benefit as follows:

- **Reduced wastewater utility fees:** Reduced costs for wastewater treatment plants could enable a municipality to meet existing needs with lower fees or forestall future rate hikes due to inflation.
- **Reduced electric utility fees:** The lower energy use of the SAF-MBR compared to many aerobic systems, coupled with the major increase in energy production from additional biogas, could reduce total demands on the energy grid while furnishing additional renewable energy to meet the state's renewable portfolio objectives at reduced costs. Coupled with biogas storage or other on-site storage, treatment plants could begin to provide some dispatchable grid services to reduce overall costs of grid operation.
- **Reduced greenhouse gases:** Lower emissions from energy consumption, increased production of renewable energy, elimination of greenhouse gas emissions from aeration basins, and reduced trips for hauling biosolids will reduce the greenhouse gas impact of wastewater treatment.

GLOSSARY AND LIST OF ACRONYMS

Term	Definition
AD	anaerobic digestion
AnMBR	anaerobic membrane bioreactor
AOP	advanced oxidation process
AWWA	American Water Works Association
BAC	biological activated carbon
BACWA	Bay Area Clean Water Agencies
BAWSCA	Bay Area Water Supply and Conservation Agency
BOD ₅	5-day biochemical oxygen demand
BSA	bovine serum albumin
CASA	California Association of Sanitation Agencies
CEB	chemically enhanced backwashing
CEC	California Energy Commission
CHO	Chinese hamster ovary
CHP	combined heat and power
Cl ⁻	chloride
cm	centimeter
CO ₂ eq	carbon dioxide equivalent
COD	chemical oxygen demand
CSTR-AnMBR	Continuously stirred tank reactor coupled with anaerobic membrane bioreactor.
CT	The product of total chlorine residual and contact time.
CWEA	California Water Environment Association
d	day
DBP	disinfection byproduct
DDW	Division of Drinking Water
DOC	dissolved organic carbon
DPD	N,N- diethyl-p-phenylenediamine
ε	molar absorptivity
EBCT	empty bed contact time
EPIC	Electric Program Investment Charge
FAT	full advanced treatment

Term	Definition
FBR	anaerobic fluidized bed reactor
FNU	Formazin Nephelometric Units
GAC	granular activated carbon
GC-TCD	gas chromatography equipped with a thermal conductivity detector
gpd	gallons per day
gpm/sf	gallons per minute per square foot
h	hour
ΔH	hydraulic head loss
H ⁺	hydrogen ion
HAA	halo-acetic acids
HLR	hydraulic loading rates
H ₂ O ₂	hydrogen peroxide
HOCl	hypochlorous acid
HPLC	high performance liquid chromatography
HRT	hydraulic retention time
HS ⁻	hydrogen sulfide ion
H ₂ S	hydrogen sulfide
IC	ion chromatography
J	RO permeate flux
kgCO ₂ e/MG	kilograms of carbon dioxide equivalent per million gallons
kWh/m ³	kilowatt-hours per cubic meter
kWh/MG	kilowatt-hours per million gallons
lbs	pounds
L/m ² /h	liters per square meter hour
LIFT	Leaders Innovation Forum for Technology
LECR	lifetime excess cancer risk
LRV	log removal value
MBR	membrane bioreactor
MC	maintenance cleanings
MCL	maximum contaminant level
m ³ /d	cubic meters per day
MF	microfiltration

Term	Definition
MG	million gallons
mg	milligram
mg/L	milligrams per liter
µg	microgram
MGD	million gallons per day
mJ cm ⁻²	millijoule per square centimeter
mL or ML	milliliter
µM	micromole
mM	millimolar
m/minute	meters per minute
MLSS	mixed liquor suspended solids
MPN	most probable number
MRL	minimum reporting level
MS2	A member of a family of closely related bacterial viruses that includes bacteriophage.
MT	membrane tank
mW	milliwatt
N	nitrogen
NaOCl	sodium hypochlorite
ng	nanogram
Nm ³ /m ² /h	normal meter cubed per hour
NTU	nephelometric turbidity units
NDMA	N-nitrosodimethylamine
NWRI	National Water Research Institute
O ₂	oxygen
OLR	organic loading rate
PFU	plaque-forming units
pH	"potential of hydrogen;" a measure of acidity or basicity.
pK _a	The negative base 10 logarithm of the acid dissociation constant, K _a .
PRAM	polarity rapid assessment method
PVDF	polyvinylidene fluoride
RC	recovery cleaning
RO	reverse osmosis

Term	Definition
SAF-MBR	staged anaerobic fluidized-bed membrane bioreactor
scfm	standard cubic feet per minute
SF	safety factor
slpm	standard liter per minute
SMP	soluble microbial products
SO ₃ ²⁻	sulfite
S ₂ O ₃ ²⁻	thiosulfate
SPE	solid phase extraction
SRB	sulfate-reducing bacteria
SRT	solids retention time
SS	suspended solids
STP	standard temperature and pressure
SVCW	Silicon Valley Clean Water
THM	tri-halo methanes
TMP	trans-membrane pressure
TSS	total suspended solids
UFC	uniform formation conditions
UFCOD	ultra-fine chemical oxygen demand
µm	micrometers
USEPA	Unites States Environmental Protection Agency
UV	ultraviolet
UV ₂₅₄	ultraviolet absorbance at 254 nm
UV/H ₂ O ₂ AOP	ultraviolet hydrogen peroxide advanced oxidation process
UVT	ultraviolet transmittance
W	watt
WEFTEC	Water Environment Federation
WERF	Water Research Foundation
WRCA	WaterReuse California
WWTP	wastewater treatment plant
VFA	volatile fatty acid
VSS	volatile suspended solids

References

- APHA. 1998. *Standard Methods for the Examination of Water and Wastewater*, 20th ed. American Public Health Association, Washington, DC.
- Ang, W.S., S. Lee, M. Elimelech. 2006. "Chemical and physical aspects of cleaning of organic-fouled reverse osmosis membranes". *Journal of Membrane Science*. 272(1-2), 198–210 (March). Available at <https://doi.org/10.1016/j.memsci.2005.07.035>
- Ang, W.S., M. Elimelech. 2007. "Protein (BSA) fouling of reverse osmosis membranes: implications for wastewater reclamation". *Journal of Membrane Science*. 296 (1-2), 83–92 (June). Available at <https://doi.org/10.1016/j.memsci.2007.03.018>
- Ang, W.S., A. Tiraferri, K.L. Chen, M. Elimelech. 2011. "Fouling and cleaning of RO membranes fouled by mixtures of organic foulants simulating wastewater effluent". *Journal of Membrane Science*. 376(1-2), 196–206 (July). Available at <https://doi.org/10.1016/j.memsci.2011.04.020>
- Bader, H., V. Sturzenegger, J. Hoigne. 1988. "Photometric method for the determination of low concentrations of hydrogen peroxide by the peroxidase catalyzed oxidation of N, N-diethyl-p-phenylenediamine (DPD)". *Water Research*. 22(9), 1109–1115 (September). Available at [https://doi.org/10.1016/0043-1354\(88\)90005-X](https://doi.org/10.1016/0043-1354(88)90005-X)
- Bae, K.S., G.-A. Shin. 2016. "Inactivation of various bacteriophages by different ultra- violet technologies: development of a reliable virus indicator system for water reuse". *Environmental Engineering Research*. 21(4), 350–354 (June). Available at <https://doi.org/10.4491/eer.2016.032>
- Bolton, J.R., M.I. Stefan, P.S. Shaw, K.R. Lykke. 2011. "Determination of the quantum yields of the potassium ferrioxalate and potassium iodide–iodate actinometers and a method for the calibration of radiometer detectors". *Journal of Photochemistry and Photobiology A*. 222(1), 166–169 (July). Available at <https://doi.org/10.1016/j.jphotochem.2011.05.017>
- Cadena, F., R.W. Peters. 1988. "Evaluation of chemical oxidizers for hydrogen sulfide control." *Journal (Water Pollution Control Federation)*. 60(7), 1259–1263 (July). Available at <https://www.jstor.org/stable/25043633>
- California Department of Public Health (CADPH). State of California Office of Administrative Law. 2021. *Title 22, California Code of Regulations, Section 60001-60355*.
- CEC (California Energy Commission). 2024. "References for Calculating Energy End-Use and GHG Emissions." Available at <https://www.energy.ca.gov/media/9207>
- Cheng, D., H.H. Ngo, W. Guo, Y. Liu, S.W. Chang, D.D. Nguyen, L.D. Nghiem, J. Zhou, B. Ni. 2018. "Anaerobic membrane bioreactors for antibiotic wastewater treatment: performance and membrane fouling issues." *Bioresource Technology*. 267, 714–724 (November). Available at <https://doi.org/10.1016/j.biortech.2018.07.133>

- Chuang, Y.H., K.M. Parker, W.A. Mitch. 2016. "Development of predictive models for the degradation of halogenated disinfection byproducts during the UV/H₂O₂ advanced oxidation process." *Environmental Science & Technology*. 50, 11209–11217 (September). ACS Publications. Available at <https://doi.org/10.1021/acs.est.6b03560>
- Chuang, Y.H., W.A. Mitch. 2017. "The effect of ozonation and biological activated carbon treatment of wastewater effluents on formation of N-nitrosamines and halogenated disinfection byproducts." *Environmental Science & Technology*. 51, 2329–2338 (January). ACS Publications. Available at <https://doi.org/10.1021/acs.est.6b04693>
- City of Oxnard. 2012. "City of Oxnard, CA, bid document comparison." Available at https://www.oxnard.org/wp-content/uploads/2016/03/08.29.12_Bid_PW-13-1_Chemicals_Summary_2012.xls. Retrieved on November 5, 2020.
- Drewes, J.E., P. Fox. 1999. "Fate of natural organic matter (NOM) during groundwater recharge using reclaimed water." *Water Science & Technology*. 40, 241–248 (November). Available at [https://doi.org/10.1016/S0273-1223\(99\)00662-9](https://doi.org/10.1016/S0273-1223(99)00662-9)
- Drewes, J.E.; T. Heberer, K. Reddersen. 2002. "Fate of pharmaceuticals during indirect potable reuse." *Water Science & Technology*. 46, 73–80. Available at <https://pubmed.ncbi.nlm.nih.gov/12227606/>
- Drewes, J.E., P. Anderson, N. Denslow, A. Olivieri, D. Schlenk, S.A. Snyder, K.A. Maruya. 2013. "Designing monitoring programs for chemicals of emerging concern in potable reuse—what to include and what not to include?" *Water Science & Technology*. 67, 433–439. Available at <https://pubmed.ncbi.nlm.nih.gov/23168646/>
- Errico, M., L.F. Sotoft, A.K. Nielsen, and B. Norddahl. 2018. "Treatment costs of ammonia recovery from biogas digestate by air stripping analyzed by process simulation." *Clean Technologies and Environmental Policy*. 20, 1479-1489 (November). Available at <https://doi.org/10.1007/s10098-017-1468-0>
- Evans, P.J., A. Doody, M. Harclerode, A. Brower, P. Vila, P.L. McCarty, W. Parker, P. Parameswaran, K. Lim., J. Bae, C. Shin, P. Lee, A. Tan, K. Guy, M. Page, and S. Maga. 2018. "Anaerobic membrane bioreactor (AnMBR) for sustainable waste-water treatment." *Environmental Security Technology Certification Program Project (ESTCP Project ER-201434)*. Available at <https://serdp-estcp.mil/projects/details/ebe45ed0-53d4-497c-a7ba-fad43f88bb2f/er-201434-project-overview>
- Feng, Y., D.W. Smith, J.R. Bolton. 2007. "Photolysis of aqueous free chlorine species (HOCl and OCl) with 254 nm ultraviolet light." *Journal of Environmental Engineering and Science*. 6, 277–284 (May). Available at <https://doi.org/10.1139/s06-052>
- Furman, C.S., D.W. Margerum. 1998. "Mechanism of chlorine dioxide and chlorate ion formation from the reaction of hypobromous acid and chlorite ion." *Inorganic Chemistry*. 37, 4321–4327 (July). ACS Publications. Available at <https://doi.org/10.1021/ic980262q>

- Furst, K.E., B.M. Pecson, B.D. Webber, W.A. Mitch. 2018. "Tradeoffs between pathogen inactivation and disinfection byproduct formation during sequential chlorine and chloramine disinfection for wastewater reuse." *Water Research*. 143, 579–588 (October). Available at <https://doi.org/10.1016/j.watres.2018.05.050>
- Giménez, J.B., A. Robles., L. Carretero, F. Durán, M.V. Ruano, M.N. Gatti,, J. Ribes, J. Ferrer, A. Seco. 2011. "Experimental study of the anaerobic urban wastewater treatment in a submerged hollow-fibre membrane bioreactor at pilot scale". *Bioresource Technology*. 102(19), 8799-8806 (October). Available at <https://doi.org/10.1016/j.biortech.2011.07.014>
- Galdi, S. and R. Luthy. 2021. "Effluent polishing for non-potable wastewater reuse from anaerobic membrane bioreactors." American Chemical Society Fall 2021. *Resilience of Chemistry* (Aug/22). Atlanta, GA. Available at <https://acs.digitellinc.com/p/s/effluent-polishing-for-non-potable-wastewater-reuse-from-anaerobic-membrane-bioreactors-176579>
- Gerrity, D., B. Pecson, R.S. Trussell, R.R. Trussell. 2013. "Potable reuse treatment trains throughout the world." *Journal of Water Supply: Research and Technology. Aqua*. 62(6), 321–338 (September). Available at <http://dx.doi.org/10.2166/aqua.2013.041>
- Goldstein, S., J. Rabani. 2008. "The ferrioxalate and iodide–iodate actinometers in the UV region." *Journal of Photochemistry and Photobiology A: Chemistry*. 193(1), 50–55 (January). Available at <https://doi.org/10.1016/j.jphotochem.2007.06.006>
- Guo, W., H.H. Ngo, J. Li. 2012. "A mini-review on membrane fouling." *Bioresource Technology*. 122, 27–34 (October). Available at <https://doi.org/10.1016/j.biortech.2012.04.089>
- Hansen, L.D., B.E. Richter, D.K. Rollins, J.D. Lamb, D.J. Eatough. 1979. "Determination of arsenic and sulfur species in environmental samples by ion chromatography." *Analytical Chemistry*. 51(6), 633–637. Available at <https://doi.org/10.1021/ac50042a010>
- Hijnen, W., E. Beerendonk, G.J. Medem. 2006. "Inactivation credit of UV radiation for viruses, bacteria and protozoan (oo)cysts in water: a review." *Water Research*. 40(1), 3–22 (May). Available at <https://doi.org/10.1016/j.watres.2005.10.030>
- Hoffmann, M.R. 1977. "Kinetics and mechanism of oxidation of hydrogen sulfide by hydrogen peroxide in acidic solution." *Environmental Science & Technology*. 11(1), 61–66 (January). Available at <https://doi.org/10.1021/es60124a004>
- Huang, B., H.C. Wang, D. Cui, B. Zhang, Z.B. Chen, A.J. Wang. 2018. "Treatment of pharmaceutical wastewater containing β -lactams antibiotics by a pilot-scale anaerobic membrane bioreactor (AnMBR)." *Chemical Engineering Journal*. 341, 238–247 (June). Available at <https://doi.org/10.1016/j.cej.2018.01.149>
- IPCC. 2019. "2019 Refinement to the 2006 IPCC Guidelines for National Greenhouse Gas Inventories, Vol. 5: Waste". Buendia, Calvo, E., Tanabe, K., Kranjc, A., Baasansuren, J., Fukuda, M., Ngarize S., Osako, A., Pyrozhenko, Y., Shermanau, P. and Federici, S.

(eds). Published: IPCC, Switzerland. Available at <https://www.ipcc-nggip.iges.or.jp/public/2019rf/vol5.html>

- de Haas, David W., G. Appleby, G. Charakos, and N. Dinesh. 2019. "Benchmarking energy use for wastewater treatment plants - A summary of the 2015-16 benchmarking study". *Water e-Journal (Online journal of the Australian Water Association)*, vol. 3(2). https://www.researchgate.net/publication/276921977_Benchmarking_Wastewater_Treatment_Plant_Energy_Use_in_Australia
- Jin, S., A.A. Mofidi, K.G. Linden. 2006. "Polychromatic UV fluence measurement using chemical actinometry, biosimetry, and mathematical techniques." *Journal of Environmental Engineering*. 132(8), 831–841 (August). [https://doi.org/10.1061/\(ASCE\)0733-9372\(2006\)132:8\(831\)](https://doi.org/10.1061/(ASCE)0733-9372(2006)132:8(831))
- Juang, L.C., D.H. Tseng, Y.M. Chen, G.U. Semblante, S.J. You. 2013. "The effect of soluble microbial products (SMP) on the quality and fouling potential of MBR effluent." *Desalination*. 326, 96–102 (October). <https://doi.org/10.1016/j.desal.2013.07.005>
- Kavvada, O., W.A. Tarpeh, A. Horvath, and K.L. Nelson. 2017. "Life-cycle cost and environmental assessment of decentralized nitrogen recovery using ion exchange from source-separated urine through spatial modeling." *Environmental Science & Technology*. 51(21), 12061-12071 (September). <https://doi.org/10.1021/acs.est.7b02244>
- King, J.F., A. Szczuka, Z. Zhang, W.A. Mitch. 2020. "Efficacy of ozone for removal of pesticides, metals and indicator virus from reverse osmosis concentrates generated during potable reuse of municipal wastewaters." *Water Research*. 176, 115744 (June). <https://doi.org/10.1016/j.watres.2020.115744>
- Komlenic, R. 2010. "Rethinking the causes of membrane biofouling." *Filtration & Separation*. 47(5), 26–28 (September – October). [https://doi.org/10.1016/S0015-1882\(10\)70211-1](https://doi.org/10.1016/S0015-1882(10)70211-1)
- Ksibi, M. 2006. "Chemical oxidation with hydrogen peroxide for domestic wastewater treatment." *Chemical Engineering Journal*. 119(2-3), 161–165 (June). <https://doi.org/10.1016/j.cej.2006.03.022>
- Lang, J., P. Schäffert, R. Böwing, S. Rivellini, F. Nota, and J. Klausner. 2017. "Development of a new generation of GE's Jenbacher type 6 gas engines." In: Siebenpfeiffer, W. (ed.). *Heavy-Duty-, On-und Off-Highway-Motoren 2016*. Springer Vieweg, Wiesbaden. 19-36 (September). https://doi.org/10.1007/978-3-658-19012-5_2
- Lee, S., J. Cho, M. Elimelech. 2004. "Influence of colloidal fouling and feed water recovery on salt rejection of RO and NF membranes." *Desalination*. 160(1), 1–12 (January). [https://doi.org/10.1016/S0011-9164\(04\)90013-6](https://doi.org/10.1016/S0011-9164(04)90013-6)
- Lee, S., W.S. Ang, M. Elimelech. 2006a. "Fouling of reverse osmosis membranes by hydrophilic organic matter: implications for water reuse." *Desalination*. 187(1-3), 313–321 (February). <https://doi.org/10.1016/j.desal.2005.04.090>

- Lee, S., M. Elimelech. 2006b. "Relating organic fouling of reverse osmosis membranes to intermolecular adhesion forces." *Environmental Science & Technology*. 40, 980–987 (January). <https://doi.org/10.1021/es051825h>
- Lens, P.N.L., A. Visser, A.J.H. Janssen, L.H. Pol, G. Lettinga. 1998. "Biotechnological treatment of sulfate-rich wastewaters." *Critical Reviews in Environmental Science and Technology*. 28(1), 41–88 (June). <https://doi.org/10.1080/10643389891254160>
- Li, Q., Z. Xu, I. Pinnau. 2007. "Fouling of reverse osmosis membranes by biopolymers in wastewater secondary effluent: Role of membrane surface properties and initial permeate flux." *Journal of Membrane Science*. 290(1-2), 173–181 (March). <https://doi.org/10.1016/j.memsci.2006.12.027>
- Li, X.-F., W.A. Mitch. 2018. "Drinking water disinfection byproducts (DBPs) and human health effects: multidisciplinary challenges and opportunities." *Environmental Science & Technology*. 52(4), 1681–1689 (December). <https://doi.org/10.1021/acs.est.7b05440>
- Liang, S., C. Liu, L. Song. 2007. "Soluble microbial products in membrane bioreactor operation: behaviors, characteristics, and fouling potential." *Water Research*. 41(1), 95–101 (January). <https://doi.org/10.1016/j.watres.2006.10.008>
- Lim, K., P.J. Evans, P. Parameswaran. 2019. "Long-term performance of a pilot-scale gas-sparged anaerobic membrane bioreactor under ambient temperatures for holistic wastewater treatment." *Environmental Science & Technology*. 53(13), 7347-7354 (June). <https://doi.org/10.1021/acs.est.8b06198>
- Lin, H., J. Chen, F. Wang, L. Ding, H. Hong. 2011. "Feasibility evaluation of submerged anaerobic membrane bioreactor for municipal secondary wastewater treatment." *Desalination*. 280 (1-3), 120-126 (October). <https://doi.org/10.1016/j.desal.2011.06.058>
- McCarty, P.L., J. Bae, J. Kim. 2011, "Domestic wastewater treatment as a net energy producer – Can this be achieved?" *Environmental Science & Technology*. 45(17), 7100-7105 (July). <https://doi.org/10.1021/es2014264>
- McCarty, P.L., J. Kim, C. Shin, P.H. Lee., J. Bae. 2015. "Anaerobic fluidized bed membrane bioreactors for the treatment of domestic wastewater." *Anaerobic biotechnology: Environmental protection and resource recovery*. 211-242. https://doi.org/10.1142/9781783267910_0010
- McCurry, D.L., S.E. Bear, J. Bae, D.L. Sedlak, P.L. McCarty, W.A, Mitch. 2014. "Superior Removal of Disinfection Byproduct Precursors and Pharmaceuticals from Wastewater in a Staged Anaerobic Fluidized Membrane Bioreactor Compared to Activated Sludge." *Environmental Science & Technology Letters*. 1(11), 459–464 (October). <https://doi.org/10.1021/ez500279a>
- Metcalf and Eddy, Inc. 1991. "Wastewater Engineering: Treatment, Disposal and Reuse". 3rd Edition. McGraw-Hill, Inc. New York, NY. 109. <https://www.scribd.com/document/476475702/WastewaterEngbyMecalfandEddy2003-pdf>

- Millero, F.J., A. LeFerriere, M. Fernandez, S. Hubinger, J.P. Hershey. 1989. "Oxidation of hydrogen sulfide with hydrogen peroxide in natural waters." *Environmental Science & Technology*. 23(2), 209–213 (February). <https://doi.org/10.1021/es00179a012>
- Morgan, M.S., P.F. Van Trieste., S.M. Garlick, M.J. Mahon, A.L. Smith. 1988. "Ultraviolet molar absorptivities of aqueous hydrogen peroxide and hydroperoxyl ion." *Analytica Chimica Acta*. 215, 325–329. [https://doi.org/10.1016/S0003-2670\(00\)85294-0](https://doi.org/10.1016/S0003-2670(00)85294-0)
- NRC (National Research Council). 2012. "Understanding Water Reuse: Potential for Expanding the Nation's Water Supply through Reuse of Municipal Wastewater." The National Academies Press. Washington, DC. <https://nap.nationalacademies.org/catalog/13514/understanding-water-reuse-potential-for-expanding-the-nations-water-supply>
- Nelson, D.P., L.A. Kiesow. 1972. "Enthalpy of decomposition of hydrogen peroxide by catalase at 25 C (with molar extinction coefficients of H₂O₂ solutions in the UV)." *Analytical Biochemistry*. 49(2), 474–478 (October). [https://doi.org/10.1016/0003-2697\(72\)90451-4](https://doi.org/10.1016/0003-2697(72)90451-4)
- National Water Research Institute (NWRI). 2012. "Ultraviolet Disinfection Guidelines for Drinking Water and Water Reuse." National Water Research Institute (August). Available at <https://www.nwri-usa.org/research>
- Pressley, T.A., D.F. Bishop, S.G. Roan. 1972. "Ammonia-nitrogen removal by break-point chlorination." *Environmental Science & Technology*. 6(7), 622–628 (July). <https://doi.org/10.1021/es60066a006>
- Rahn, R.O., M.I. Stefan, J.R. Bolton, E. Goren, P.S. Shaw, K.R. Lykke. 2003. "Quantum yield of the iodide-iodate chemical actinometer: dependence on wavelength and concentration." *Photochemistry and Photobiology*. 78(2), 146–152 (August). [https://doi.org/10.1562/0031-8655\(2003\)078%3C0146:qyotic%3E2.0.co;2](https://doi.org/10.1562/0031-8655(2003)078%3C0146:qyotic%3E2.0.co;2)
- Ridgway, H.F., C.A. Justice, C. Whittaker, D.G. Argo, B.H. Olson. 1984. "Biofilm fouling of RO membranes—its nature and effect on treatment of water for reuse." *Journal AWWA*. 76, 94–102. <https://doi.org/10.1002/j.1551-8833.1984.tb05355.x>
- Rittmann, B.E., W. Bae, E. Namkung, C.J. Lu. 1987. "A critical evaluation of microbial product formation in biological processes." *Water Science & Technology*. 19(3-4), 517–528 (March). <https://doi.org/10.2166/wst.1987.0231>
- Rittmann, B.E., P.L. McCarty. 2020. *Environmental biotechnology: principles and applications*. McGraw-Hill Education. <https://www.accessengineeringlibrary.com/content/book/9781260440591>
- Robles, A., M.V. Ruano, J. Ribes, J. Ferrer. 2013. "Performance of industrial scale hollow-fibre membranes in a submerged anaerobic MBR (HF-SAnMBR) system at mesophilic and psychrophilic conditions." *Separation and Purification Technology*. 104, 290-296 (February). <https://doi.org/10.1016/j.seppur.2012.12.004>

- Rosario-Ortiz, F.L., S.A. Snyder, I.M. Suffet. 2007a. "Characterization of dissolved organic matter in drinking water sources impacted by multiple tributaries." *Water Research*. 41(18), 4115–4128 (October). <https://doi.org/10.1016/j.watres.2007.05.045>
- Rosario-Ortiz, F.L., S. Snyder, I.H. Suffet. 2007b. "Characterization of the polarity of natural organic matter under ambient conditions by the polarity rapid assessment method (PRAM)." *Environmental Science & Technology*. 41, 4895–4900 (June). <https://doi.org/10.1021/es062151t>
- Sarti, A., E. Pozzi, F.A. Chinalia., A. Ono, E. Foresti. 2010. "Microbial processes and bacterial populations associated to anaerobic treatment of sulfate-rich wastewater." *Process Biochemistry*. 45(2), 164–170 (February). <https://doi.org/10.1016/j.procbio.2009.09.002>
- Schreiber, I.M., W.A. Mitch. 2005. "Influence of the order of reagent addition on NDMA formation during chloramination." *Environmental Science & Technology*. 39(10), 3811–3818 (April). <https://doi.org/10.1021/es0483286>
- Shin, C., E. Lee, P.L. McCarty, J. Bae. 2011. "Effects of influent DO/COD ratio on the performance of an anaerobic fluidized bed reactor fed low-strength synthetic wastewater." *Bioresource Technology*. 102(21), 9860-9865 (November). <https://doi.org/10.1016/j.biortech.2011.07.109>
- Shin, C., J. Bae, P.L. McCarty. 2012. "Lower operational limits to volatile fatty acid degradation with dilute wastewaters in an anaerobic fluidized bed reactor." *Bioresource Technology*. 109, 13-20 (April). <https://doi.org/10.1016/j.biortech.2012.01.014>
- Shin, C., P.L. McCarty, J. Kim, and J. Bae. 2014. "Pilot-scale temperate-climate treatment of domestic wastewater with a staged anaerobic fluidized membrane bioreactor (SAF-MBR)." *Bioresource Technology*. 159, 95-103 (May). <https://doi.org/10.1016/j.biortech.2014.02.060>
- Shin, C., S.H. Tilmans, F. Chen, P.L. McCarty, C.S. Criddle. 2021a. "Temperate Climate Energy-positive Anaerobic Secondary Treatment of Domestic Wastewater at Pilot-scale." *Water Research*. 204, 117598 (October). <https://doi.org/10.1016/j.watres.2021.117598>
- Shin, C., S.H. Tilmans, F. Chen, C.S. Criddle. 2021b. "Anaerobic membrane bioreactor model for design and prediction of domestic wastewater treatment process performance." *Chemical Engineering Journal*. 426, 131912 (December). <https://doi.org/10.1016/j.cej.2021.131912>
- Shin, C., A. Szczuka., R. Jiang, W.A. Mitch., C.S. Criddle. 2021c. "Optimization of reverse osmosis operational conditions to maximize ammonia removal from the effluent of an anaerobic membrane bioreactor." *Environmental Science: Water Research & Technology*. 7(4), 739-747 (February). <https://doi.org/10.1039/D0EW01112F>
- Shin, C., A. Szczuka, M.J. Liu., L. Mendoza, R. Jiang, S.H. Tilmans, W.A. Tarpeh, W.A. Mitch, C.S. Criddle. In preparation. "Conventional energy-intensive water and ammonia supply chains verses short-cut reuse cycles: a systems-level comparison."

- Shon, H.K., S.H. Kim, L. Erdei, S. Vigneswaran. 2006. "Analytical methods of size distribution for organic matter in water and wastewater." *Korean Journal of Chemical Engineering*. 23, 581–591 (July). <https://doi.org/10.1007/BF02706798>
- Smith, A.L., L.B. Stadler, N.G. Love, S.J. Skerlos., L. Raskin. 2012. "Perspectives on anaerobic membrane bioreactor treatment of domestic wastewater: a critical review." *Bioresource Technology*. 122, 149–159 (October). <https://doi.org/10.1016/j.biortech.2012.04.055>
- Snoeyink, V.L., D. Jenkins. 1980. *Water Chemistry*. John Wiley & Sons, New York. 6. <https://eclass.upatras.gr/modules/document/file.php/CMNG2125/Water%20Chemistry%20-%20V.L.Snoeyink%3B%20D.Jenkins.pdf>
- Song, Y., B. Dong, N. Gao, S. Xia. 2010. "Huangpu River water treatment by microfiltration with ozone pretreatment." *Desalination*. 250(1), 71–75 (January). <https://doi.org/10.1016/j.desal.2009.06.047>
- Stanford, B.D., A.N. Pisarenko, R.D. Holbrook, S.A. Snyder. 2011. "Preozonation effects on the reduction of reverse osmosis membrane fouling in water reuse." *Ozone: Science & Engineering*. 33, 379–388 (February). <https://doi.org/10.1016/j.memsci.2019.117546>
- Steiner, N., R. Gec. 1992. "Plant Experience Using Hydrogen Peroxide for Enhanced Fat Flotation and BOD Removal." *Environmental Progress & Sustainable Energy*. 11, 261–264 (November). <https://doi.org/10.1002/ep.670110412>
- Steinle-Darling, E., M. Zedda, M.H. Plumlee, H.F. Ridgway, M. Reinhard. 2007. "Evaluating the impacts of membrane type, coating, fouling, chemical properties and water chemistry on reverse osmosis rejection of seven nitrosoalkylamines, including NDMA." *Water Research*. 41(17), 3959–3967 (September). <https://doi.org/10.1016/j.watres.2007.05.034>
- Sun, P., C. Tyree, C.H. Huang. 2016. "Inactivation of Escherichia coli, bacteriophage MS₂, and Bacillus spores under UV/H₂O₂ and UV/peroxydisulfate advanced disinfection conditions." *Environmental Science & Technology*. 50(8), 4448–4458 (March). <https://doi.org/10.1021/acs.est.5b06097>
- Sunden, T., M. Lindgren, A. Cedergren, D.D. Siemer. 1983. "Separation of sulfite, sulfate, and thiosulfate by ion chromatography with gradient elution." *Analytical Chemistry*. 55(1), 2–4 (January). <https://doi.org/10.1021/ac00252a004>
- Świetlik, J., E. Sikorska. 2004. "Application of fluorescence spectroscopy in the studies of natural organic matter fractions reactivity with chlorine dioxide and ozone." *Water Research*. 38(17), 3791–3799 (October). <https://doi.org/10.1016/j.watres.2004.06.010>
- SWRCB (State Water Resources Control Board). 2019. "Co-Digestion Capacity Analysis Prepared for the California State Water Resources Control Board under Agreement #17-014-240." Available at https://www.waterboards.ca.gov/climate/docs/co_digestion/final_co_digestion_capacity_in_california_report_only.pdf. Last accessed on April 4, 2022.

- Szczuka, A., K.M. Parker, C. Harvey, E. Hayes, A. Vengosh, W.A. Mitch. 2017. "Regulated and unregulated halogenated disinfection byproduct formation from chlorination of saline groundwater." *Water Research*. 122, 633–644. <https://doi.org/10.1016/j.watres.2017.06.028>
- Szczuka, A., J.P. Berglund-Brown, H.K. Chen, A.N. Quay, W.A. Mitch. 2019. "Evaluation of a pilot anaerobic secondary effluent for potable reuse: impact of different disinfection schemes on organic fouling of RO membranes and DBP formation." *Environmental Science & Technology*. 53(6), 3166-3176 (February). <https://doi.org/10.1021/acs.est.8b05473>
- Szczuka, A., Y.H. Chuang, F.C. Chen, Z. Zhang, E. Desormeaux, M. Flynn, J. Parodi, W.A. Mitch. 2020. "Removal of pathogens and chemicals of emerging concern by pilot-scale FO-RO hybrid units treating RO concentrate, graywater, and sewage for centralized and decentralized potable reuse." *ACS ES&T Water* 1(1) 89-100 (August). <https://doi.org/10.1021/acsestwater.0c00006>
- Szczuka, A., J.P. Berglund-Brown, J.A. MacDonald, W.A. Mitch. 2021. "Control of sulfides and coliphage MS₂ using hydrogen peroxide and UV disinfection for non-potable reuse of pilot-scale anaerobic membrane bioreactor effluent." *Water Research*. X, 11, 100097 (May). <https://doi.org/10.1016/j.wroa.2021.100097>
- Takenaka, N., S. Furuya, K. Sato, H. Bandow, Y. Maeda, Y. Furukawa. 2003. "Rapid reaction of sulfide with hydrogen peroxide and formation of different final products by freezing compared to those in solution." *International Journal of Chemical Kinetics*. 35, 198–205 (February). <https://doi.org/10.1002/kin.10118>
- Tang, S., Z. Wang, Z. Wu, Q. Zhou. 2010. "Role of dissolved organic matters (DOM) in membrane fouling of membrane bioreactors for municipal wastewater treatment." *Journal of Hazardous Material*. 178(1-3), 377– 384 (June). <https://doi.org/10.1016/j.jhazmat.2010.01.090>
- Templeton, M.R., R.C. Andrews, R. Hofmann. 2006. "Impact of iron particles in groundwater on the UV inactivation of bacteriophages MS₂ and T4." *Journal of Applied Microbiology*. 101(3), 732–741 (September). <https://doi.org/10.1111/j.1365-2672.2006.02980.x>
- USEPA (U.S. Environmental Protection Agency). 1980. "Construction Costs for Municipal Wastewater Treatment Plants: 1973-1978." Technical Report, EPA/430/9-80-003. Available at https://www.fs.usda.gov/Internet/FSE_DOCUMENTS/stelprdb5336487.pdf. Accessed on February 28, 2022
- USEPA (U.S. Environmental Protection Agency). 2012. *Guidelines For Water Reuse*. United States Environmental Protection Agency. AR-1530, EPA/600/R-12/618 (September). Available at <https://www.epa.gov/sites/default/files/2019-08/documents/2012-guidelines-water-reuse.pdf>
- USEPA (U.S. Environmental Protection Agency). 2000. "Wastewater technology fact sheet." EPA 832-F-00-017. <https://nepis.epa.gov/Exe/ZyPURL.cgi?Dockey=P1001QTK.txt>

- USEPA (U.S. Environmental Protection Agency). 2024. "Secondary Drinking Water Standards: Guidance for Nuisance Chemicals." United States Environmental Protection Agency. Available at <https://www.epa.gov/sdwa/secondary-drinking-water-standards-guidance- nuisance-chemicals>
- Van Geluwe, S., L. Braeken, B. van der Bruggen. 2011a. "Ozone oxidation for the alleviation of membrane fouling by natural organic matter: A review." *Water Research*. 45(12), 3551–3570 (June). <https://doi.org/10.1016/j.watres.2011.04.016>
- Van Geluwe, S., C. Vinckier, L. Braeken, B. van der Bruggen. 2011b. "Ozone oxidation of nanofiltration concentrates alleviates membrane fouling in drinking water industry." *Journal of Membrane Science*. 378, 128–137 (August). <https://doi.org/10.1016/j.memsci.2011.04.059>
- Vatankhah, H., C.C. Murray, J.W. Brannum, J. Vanneste, C. Bellona. 2018. "Effect of pre-ozonation on nanofiltration membrane fouling during water reuse applications." *Separation and Purification Technology*. 205, 203–211 (October). <https://doi.org/10.1016/j.seppur.2018.03.052>
- Verlicchi, P., M. Al Aukidy, E. Zambello. 2012. "Occurrence of pharmaceutical compounds in urban wastewater: removal, mass load and environmental risk after a secondary treatment—a review." *Science of the Total Environment*. 429, 123–155 (July). <https://doi.org/10.1016/j.scitotenv.2012.04.028>
- von Sonntag, C., U. von Gunten. 2012. *Chemistry of Ozone in Water and Wastewater Treatment: From Basic Principles to Application*. IWA Publishing. London (August). <https://doi.org/10.2166/9781780400839>
- Xu, P., C. Bellona, J.E. Drewes. 2010. "Fouling of nanofiltration and reverse osmosis membranes during municipal wastewater reclamation: membrane autopsy results from pilot-scale investigations." *Journal of Membrane Science*. 353(1-2), 111–121 (May). <https://doi.org/10.1016/j.memsci.2010.02.037>
- Yang, X., R.C. Flowers, H.S. Weinberg, P.C. Singer. 2011. "[Occurrence and removal of pharmaceuticals and personal care products \(PPCPs\) in an advanced wastewater reclamation plant.](#)" *Water Research*. 45(16), 5218–5228 (October). <https://doi.org/10.1016/j.watres.2011.07.026>
- Ye, Y., P.H. Chang, J. Hartert, K.R. Wigginton. 2018. "[Reactivity of enveloped virus genome, proteins, and lipids with free chlorine and UV₂₅₄.](#)" *Environmental Science & Technology*. 52(14), 7698–7708 (June). <https://doi.org/10.1021/acs.est.8b00824>
- Yoo, R., J. Kim, P.L. McCarty, J. Bae. 2014. "[Anaerobic treatment of municipal wastewater with a staged anaerobic fluidized membrane bioreactor \(SAF-MBR\) system.](#)" *Bioresource Technology*. 120, 133–139 (September). <https://doi.org/10.1016/j.biortech.2012.06.028>

- Zeng, T., C.J. Wilson, W.A. Mitch. 2014. "[Effect of chemical oxidation on the sorption tendency of dissolved organic matter to a model hydrophobic surface.](#)" *Environmental Science & Technology*. 48(9), 5118–5126 (April). <https://doi.org/10.1021/es405257b>
- Zeng, T., M.J. Plewa, W.A. Mitch. 2016a. "[N-Nitrosamines and Halogenated Disinfection Byproducts in U.S. Full Advanced Treatment Trains for Potable Reuse.](#)" *Water Research*, 101, 176–186 (September). <https://doi.org/10.1016/j.watres.2016.03.062>
- Zeng, T., W.A. Mitch. 2016b. "[Impact of Nitrification on N- Nitrosamine and Halogenated Disinfection Byproduct Formation within Drinking Water Storage Facilities.](#)" *Environmental Science & Technology*. 50(6), 2964–2973 (February). <https://doi.org/10.1021/acs.est.5b05668>
- Zhang, Z., Y.H. Chuang, A. Szczuka, K.P. Ishida, S. Roback, M.H. Plumlee, W.A. Mitch. 2019. "[Pilot-scale evaluation of oxidant speciation, 1, 4-dioxane degradation and disinfection byproduct formation during UV/hydrogen peroxide, UV/free chlorine and UV/chloramines advanced oxidation process treatment for potable reuse.](#)" *Water Research*. 164, 114939 (November). <https://doi.org/10.1016/j.watres.2019.114939>
- Zhang, Z., J.F. King, A. Szczuka, Y.H. Chuang, W.A. Mitch. 2020. "[Pilot-scale ozone/biological activated carbon treatment of reverse osmosis concentrate: potential for synergism between nitrate and contaminant removal and potable reuse.](#)" *Environmental Science: Water Research & Technology*. 6, 1421–1431 (March). <https://doi.org/10.1039/D0EW00013B>
- Zularisam, A.W., A.F. Ismail, M.R. Salim, M. Sakinah, H. Ozaki. 2007. "[The effects of natural organic matter \(NOM\) fractions on fouling characteristics and flux recovery of ultrafiltration membranes.](#)" *Desalination*. 212(1-3), 191–208 (June). <https://doi.org/10.1016/j.desal.2006.10.010>
- Zuman, P., W. Szafranski. 1976. "[Ultraviolet spectra of hydroxide, alkoxide, and hydrogen sulfide anions.](#)" *Analytical Chemistry*. 48(14), 2162–2163 (December). <https://doi.org/10.1021/ac50008a027>